# Adaptive control of eye movement accuracy by the cerebellum: the site of plasticity and functional mechanisms

Dissertation

zur Erlangung des Grades eines Doktors
der Naturwissenschaften

der Fakultät für Biologie
und
der Medizinischen Fakultät
der Eberhard-Karls-Universität Tübingen

vorgelegt
von

***Mario Prsa***
aus Montreal, Canada

November - 2010

| | |
|---|---|
| Dekan der Fakultät für Biologie: | Prof. Dr. H. A. Mallot |
| Dekan der Medizinischen Fakultät: | Prof. Dr. I. B. Autenrieth |
| 1. Berichterstatter: | Prof. Dr. Peter Thier |
| 2. Berichterstatter: | PD Dr. Cornelius Schwarz |
| Prüfungskommission: | Prof. Dr. Peter Thier |
| | Prof. Dr. Hanspeter Mallot |
| | PD Dr. Cornelius Schwarz |
| | PD Dr. Marc Ernst |
| | Prof. Dr. Hansjörg Scherberger |
| Defense date: | Monday, October 25th, 2010 |

“I declare that I have produced the work entitled: “Adaptive control of eye saccade accuracy by the cerebellum: the site of plasticity and functional mechanisms” submitted for the award of a doctorate, on my own (without external help), have used only the sources and aids indicated and have marked passages included from other works, whether verbatim or in content, as such. I swear upon oath that these statements are true and I have not concealed anything. I am aware that making a false declaration under oath is punishable by a term of imprisonment of up to three year or by a fine. I also declare that this version of the work does not differ in form or contents from the one submitted to the evaluation committee for review purposes.”

Mario Prsa
Tübingen, 2010

# Preface

At the 1936 Olympic Games in Berlin, the Slovenian gymnast Leon Štukelj won his sixth and final Olympic medal. In 1998, at one hundred years of age, he was known as the oldest living Olympic gold medalist and famous for his impressive abilities to replicate in front of journalists some of the same gymnastic stances that he used to do more than 60 years ago. The physical capability of this legendary Olympian highlights the important faculty of our brains to adapt to our ever-changing physiology. Growing evidence suggests that the cerebellum mediates such adaptive processes.

The work presented in this thesis uses the simple model of eye movement control in behaving macaque monkeys to reveal important aspects of cerebellum-dependent adaptation of motor function.

**Berlin, 1936:** 38 years old

**1998:** 100 years old

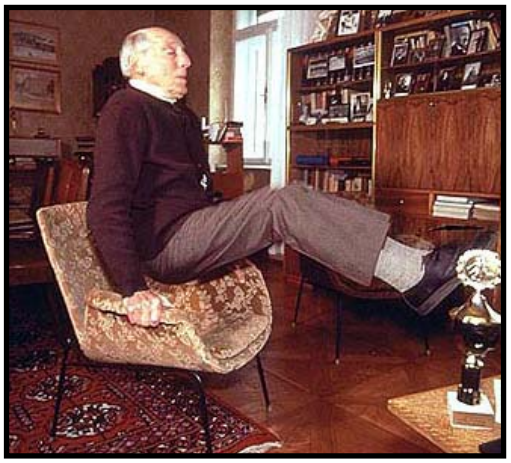

## Table of contents

# Chapter 1:

# Introduction

## *1.1 General introduction*

Throughout the animal kingdom we can marvel at the impressive accuracy of coordinated movements that living organisms are capable of. Whether it is a chameleon shooting out his tongue to catch an insect sitting on a distant flower or the swift changes in running directions of a cheetah chasing a gazelle at furious speeds, the ability of the nervous system to generate precisely tuned motor commands that will guide the physical periphery towards a desired position in space is of vital importance. From a computational standpoint, even the simplest shift in gaze direction and a subsequent reaching movement of a 1-year-old child trying to grasp her favorite toy is quite a remarkable ability of the brain.

In the case of robotic control, motors can be carefully designed so they do not overheat, a constant power supply can be assured, sensors that record motion are highly precise and transmit information to the controller which computes and issues commands by means of unfailing silicon transistors, all on the timescale of microseconds. In contrast, biological movement control relies on noisy and slow sensory feedback, neural transmission and processing operates in the millisecond range and can also be corrupted by noise, and most importantly, the whole motor apparatus is subject to change with time. Therefore, in order to preserve the vital importance of accurate movements, the nervous system must have the additional ability to compensate for these limitations and be adaptable to physiological changes. For example, the motor commands issued by the brain of the 1-year-old reaching for an object are of little use to this individual as a grown adult, with larger bones and increased muscle mass. Such changes in the dynamic relationship between the neural motor commands and the resulting movements must continuously be compensated for as they occur on much shorter time scales; when for instance our muscles fatigue, we wear heavy equipment or manipulate a tool.

Numerous lines of evidence suggest that the cerebellum is the key brain structure that mediates such adaptive or compensatory processes. Following a brief

introductory description of cerebellar function and the neuronal basis of eye movement control, the work presented in this thesis uses the oculomotor system as a model of biological motor control to investigate various aspects of cerebellum-dependent motor adaptation:

- chapter 2 provides novel evidence for a cerebellum-dependent compensation of a purely cognitive disturbance of motor function,

- chapter 3 identifies the site of neural plasticity in the micro circuitry of the cerebellar cortex that takes place during motor adaptation,

- chapter 4 reveals at what stage of sensori-motor processing the cerebellum interacts with the neural control of eye movements during adaptive behavior,

- chapter 5 is a brief synopsis of the three aforementioned studies and elucidates how they collectively contribute to a much broader understanding of the role of the cerebellum in motor adaptation.

## *1.2 The cerebellum*

The cerebellum, a phylogenetically ancient structure, is present in all vertebrates and analogous brain areas can also be found in cephalopods. In humans, it constitutes about 10% of the total brain volume but contains roughly half of all its neurons. A salient characteristic of the cerebellar cortex is its crystal-like structural regularity. Neurons and their underlying circuits are arranged in highly uniform and repetitive modules across the entire cortical volume. Therefore, it may be firmly assumed that the same neuronal computations are carried anywhere in the cerebellar cortex. Moreover, as the horizontal extent of intracortical fibers is confined to a few millimeters only, neural computations are necessarily local, and hence specific to the afferent and efferent connections a particular part of the cortex maintains with extra-cerebellar structures involved in a particular sensori-motor function. This contrast between structural regularity and regional specificity suggests that the cerebellum

provides the same neural processing to the pathways of different motor systems. It follows that functional findings about a cortical area of the cerebellum specialized in a specific motor function are also descriptive of the broader role the cerebellum has in motor control. Accordingly, the control of saccadic eye movements is used in this thesis to investigate cerebellar function, and the relevant cortical area is the midline of lobuli VIc and VIIA, also known as the oculomotor vermis and is highlighted in Figure 1.1.

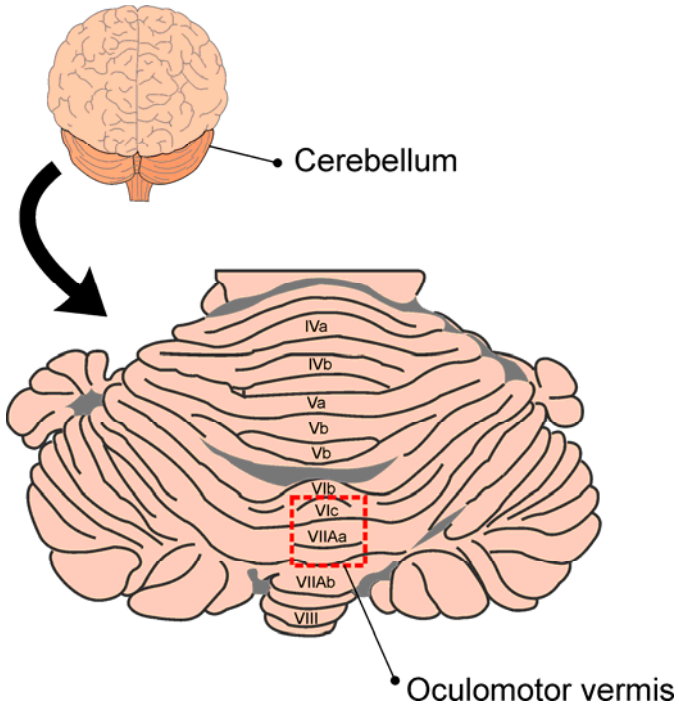


**Figure 1.1: dorsal view of the cerebellar cortex with the oculomotor vermis (midline of lobuli VIc and VIIA) highlighted.**

Surgical lesions in animals and studies of patients with cerebellar pathologies reveal that the absence of a normal functioning cerebellum does not lead to paralysis, but suggest instead that its primary role would be the fine-tuning of motor function. For example, patients with focal cerebellar lesions show an increased variability in the end-point accuracy of voluntary leg placement (Ilg et al., 2008), while others exhibit abnormal upper limb movements during a finger pointing task (Konczak et al., 2005). Monkeys with a surgically removed oculomotor vermis, after an initial recovery period, are still able to accurately execute visually guided eye movements, however not without a significant impairment in end-point precision (Barash et al., 1999). The most immediate function of the cerebellum is therefore to

monitor the progress of each individual movement and ensure that the desired movement goal is reached by tweaking, as necessary, the underlying cortical, spinal or brainstem motor pathways.

On a different time scale, the cerebellum participates in the vital process of learning new motor skills; or adapting the nervous system to any novel changes in the physical dynamics of the motor periphery or in the external environment. This ability can be studied by for example having subjects manipulate a robotic arm and having to adapt their reaching movements to novel dynamics imposed by that manipulandum. Patient and lesion studies again reveal that an intact cerebellum is necessary for such adaptive behavior to take place, whether it is adaptation to modified arm dynamics (Smith and Shadmehr, 2005), visuo-motor disturbances (Martin et al., 1996; Rambold et al., 2002; Tseng et al., 2007), surgical weakening of eye muscles (Optican and Robinson, 1980) or forced asymmetric locomotion (Morton and Bastian, 2006). The role of the cerebellum in motor adaptation can easily be investigated with saccadic eye movements. First, the ability for monkeys to maintain movement accuracy despite a gradual decrease in eye velocity during a long sequence of repetitive saccades depends on the integrity of the oculomotor vermis (Barash et al., 1999). The underlying cerebellum-dependent fatigue compensation mechanism is the subject of chapter 2. Second, when the oculomotor vermis is surgically removed, monkeys are also unable to adaptively adjust the amplitude of their saccades after an unperceived displacement of the visual target (Barash et al., 1999). This classic example of short-term motor learning is more commonly referred to as saccadic adaptation and is used in chapters 3 and 4 to investigate, respectively, the site of plasticity and functional mechanisms of the adaptive process.

## *1.3 Neural control of saccadic eye movements*

Eye movements are probably the most studied example of biological motor control. The wealth of data from electrophysiology, anatomy, lesion and patient studies about the oculomotor system is overwhelming. The reasons lie, on the one hand in the mechanical simplicity of eye movements, and on the other, in the experimental ease of measuring eye globe rotation from behaving animals in laboratory settings. If movements are limited to purely horizontal eye saccades, the motor periphery is

limited to two pairs of muscles only; the lateral recti, which rotate the ipsilateral eye temporally and the medial recti, which rotate the contralateral eye nasally. The neural control of saccadic eye movements then describes the flow of neural information that transforms the sensory encoding of target location into motor commands issued by neurons that innervate the two muscle pairs.

The location of the spatial target is initially encoded as a retinal error (i.e. the distance between the fovea and the location on the retina of photoreceptors responsive to the visual target) in the visual cortex and the frontal eye fields on spatial retinotopic maps. These cortical areas then convey this information to the superior colliculus (SC) in the optic tectum of the midbrain. The SC is a layered structure of topographically organized maps of the visual space. A dorso-ventral relay of sensory visual information encoded on the superficial layers is eventually converted into motor responses encoding the desired eye displacement in the deeper layers. This desired eye displacement signal is then provided by the SC to the brainstem saccade generator where the kinematics of horizontal eye saccades are dictated by the temporal spiking rates of specialized subgroups of pre-motor and motor neurons (Figure 1.2).

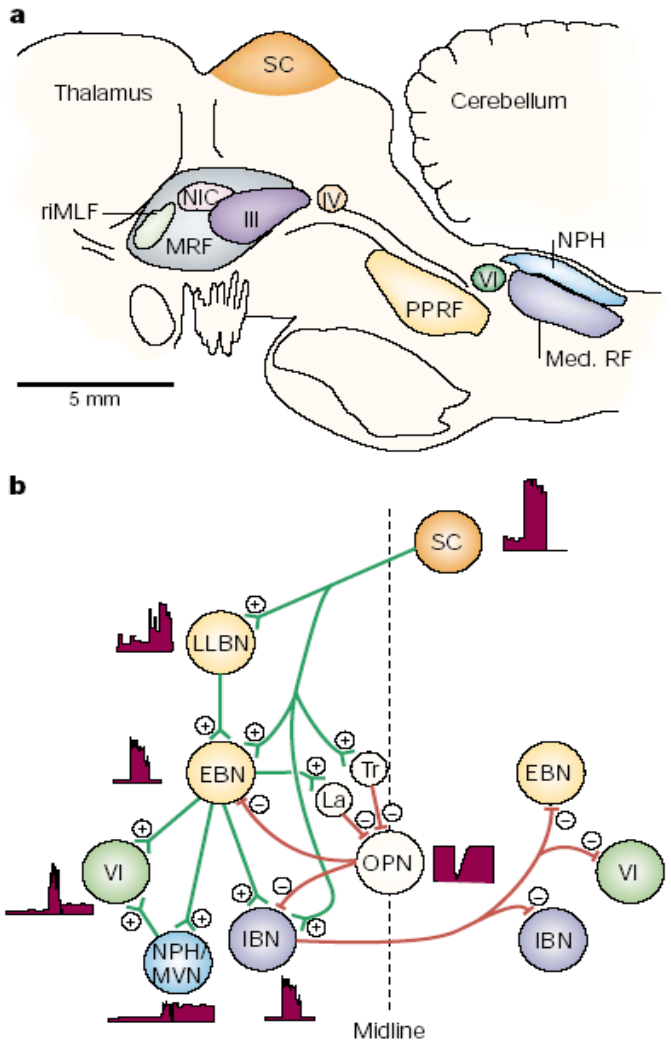


**Figure 1.2: the brainstem eye saccade controler; relevant regions (a) and functional network (b) (from Sparks, 2002).**

Medium and short lead excitatory burst neurons (EBN) in the paramedian pontine reticular formation (PPRF) embody the saccadic pulse generator acting inside a local feedback circuit (van Gisbergen et al., 1981). The local feedback tailors

the pulse command of EBNs so that the retinal error is reduced to zero. This pulse of spikes excites motor neurons in the abducens nucleus whose axons give rise to the sixth cranial nerve which innervate the lateral rectus muscle of the ipsilateral eye. The pulse is simultaneously integrated by the so called “neural integrator” in the nucleus prepositus hypoglossi (NPH) into a step command which is added to the pulse in the abducens nucleus to produce the typical pulse-step discharge patterns of these neurons (Robinson, 1970). The phasic burst of spikes accelerates the eyes during the saccadic component of movement against the viscous forces acting on the eye globe, and the tonic discharge holds the eyes fixed at the peripheral position by counteracting the elastic forces that pull the eye back towards midline. A second class of inter-neurons in the abducens nucleus exhibits the same discharge patterns and hence provides an identical command to a subgroup of motor units in the oculomotor nucleus which directly innervate the medial rectus muscle of the contralateral eye. Moreover, EBNs also excite their inhibitory counterparts (IBNs) in the medullary reticular formation (MRF), which in turn inhibit the EBNs, IBNs and abducens neurons on the other side of the brainstem in order to prevent contraversive ocular rotation. The overall result is a horizontal ipsiversive binocular eye movement to the visual target.

As is the case with all motor systems, the cerebellum (i.e. oculomotor vermis) is functionally connected with the neural circuit controlling eye saccades. It receives extensive information about eye movements from all key cortical and subcortical areas (Thielert and Thier, 1993), whereas the output projections are more limited. Output from the oculomotor cerebellum relevant for horizontal saccades targets mainly the EBNs, IBNs and the SC (May et al., 1990; Noda et al., 1990).

# Chapter 2:

## The cerebellum compensates for cognitive disturbances of movement

*The work summarized in this chapter is based on the following manuscript:*

Mario Prsa, Peter W. Dicke and Peter Thier. The absence of eye muscle fatigue indicates that the nervous system compensates for non-motor disturbances of oculomotor function. *Journal of Neuroscience,* 30:15834-15842, 2010.

As described in the previous chapter, motor adaptation refers to the ability of the central nervous system to adjust motor commands whenever the dynamics of the body or the external environment are modified. This ability is shown to be cerebellum-dependent and is most often investigated by visual perturbations or artificial modifications of peripheral dynamics. In the present work we trained monkeys to perform a fatiguing eye saccade task which brings about significant changes in eye saccade kinematics which, if left uncompensated, lead to hypometric movements (Figure 2.1). Lesions of the oculomotor vermis in monkeys (Barash et al., 1998) and studies of cerebellar patients (Golla et al., 2008; Xu-Wilson et al., 2009) confirm that the cerebellum plays the key role in this particular case of motor adaptation as well. The conventional view of motor adaptation posits that the cerebellum compensates for a progressive weakening of eye muscles during the fatigue task in order to maintain accurate saccades. We tested this hypothesis by recording motor-neuronal activity from the abducens nucleus before, after and during the fatigue task.

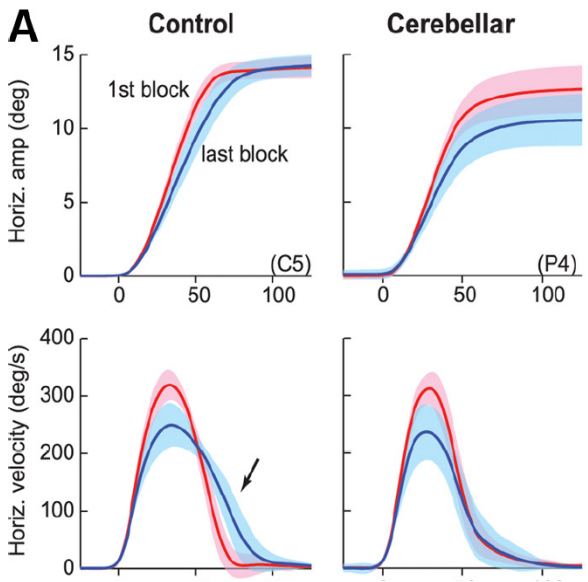


**Figure 2.1: comparison of eye position (top) and velocity (bottom) traces between healthy subjects and cerebellar patients pre (red) and post (blue) fatigue (from Xu-Wilson et al., 2009).**

As desribed in the previous chapter, motor neurons in the abducens nucleus directly innervate the lateral recti muscles of the eye and their temporal discharge thus constitutes the motor command for horizontal ocular rotations. Their typical pulse-step firing pattern during saccades reflects the dynamic properties of the "eye plant" (production of muscle force and the action of that force on the surrounding orbital tissues) that need to be overcome to produce the desired ocular rotation. A simultaneous recording of the motor command in the abducens nucleus (the input to the eye plant) and of the resulting instantaneous eye position during the saccade (the output of the eye plant) allows one to identify the dynamic properties of the oculomotor periphery. By resorting to system identification techniques, we have in this manner computed a parametric description of eye plant's physical dynamics just prior and immediately after the fatigue task. We have moreover monitored how well the plant parameters identified pre-fatigue could predict the firing rate of the abducens motoneurons during the course of the fatigue itself. If a weakening of eye muscles were responsible for the slower saccades that the cerebellum needs to compensate for, than this would necessarily be reflected by significantly different parameters describing the plant after the fatigue task. Moreover, during the course of fatigue, the identified dynamics would progressively underestimate the firing rates of motoneurons. Our results strikingly demonstrate that no such changes in eye plant dynamics occur as a result of fatigue. In simpler terms, the observed changes in saccade kinematics were always followed by parallel changes in the discharge rate of abducens neurons and therefore point to the absence of any muscular changes of the oculomotor periphery (Figure 2.2). This finding becomes pregnant with meaning when considering that the source of fatigued saccades must therefore be of non-motor (i.e. cognitive) origin and that the cerebellum compensates for this type of physiological changes as well.

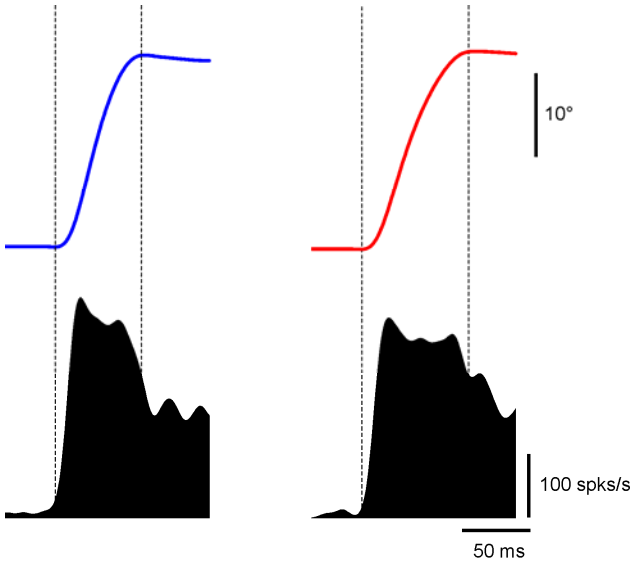


**Figure 2.2: slower and longer saccades after fatigue (red) were followed by parallel weaker and longer discharges of abducens units (bottom) as compared to before fatigue (blue).**

# Chapter 3:

## Adaptation driven plasticity in the cerebellar cortex first occurs at the level of Purkinje cells

*The work summarized in this chapter is based on the following publication:*

Mario Prsa, Suryadeep Dash, Nicolas Catz, Peter W. Dicke and Peter Thier. Characteristics of responses of Golgi cells and mossy fibers to eye saccades and saccadic adaptation recorded from the posterior vermis of the cerebellum. *Journal of Neuroscience*, 29(1):250-262, 2009.

In this work we trained monkeys to perform the classic saccadic adaptation task (Figure 3.1) and looked for any simultaneous signs of changes in the firing rates of cerebellar cortical neurons.

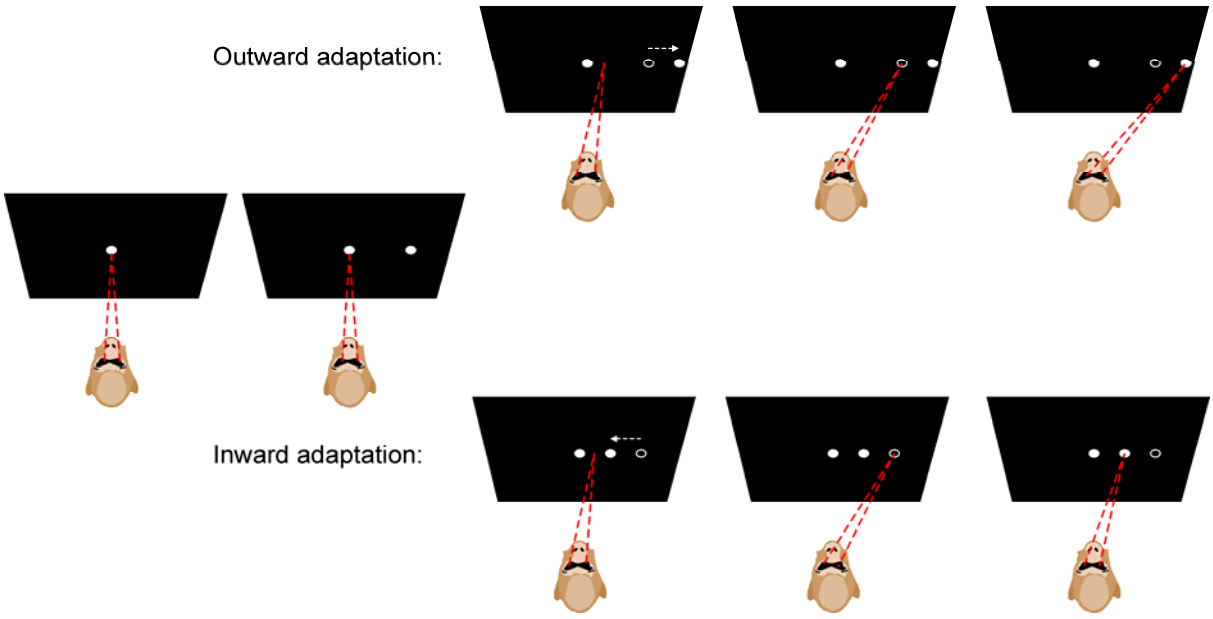


**Figure 3.1: in the saccadic adaptation paradigm monkeys are trained to adapt the amplitudes of their saccades to a non-perceived shift of the visual target.**

Previous studies revealed that both simple and complex spikes of individual Purkinje cells (PC) in the oculomotor vermis undergo significant changes in their firing patterns during the course of adaptation (Catz et al., 2005, 2008). Because they are the only neurons where the two inputs to the cerebellar cortex (mossy fibers and climbing fibers) converge, they have attracted an almost exclusive attention from

electrophysiological investigations, much to the detriment of other large-sized interneurons located in the neighboring layers. While the climbing fiber input to the PCs is direct, the mossy fibers first make synapses with granule cells which are modulated by other neuronal types in the granular layer before transmitting the relevant signals to the PCs. One such interneuron is the Golgi cell (GC); it receives both a direct and indirect excitation from the mossy fiber input and exhibits an exclusive inhibition of granule cells. It is then conceivable that the plastic changes observed in the firing patterns of PC simple spikes are a mere reflection of a prior processing of the mossy fiber input in the granular layer by interneurons such as the GCs or are perhaps even of pre-cerebellar origin.

To test this hypothesis we made an attempt to putatively identify GCs and record their spiking activity during the saccadic adaptation task. Our cellular identification was based on previously established correlations between cell morphology and physiological parameters (spike rates, inter-spike-interval regularity and length and shape of the action potential waveform) in juxtacellular labeling studies of cerebellar inter-neurons. Because this was the first ever recording of putative GCs from the oculomotor vermis, we additionally described several discharge properties of theses neurons relative to saccadic eye movements and speculated on the possible role they might play in the cerebellar processing of information. The same was also the case with mossy fibers, which were recorded simultaneously.

The saccade-related activity of individual mossy fibers was found to be highly specific for a particular direction of movement, whereas that of GCs did not show any strong directional preference. This result is consistent with the fact that individual GCs receive inputs from many mossy fibers, and their broad directional tuning therefore results from a compound of inputs, each tuned to a particular direction. The finding also indicates that individual GCs are well suited to provide inhibition of a large number of granule cells regardless of the saccade direction they prefer. Authors of early theoretical work on the cerebellum (Marr, 1969; Albus 1971; Ito, 1984) have postulated that GCs exhibit gain-control over the mossy fiber-granule cell-parallel fiber transmission to the PCs. According to this scheme, their role would be to limit the amount of mossy fiber excitation that is conveyed to PCs via their inhibitory action on granule cells. We have however found that the saccade-related activity of GCs is inconsistent with the traditional gain-control theory. The activity of

individual GCs as well as their population response was found to be highly unspecific to the timing, duration or amplitude of saccades. On the other hand, mossy fibers fired both more intensely and with longer bursts as saccade size and duration increased. This means that increased excitation of granule cells by mossy fibers is not accompanied by a proportionally larger inhibition from GCs and therefore contradicts the traditional role attributed to this inter-neuron.

The main aim of this study was however to investigate whether GCs exhibit any plastic changes analogous to those observed in PC simple spikes. We have therefore recorded the activity of many putative GCs while the monkeys adaptively both increased and decreased the amplitudes of their saccades. We consistently found that the discharge pattern of individual neurons (Figure 3.2) and also that of a GC population response failed to display any signs of plastic changes that could account for the adaptive behavior. If one then assumes that the firing properties of a major interneuron are reflective of the granular layer at large, one comes to the conclusion that neuronal adaptive changes only emerge at the level of PCs and are not reflective of previous adjustments of the mossy fiber input.

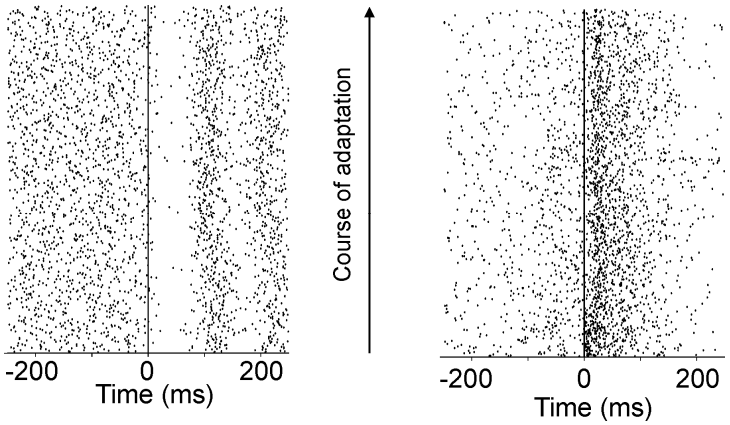


**Figure 3.2: examples of two Golgi cells that do not change their initial discharge patterns throughout the course of saccadic adaptation.**

# Chapter 4:

## The cerebellum adapts horizontal eye movements by its action on the PPRF pre-motor neurons

*The work summarized in this chapter is based on the following manuscript:*

Mario Prsa, Suryadeep Dash and Peter Thier. Adaptation of saccade amplitude is organized in Cartesian coordinates: evidence from behavioral studies of directional transfer of learning.

Cortical and brainstem structures implicated in the neural control of eye movements were described in the introductory chapter. A pertinent issue is to identify at what sites along these oculomotor pathways the cerebellum fine-tunes the system during adaptive behavior. As previously described, the cerebellum receives rich information about eye movements and its outputs target, amongst others, the SC, the EBNs in the PPRF and their inhibitory counterparts (IBNs) in the MRF.

In the present work, we used the saccadic adaptation paradigm (Figure 3.1) in both monkey and human subjects to explore this issue. The indirect method that we used to identify the neural site for saccadic adaptation was to determine whether the saccadic movement is adapted as a vector, or in its vertical and/or horizontal components. If the former is true, then “early” stages of neural processing, such as the SC, where desired saccade amplitude is still encoded as a vector on spatial topographic maps, is the most likely candidate. In contrast, the temporal spiking profile of EBNs and IBNs reflects mainly the kinematics of the horizontal component of saccades (Cromer and Waitzmann, 2007). Adaptive changes in the firing rates of these neurons, mediated by their cerebellar afferents, would thus translate in the adaptation of the horizontal component only.

Accordingly, the monkey and human subjects behaviorally adapted the amplitude of horizontally directed saccades and saccades to oblique targets, with identical horizontal components, were prompted during adaptation to investigate how the adjustment of horizontal amplitude transferred to these oblique directions. Results obtained from both primate species unequivocally revealed that only the horizontal component of oblique saccades was modified by the motor adaptation, whereas any influence on the vertical direction was negligible. Horizontal saccadic

eye movements are therefore most likely adapted via a cerebellar modulation of the temporal spiking rates of pre-motor neurons in the PPRF/MRF. In more general terms, during adaptation, the cerebellum seems to act on pre-motor structures that control the components making up a movement vector, rather than on structures that encode the vector itself.

# Chapter 5:

## Synopsis

In order to execute accurate movements, the neural system must produce motor commands that guide the muscular periphery along a desired trajectory. However, errors or deviations from the desired trajectory can occur and compromise accurate performance. As described in the introductory chapter, growing evidence shows that the cerebellum adapts the neural control of movement in order to counteract such errors. The three studies presented in this thesis collectively contribute in revealing important aspects of this cerebellum-dependent mechanism of motor adaptation (Figure 5.1).

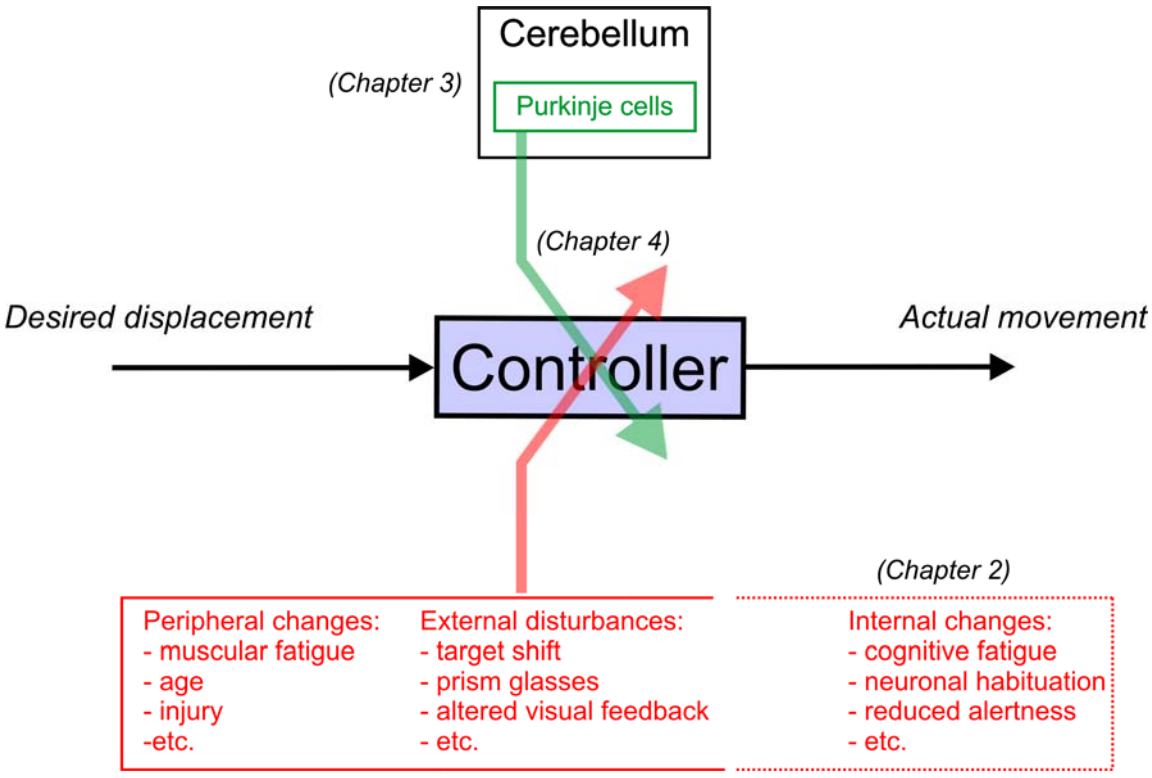


**Figure 5.1: a conceptual illustration of the cerebellum-dependent mechanism for motor adaptation. The transformation of the desired displacement into the actual movement can be corrupted by many different sources (in red) including cognitive factors (chapter 2). The cerebellum adjusts the controller (in green) by acting on segregated pre-motor structures (chapter 4) to counteract these disturbances by means of plastic changes that first occur at the level of Purkinje cells (chapter 3).**

Previous investigations of motor adaptation have been concerned with the ability of the cerebellum to adapt motor behavior when the dynamics of the muscular periphery or the external environment change. The study presented in chapter 2 indicates that the role of the cerebellum is actually more general than that. The cerebellum additionally takes into account and adapts to any disruptive processes that originate within the brain itself (neuronal fatigue, drowsiness etc.). A striking contrast then exists between the variety of potential sources of inaccuracy that the cerebellum has to compensate for and, as described in chapter 4, the specificity with which the cerebellum acts on pre-motor centers in the brainstem to “repair” the motor commands. It follows that the cerebellum does not actively discriminate between the different potential sources of inaccuracy in order to adapt to each independently. Instead, the cerebellum uses the same dependable mechanism to compensate for all sources of error, regardless of their origin. The only necessary information that therefore needs to be conveyed to the cerebellum is that an error in movement is about to be made and that the cerebellar output needs to be adjusted accordingly. As demonstrated in chapter 3, the site where these error-correcting changes first take place is at the level of Purkinje cells.

# References


Albus, J.S. (1971). A theory of cerebellar function. *Math Biosci*, 10:25–61.

Barash, S., Melikyan, A., Sivakov, A., Zhang, M., Glickstein, M., and Thier, P. (1999). Saccadic dysmetria and adaptation after lesions of the cerebellar cortex. *J Neurosci*, 19(24):10931–10939.

Catz, N., Dicke, P. W., and Thier, P. (2005). Cerebellar complex spike firing is suitable to induce as well as to stabilize motor learning. *Curr Biol*, 15(24):2179–2189.

Catz, N., Dicke, P. W., and Thier, P. (2008). Cerebellar-dependent motor learning is based on pruning a purkinje cell population response. *Proc Natl Acad Sci U S A*, 105(20):7309–7314.

Cromer, J. A. and Waitzman, D. M. (2007). Comparison of saccade-associated neuronal activity in the primate central mesencephalic and paramedian pontine reticular formations. *J Neurophysiol*, 98(2):835–850.

Gisbergen, J. A. V., Robinson, D. A., and Gielen, S. (1981). A quantitative analysis of generation of saccadic eye movements by burst neurons. *J Neurophysiol*, 45(3):417–442.

Golla, H., Tziridis, K., Haarmeier, T., Catz, N., Barash, S., and Thier, P. (2008). Reduced saccadic resilience and impaired saccadic adaptation due to cerebellar disease. *Eur J Neurosci*, 27(1):132–144.

Ilg, W., Giese, M. A., Gizewski, E. R., Schoch, B., and Timmann, D. (2008). The influence of focal cerebellar lesions on the control and adaptation of gait. *Brain*, 131(Pt 11):2913–2927.

Ito, M. (1984). The cerebellum and neural control. New York: Raven Press.

Konczak, J., Schoch, B., Dimitrova, A., Gizewski, E., and Timmann, D. (2005). Functional recovery of children and adolescents after cerebellar tumour resection. *Brain*, 128(Pt 6):1428–1441.

Marr, D. (1969) A theory of cerebellar cortex. *J Physiol* 202:437–470.

Martin, T. A., Keating, J. G., Goodkin, H. P., Bastian, A. J., and Thach, W. T. (1996). Throwing while looking through prisms. i. focal olivocerebellar lesions impair adaptation. *Brain*, 119 ( Pt 4):1183–1198.

May, P. J., Hartwich-Young, R., Nelson, J., Sparks, D. L., and Porter, J. D. (1990). Cerebellotectal pathways in the macaque: implications for collicular generation of saccades. *Neuroscience*, 36(2):305–324.

Morton, S. M. and Bastian, A. J. (2006). Cerebellar contributions to locomotor adaptations during splitbelt treadmill walking. *J Neurosci*, 26(36):9107–9116.

Noda, H., Sugita, S., and Ikeda, Y. (1990). Afferent and efferent connections of the oculomotor region of the fastigial nucleus in the macaque monkey. *J Comp Neurol*, 302(2):330–348.

Optican, L. M. and Robinson, D. A. (1980). Cerebellar-dependent adaptive control of primate saccadic system. *J Neurophysiol*, 44(6):1058–1076.

Rambold, H., Churchland, A., Selig, Y., Jasmin, L., and Lisberger, S. G. (2002). Partial ablations of the flocculus and ventral paraflocculus in monkeys cause linked deficits in smooth pursuit eye movements and adaptive modification of the vor. *J Neurophysiol*, 87(2):912–924.

Robinson, D. A. (1970). Oculomotor unit behavior in the monkey. *J Neurophysiol*, 33(3):393–403.

Thielert, C. D. and Thier, P. (1993). Patterns of projections from the pontine nuclei and the nucleus reticularis tegmenti pontis to the posterior vermis in the rhesus monkey: a study using retrograde tracers. *J Comp Neurol*, 337(1):113–126.

Tseng, Y.-W., Diedrichsen, J., Krakauer, J. W., Shadmehr, R., and Bastian, A. J. (2007). Sensory prediction errors drive cerebellum-dependent adaptation of reaching. *J Neurophysiol*, 98(1):54–62.

Xu-Wilson, M., Chen-Harris, H., Zee, D. S., and Shadmehr, R. (2009). Cerebellar contributions to adaptive control of saccades in humans. *J Neurosci*, 29(41):12930–12939.

# Publications

## Adaptation of saccade amplitude is organized in Cartesian coordinates: evidence from behavioral studies of directional transfer of learning

Mario Prsa, Suryadeep Dash, Peter Their
Department of Cognitive Neurology, Hertie Institute for Clinical Brain Research, University of Tübingen, Tübingen, Germany

**The adaptation of saccadic eye movement amplitude has undoubtedly been the most useful model for investigating neuronal plasticity during short-term motor learning. Although converging evidence suggests that the site of plasticity are the Purkinje cells in the cerebellar cortex, determining what extra-cerebellar structures this signal influences to influence the learned behavior has been controversial. To address this issue, we conducted identical experiments in monkey and human subjects where the amplitude of horizontally directed saccades was adaptively decreased and investigated how these changes transferred to the metrics of oblique saccades. Our results reveal that, in both primate species, adaptation transferred only to the horizontal component of oblique saccades, whereas any changes in the vertical direction were negligible. This finding is compatible with the notion that during adaptation, the cerebellum acts on spatially segregated pre-motor structures for the horizontal and vertical components of saccades.**

### Introduction

The ability of our central nervous system to learn new motor skills or adapt to continual physiological changes is quite impressive. Eye movement control offers many advantages as a model to study the neuronal underpinnings of motor learning. It is possibly the most thoroughly studied and understood example of biological motor control. Eye movements can

easily and accurately be measured in experimental settings and a simple visual paradigm can be used to study the adaptive behavior of saccadic eye movements (McLaughlin 1967). The latter consists of having a subject execute an eye saccade from an initial fixation point towards a peripheral target. Following the initiation of the saccade, the target is displaced to a different eccentricity, which is not perceived by the moving eyes of the subject due to the suppression of visual feedback. The eyes therefore land at the original target location and a mismatch between the actual (visual) and predicted (efference copy) sensory information ensues. This mismatch signals to the nervous system that an error has been made, which then progressively updates motor commands and corrects this inaccuracy by adjusting the amplitude of saccades toward the "correct" target over many consecutive trial repetitions (Figure 1).

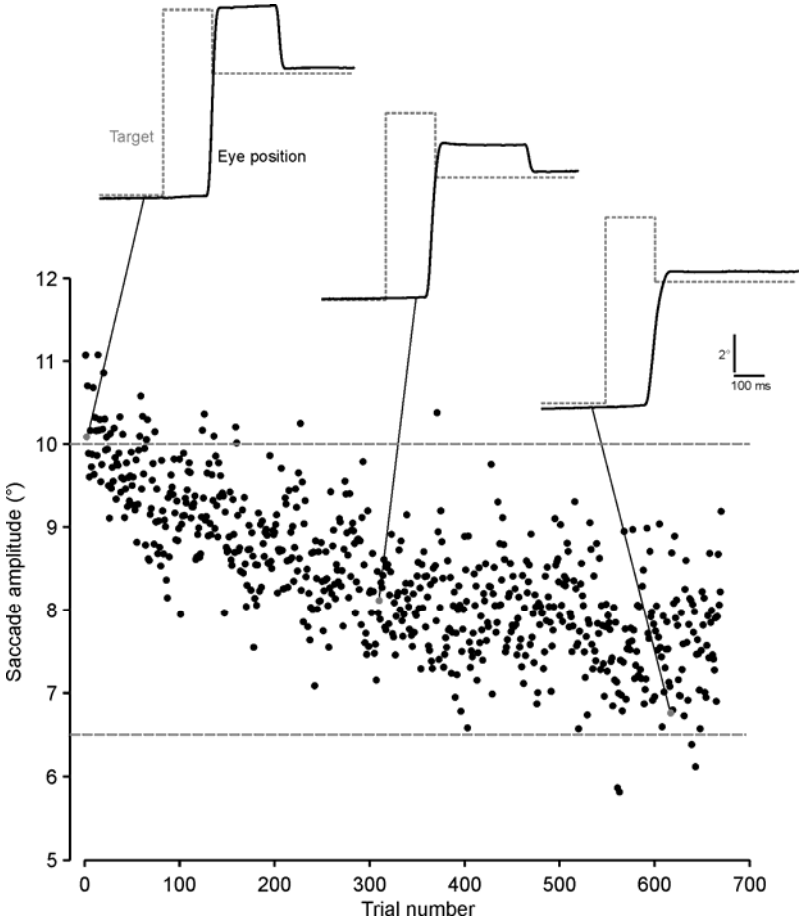


Figure 1. Typical changes in saccade amplitude during an adaptation paradigm where the visual target is displaced from a 10° to a 6.5° horizontal eccentricity shortly after the onset of the saccadic eye movement. Insets show horizontal eye position and target traces at three different instances during the course of adaptation.

Surgical lesions in monkeys (Barash et al. 1999; Takagi et al. 2000) and human patient studies (Golla et al. 2008) reveal that the integrity of the posterior vermis of the

cerebellum is necessary for saccadic adaptation to occur. Changes in the properties of the population signal of simple spikes recorded from Purkinje cells (PC) in this area have been found to give a perfect account for the adaptive changes in saccade amplitude (Catz et al. 2008). Moreover, the target neurons of Purkinje cells in the caudal fastigial nucleus (cFN) also exhibit adaptation-related changes in their firing properties (Inaba et al. 2003; Scudder and McGee 2003) whereas Golgi cells, the large-sized interneurons that inhibit granule cells in the cerebellum immediately upstream of the PCs, do not (Prsa et al. 2009). The site of plasticity seems therefore to be firmly established at the level of PCs in the cerebellar cortex. This adaptive signal is first conveyed to the saccade representation in the cFN, which in turn contacts the many brainstem centers for saccades (May et al. 1990; Noda et al. 1990). A cerebellar modulation of many of these centers could in principle bring about the changes in saccade amplitude during adaptation. However, the cFN output primarily targets brainstem nuclei with direct projections to horizontal and vertical extra-ocular motor nuclei, namely the paramedian pontine reticular formation (PPRF), the dorsomedial reticular formation (DMRF) and the rostral interstitial nucleus of the medial longitudinal fasciculus (riMLF) (Noda et al. 1990). The PPRF and DMRF harbor respectively the excitatory and inhibitory premotor neurons (EBN/IBN) whose temporal spiking profile reflects mainly the kinematics of the horizontal component of saccades (Cromer and Waitzman 2007), while the riMLF contains premotor neurons which directly activate the vertical extra-ocular motoneurons (Buttner et al. 1977). A much smaller portion of cFN fibers terminate at even “earlier” sites of oculomotor processing, such as the superior colliculus (SC) and the nucleus reticularis tegmentis pontis (NRTP) (May et al. 1990; Noda et al. 1990), where desired saccade amplitudes are still encoded as vectors by neurons with retinotopically organized movement fields (Sparks et al. 1976; Crandall and Keller 1985).

An indirect method that can be used to explore which of these two distinct pathways is most likely to be involved in saccade adaptation is to determine whether the saccadic movement is adapted as a vector, or in its vertical and/or horizontal components. To this end, one can adapt the amplitude of purely horizontal saccades and observe how this adaptation is transferred to the components of oblique non-adapted saccades. Adaptive changes in the firing rates of neurons in the PPRF and DMRF, mediated by their cerebellar afferents, would translate in a modification of only the horizontal component, whereas a modulation of SC or NRTP neurons would have an effect on the amplitude of the vector representation, without directional changes, of the oblique saccades. Previous such investigations (Deubel 1987; Kojima et al. 2005; Hopp and Fuchs 2006) have claimed or at least implied that their results

indicate that saccade adaptation does not occur at the level of horizontal and vertical representations of saccade components in premotor structures. Such a conclusion is vexingly in discord with the above described anatomy because it renders the cerebello-reticular pathway, the most prominent and straightforward path for the cerebellum to influence eye movements, unexploited for the purposes of saccade adaptation.

In light of this predicament and also of some contradictory results obtained by recent investigations addressing this issue in human (Hopp and Fuchs 2006) and monkey (Kojima et al. 2005) subjects, we conducted identical experiments in both primate species which indicate that adaptation of horizontal eye saccade amplitude indeed occurs mainly at neural stages where the desired movement vector is decomposed in its components. We subsequently discuss the shortcomings and offer a reinterpretation of the seemingly contradictory data of previous studies.

## Methods

### *Animals*

Two rhesus monkeys (*Macaca mulatta*) were surgically prepared for head-fixed eye movement recording using the scleral search coil technique as described previously (Prsa et al. 2009). All procedures followed the guidelines set by the National Institutes of Health and national law and were approved by the local committee supervising the handling of experimental animals. The monkeys sat head-fixed in a primate chair in complete darkness and stimuli were presented on a monitor positioned 45 cm in front of them. A liquid reward was delivered for each successfully completed eye saccade trial. The eye movement records were digitally sampled at 1 kHz and all further analysis was carried offline.

### *Human subjects*

Six adult human subjects (2 female and 4 male, ages 25-30) participated in the experiments. One was one of the authors (M.P.) and all others were naïve with respect to the goals of the investigation. The subjects sat in quasi-total darkness and eye position was recorded at 400 Hz by means of an infra-red eye tracker system (Chronos Vision, Berlin, Germany). Stimuli were displayed by a video projector on a large screen positioned 150 cm in front of the subjects. Head movement was restrained in one subject by means of a dental bite bar. In the

others an elastic band firmly attached to the fixed frame of the eye tracking apparatus turned out to be sufficient.

*Experimental paradigms and data analysis*

In pre-adaptation trials, the subjects were instructed to execute saccadic eye movements from a central fixation point towards a peripheral target in any of four randomly selected locations (10° and 0°, 10° and 6.5°, 10° and 10°, 0° and 10° horizontal and vertical eccentricities, respectively).During adaptation sessions, the amplitude of saccades to the horizontal target (10°, 0°) were adaptively decreased by prompting a velocity dependent displacement of the target to a less eccentric horizontal position (between 6° and 7°). Adaptation sessions lasted between 500 and 1000 trials for the monkeys, and between 200 and 400 trials in the case of human subjects. In 30% of cases, trials to any of the remaining three targets (two oblique and one vertical) were randomly interleaved during the course of adaptation. We preferred to test the transfer of adaptation in this way rather than in post-adaptation test blocks in order to avoid any effects of recovery from adaptation. Correct trials were indicated by an acoustic sound (and a liquid reward for monkeys) and required that eye position be maintained inside a window around the visual target for at least 400 ms both before and after the saccadic eye displacement.

The horizontal and vertical eye positions were smoothed with a Savitzky-Golay filter (window = 10 points, polynomial degree = 4), which replaces the data points in the specified window by a polynomial regression fit of the chosen degree. With a window of 10 points and a fourth degree polynomial, the eye position data are low-pass filtered with a bandwidth of ~100 Hz, which is appropriate for frequencies of natural eye movements (20-30 Hz). Two-dimensional velocity vectors were computed by taking digital derivatives and we used the 20°/s velocity criterion for detecting saccade start and end. Horizontal and vertical components of each movement were then evaluated between those two time stamps. In all cases, the last ten trials of the adaptation session for each target direction were compared to the saccades executed to the same target during the pre-adaptation trials. Student's t-tests were used to evaluate whether data samples come from same distributions with equal means and normality of data was tested with the Kolmogorov-Smirnov test. All analyses and statistical testing were performed with custom programs in Matlab (MathWorks).

## Results

We had both monkeys and humans perform an identical saccade adaptation experiment. The subjects had to adaptively decrease the amplitude of their saccades, according to the McLaughlin (1967) paradigm, executed toward a target located at 10° horizontal and 0° vertical eccentricity. During the course of this adaptation, additional saccades were randomly prompted towards targets in three other directions; two oblique (located at 10° horizontally and 6.5° and 10° vertically) and one purely vertical direction (0° horizontal and 10° vertical). The latter was used to monitor any idiosyncratic changes, while the other two to reveal if and how the adaptation of horizontal eye movement amplitude is transferred to oblique saccades with equal horizontal components. We compared the vertical and horizontal components of each saccadic eye movement at the end of the adaptation sessions to those executed towards the same targets in pre-adaptation trials (see Methods for details).

### *Monkey data*

Two rhesus monkeys (S and E) completed seven adaptation sessions each, preceded by the pre-adaptation trials. The horizontally adapted saccades showed a significant decrease of their mean horizontal components in both cases (mean change ± s.d.: -1.94° ± 0.38 (-20%) for monkey S and -2.11 ± 0.38 (-22%) for monkey E). Even though the targets were purely horizontal, the executed saccades were slightly oblique and minor reductions in the vertical component means (mean change ± s.d.: -0.17° ± 0.14 for monkey S and -0.24 ± 0.36 for monkey E) were therefore also observed (Figure 2b). As can be deduced from the depictions of saccade end-points for two exemplary pre- and post-adaptation periods (Figure 2a), the transfer of adaptation to obliquely directed saccades reduced mainly their horizontal amplitudes. The significant increases in the mean slopes (ratio of vertical to horizontal component) of oblique saccades during adaptation demonstrates that the reduction of saccade amplitude was dominated by a decrease in the size of horizontal components, despite the significant changes of the vertical component means that occurred in some cases (Figure 2b). Had the two components changed by the same multiplicative factor, as would be the case of a change in amplitude along the direction of the saccade vector, the mean slopes would have remained unchanged.

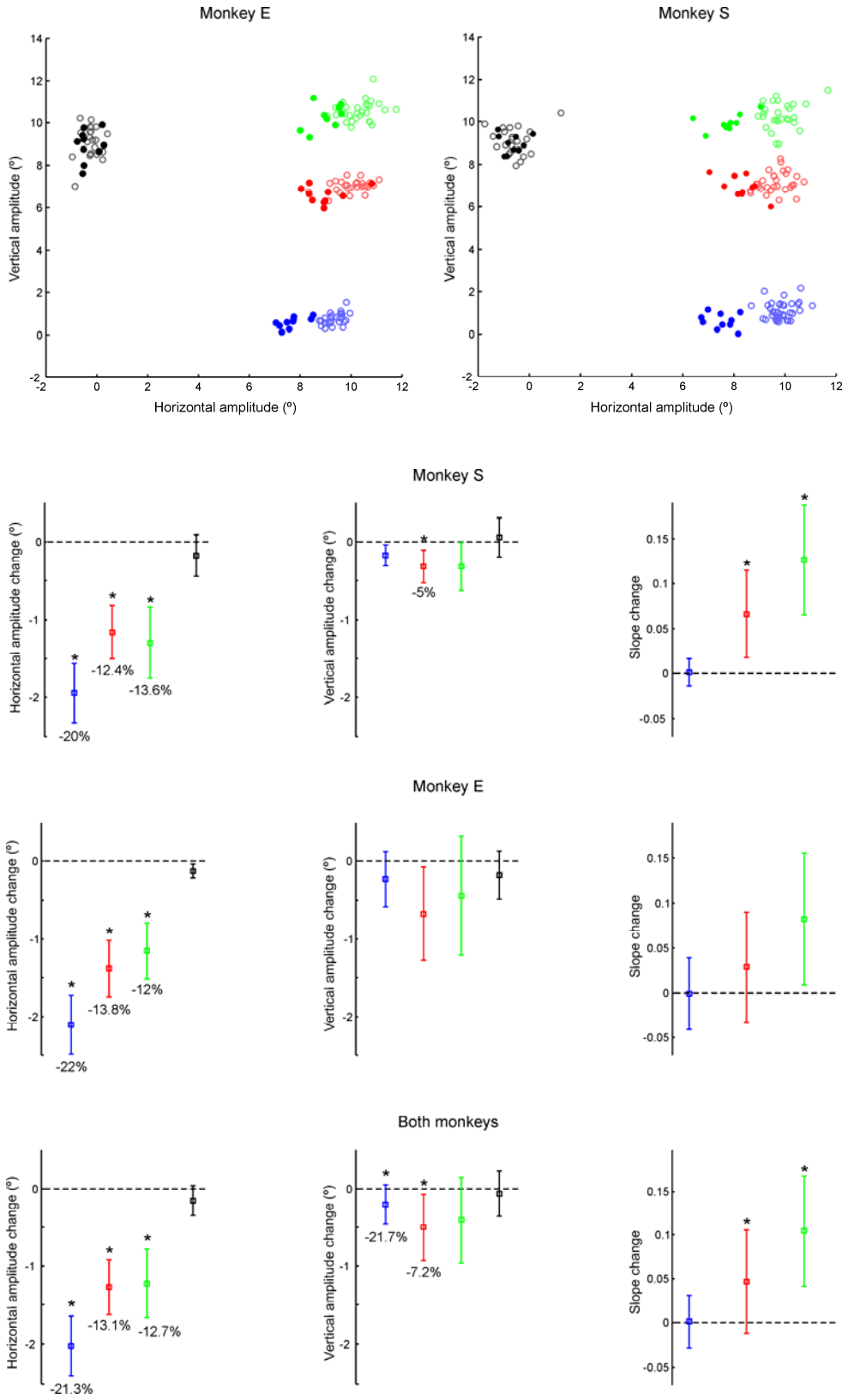


Figure 2. Comparison of pre- and post-adaptation amplitudes of the horizontal and vertical components of saccades in monkeys. A, Pre- (open circles) and post-adaptation (filled circles) saccade end-points executed towards the horizontal (blue), the two oblique (red and green) and vertical (black) targets for one example session completed by each monkey. B, average (± SD) changes across all sessions in the horizontal and vertical

amplitudes of saccades and their respective slopes (ratio of vertical to horizontal component) for each direction (color code as in A) as a result of adapting the amplitudes of the horizontally directed saccadic eye movements. *: the null hypothesis that the mean values are equal to zero cannot be rejected at a significant level (Student's t-tests, $p<0.05$, Bonferroni correction).

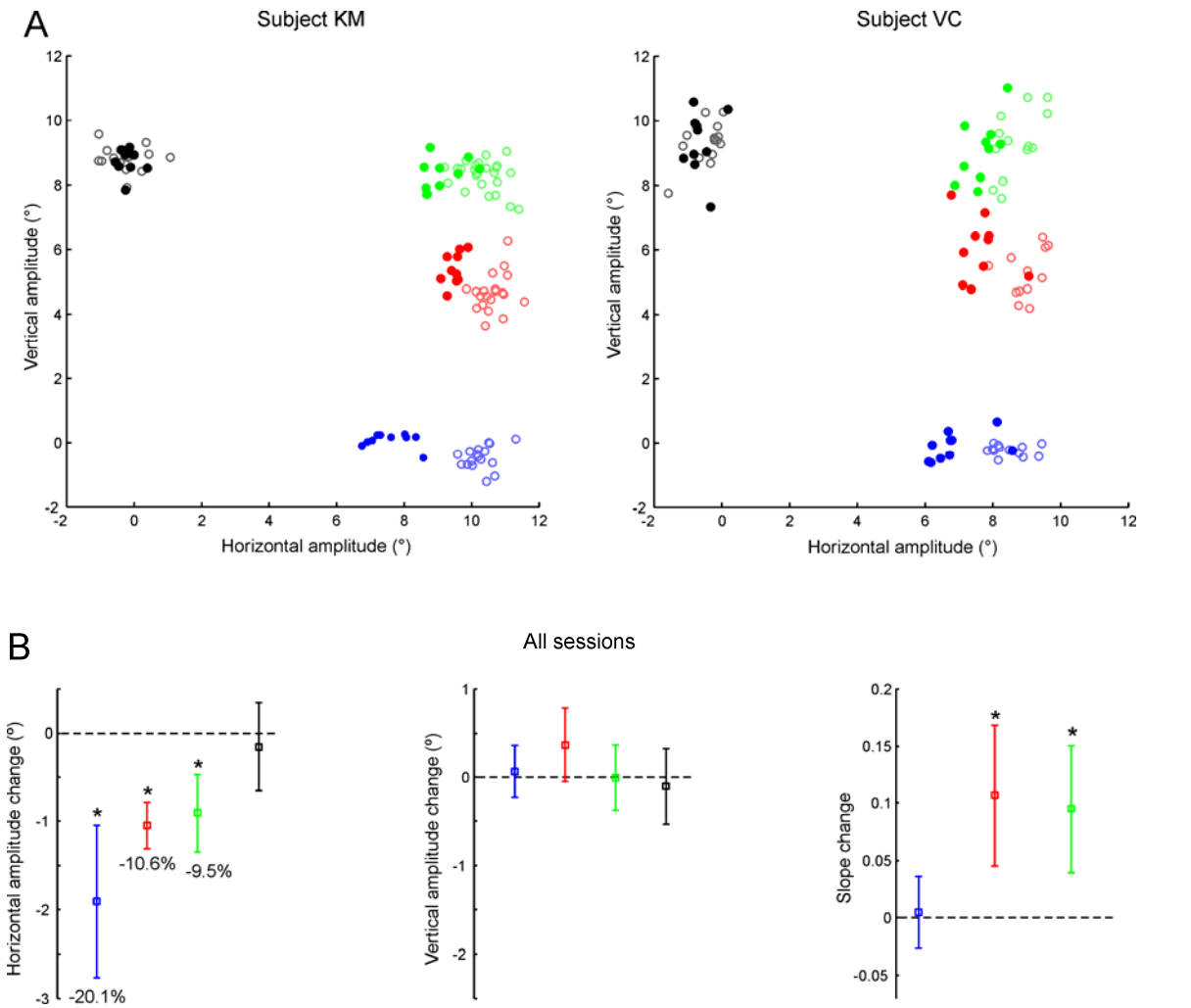


Figure 3. Comparison of pre- and post-adaptation amplitudes of the horizontal and vertical components of saccades in human subjects. A-B, examples for two subjects and average changes across all sessions for data analogous to that shown in Figure 2.

The reduction in the horizontal component of adapted saccades (mean change ± s.d.: -2.03° ± 0.38 (-21.3%) for all 14 sessions) was however only partially transferred to the two oblique directions (mean change ± s.d.: -1.27° ± 0.34 (-13.1%) for the (10°; 6.5°) direction and -1.24 ± 0.42 (-12.7%) for the (10°; 10°) direction); the amounts of decrease were statistically smaller for both directions (paired t-test: $p<10^{-4}$, uncorrected) when compared to the horizontal one. Changes in saccade end points in the purely vertical direction during adaptation were never statistically significant. This affirms that changes of the horizontal saccade component do not transfer to the vertical. Moreover, it also emphasizes that in our experiments, the metric of the vertical component was not subject to unspecific, non-adaptation related influences that might have distorted the analysis of the adaptation transfer onto oblique saccades.

*Human data*

A total of eight adaptation sessions were completed by six human subjects. Unlike the highly trained monkeys, for most subjects this was their first participation in an experimental oculomotor task, which, in comparison, translated into more imprecise saccades and increased inter-subject variability. Nonetheless, the average performance closely matched the monkey data; the mean amplitude changes in the horizontally adapted saccades, computed across all sessions, provoked in the obliquely directed saccades a significant decrease of the mean horizontal components only (Figure 3b).

In spite of the inter-subject variability and rare manifestations of idiosyncratic behavior, all subjects consistently showed a tendency to maintain constant (or in a few cases even increase) the vertical and reduce the horizontal amplitude of oblique saccades during adaptation (Table 1). This is exemplified by a comparison of pre- and post-adaptation saccade end-points of two subjects (Figure 3a) and a significant increase in the slopes of oblique saccades (Figure 3b). As with monkey subjects, the mean decrease in the oblique saccade horizontal components (mean change ± s.d.: -1.05° ± 0.26 (-10.6%) for the (10°; 6.5°) direction and -0.91 ± 0.26 (-9.5%) for the (10°; 10°) direction) was smaller (paired t-test: $p<0.04$, uncorrected) than that of the horizontally adapted saccades (mean change ± s.d.: -1.91° ± 0.86 (-20.1%)).

| *Subject* | *Target coordinates (x, y)* | *Mean horizontal amplitude change* | | *Mean vertical amplitude change* | | *Mean slope change* |
|---|---|---|---|---|---|---|
| MJ (session 1) | (10,0) | **-1.94** | | **-0.41** | | **-0.04** |
| | (10,6.5) | **-0.64** | | 0.42 | | **0.08** |
| | (10,10) | -0.35 | | 0.04 | | 0.04 |
| | (0,10) | 0.20 | | 0.05 | | |
| MJ (session 2) | (10,0) | -0.61 | | -0.08 | | -0.01 |
| | (10,6.5) | **-1.30** | | 0.25 | | **0.11** |
| | (10,10) | **-1.28** | | 0.00 | | **0.13** |
| | (0,10) | -0.24 | | -0.24 | | |
| MP (session 1) | (10,0) | **-2.09** | | -0.16 | | -0.03 |
| | (10,6.5) | **-1.13** | | -0.41 | | 0.02 |
| | (10,10) | -0.10 | | 0.23 | | 0.03 |
| | (0,10) | **0.44** | | -0.49 | | |
| MP (session 2) | (10,0) | **-2.61** | | 0.28 | | 0.03 |
| | (10,6.5) | **-0.74** | | 0.23 | | **0.06** |
| | (10,10) | **-0.99** | | -0.18 | | 0.08 |
| | (0,10) | -0.11 | | -0.45 | | |
| LK | (10,0) | **-0.81** | | -0.06 | | 0.00 |
| | (10,6.5) | **-0.94** | | 0.10 | | 0.07 |
| | (10,10) | **-1.12** | | -0.63 | | 0.05 |
| | (0,10) | -0.17 | | -0.43 | | |
| AA | (10,0) | **-2.93** | | 0.27 | | 0.02 |
| | (10,6.5) | **-1.16** | | **0.81** | | **0.17** |
| | (10,10) | **-1.19** | | 0.67 | | **0.20** |
| | (0,10) | **-1.26** | | **0.83** | | |
| KM | (10,0) | **-2.68** | | **0.54** | | **0.06** |
| | (10,6.5) | **-1.14** | | **0.73** | | **0.13** |
| | (10,10) | **-1.22** | | 0.04 | | **0.11** |
| | (0,10) | 0.09 | | -0.13 | | |
| VC | (10,0) | **-1.62** | | 0.11 | | 0.01 |
| | (10,6.5) | **-1.37** | | 0.78 | | **0.21** |
| | (10,10) | **-1.03** | | -0.23 | | **0.11** |
| | (0,10) | -0.19 | | 0.01 | | |

Table 1. Adaptation-related average changes in humans of horizontal and vertical amplitudes, and saccade slopes (ratio of vertical to horizontal component) in all four directions for each individual subject. Significant changes (Student's t-test, $p<0.05$, Bonferroni correction) are indicated in bold.

## Discussion

Our results clearly demonstrate that after the amplitude of horizontal saccades is adaptively decreased, oblique saccades towards targets in the same visual hemifield exhibit a significant reduction in their horizontal components while any influence on their vertical extension is negligible. Previous similar experiments in monkeys conducted by Kojima et al. (2005) reached the same conclusion, whereas Noto et al. (1999) and Wallman and Fuchs (1998) also found significant decreases of horizontal components of oblique saccades but unfortunately did not report any information about the vertical direction. Similarly, Deubel (1987) conducted the same experiments also in human subjects but only investigated amplitude changes in the radial direction without analyzing the effects of adaptation on the individual x- and y-components. Therefore, even though the same experiments have already been carried out by previous investigators, our study is the first one to statistically evaluate the amount of adaptation transfer from the horizontal direction to *both* horizontal and vertical components of oblique saccades in an identical paradigm in *both* primate species.

Identical results obtained from monkey and human subjects indicate that saccadic adaptation addresses the components making up a saccade vector and not the vector itself and therefore, during the adaptation of horizontally directed saccades, movement amplitude is being adjusted by a cerebellar modulation of excitatory and inhibitory burst neurons (EBN/IBN) in the PPRF and DMRF respectively. A correction of their temporal spiking rate seems indeed metabolically less demanding than a reorganization of specific regions on topographic spatial maps in the SC or NRTP, where movement fields of individual neurons need to be modified. However, the same results obtained by Kojima et al. (2005) merited a very different explanation, namely the one proposed by Deubel (1987) which states that the *direction of change* in adapted saccades is transferred to saccades in the tested non-adapted directions. In other words, only the horizontal component of oblique saccades is reduced in our data because this corresponds to the direction in which the amplitude of the horizontal saccades is adapted. Even though we agree that Deubel's interpretation can also account for the observed adaptation effects, we find it very unsettling because it assumes the existence of independent neural controllers, each specific for an individual movement direction. Not only is this assumption, to our knowledge, unsupported by any physiological evidence, it also seems like an extremely uneconomical strategy for the neural representation of movement. More importantly, in instances where oblique saccades were adapted and transfer to adjacent directions was tested, Deubel (1987) failed to provide any statistical analysis demonstrating

that the direction of induced changes in the tested directions was indeed not significantly different from the direction of amplitude change in the adapted saccades.

It is evident that the main reason why Deubel, as well as others (Hopp and Fuchs 2006), rejected that adaptation occurs where saccades are decomposed into independent x- and y-components, is the existence of adaptation fields. We showed that the transfer of horizontal saccade adaptation (~2° decrease) to oblique saccades with 6.5° and 10° vertical components is attenuated by ~50%, confirming previous observations that there is a Gaussian-like decay of adaptation effects (i.e. an adaptation field) with spatial distance (Deubel 1987; Frens and Van Opstal 1994; Wallman and Fuchs 1998; Noto et al. 1999). Adaptation fields, where the amount of adaptation reduces with spatial distance, do seem to be reflective of a topographic organization. In other words, in contrast to the notion of a component based adjustment of saccade amplitude accommodated by the lower brainstem machinery, the existence of adaptation fields may implicate changes in a structure with a clear two-dimensional topography like the SC. Actually, a spatial organization for saccades has also been proposed in models of the cerebellum (Lefevre et al. 1998; Quaia et al. 1999), but is unfortunately not borne out by any physiological finding. We think however that features of the saccade-related cerebellum may nevertheless be able to account for the existence of adaptation fields. Cerebellar signals for the control of saccades are based on a PC population signal, a direct consequence of the convergence of some hundred PCs on individual target neurons in the deep cerebellar nuclei (Palkovits et al. 1977; Thier et al. 2000). Catz et al. (2008) have recently demonstrated that saccadic adaptation is based on the precise adjustment of the duration of the saccade related PC population burst. Most of the members of the population have directional preferences and we may safely assume that all directions are represented (Ohtsuka and Noda 1995). Horizontal adaptation will change the duration of the burst fired by PCs preferring the horizontal, and these PCs will dominate the duration of the overall population response. Then, when oblique saccades are prompted, the more the saccade vector rotates away from the horizontal, the less the population signal will be influenced by the horizontal PCs and their information on saccade duration. The consequence will be a gain modulation of the adaptation effect set by the angular distance from the adaptation axis. Such a weighted cerebellar modulation of the brainstem pre-motor structures can fully account for the existence of adaptation fields, and moreover maintains that the dominant cerebello-reticular pathways are used for the adaptation of saccade amplitude instead of having to relay this role to anatomically and physiologically less relevant oculomotor sites.

In contradiction with the monkey data obtained by Kojima et al. (2005), Hopp and Fuchs (2006) claimed that in human subjects, adaptation of horizontal saccades did not transfer to oblique directions, which is why a considerable species difference was assumed. In one instance, their subjects adaptively decreased (by 0.64° on average) the amplitude of their saccades towards a horizontal target (at 4° eccentricity) and no transfer to oblique saccades made to a target at 4° horizontal and 15.5° vertical eccentricity was observed. We found that a 2° adaptive amplitude decrease in the horizontal direction does indeed transfer to oblique saccades also in humans, but was already attenuated by ~50% in saccades with 6.5° and 10° vertical components. The failure by Hopp and Fuchs (2006) to observe any significant transfer might therefore be due to a combination of both an insufficient amount of horizontal amplitude decrease and a relatively distant oblique target. Furthermore, in a second set of experiments, Hopp and Fuchs (2006) demonstrated that when subjects adaptively reduced the amplitude of oblique saccades, both the horizontal and vertical components of oblique saccades in the opposite visual hemifield significantly decreased in some cases. It seems that the movement vector of saccades is adapted in that case, because a lone adaptation of the horizontal component should not transfer to horizontal movements in the opposite direction, which are controlled by a completely distinct pair of muscles. Moreover, inconsistent with Deubel's model of adaptation transfer, the direction of change in tested saccades was clearly not the same as that in adapted saccades. Although the cerebellar projection to EBNs/IBNs that control the activity of horizontal muscle motoneurons is undoubtedly the dominant pathway, it cannot account for all the observations that occur during a directional transfer of saccadic adaptation. The vector based effects on oblique saccades could reflect cognitive strategies preferred by some humans but not others. This would also explain the variability between individual subjects as well as between experiments performed by the same subjects in different sessions (Hopp and Fuchs 2006). We therefore propose that the seeming discrepancies between previous findings (Kojima et al. 2005; Hopp and Fuchs 2006) are not attributable to a species difference; the directional transfer of cerebellum based learning is the same in both monkeys and humans, but humans additionally use a supra-cerebellar cognitive influence.

**References**


Barash S, Melikyan A, Sivakov A, Zhang M, Glickstein M, Thier P (1999) Saccadic dysmetria and adaptation after lesions of the cerebellar cortex. J Neurosci 19: 10931-10939

Buttner U, Buttnerennever JA, Henn V (1977) Vertical eye-movement related unit-activity in rostral mesencephalic reticular-formation of alert monkey. Brain Research 130: 239-252

Catz N, Dicke PW, Thier P (2008) Cerebellar-dependent motor learning is based on pruning a Purkinje cell population response. Proceedings of the National Academy of Sciences of the United States of America 105: 7309-7314

Crandall WF, Keller EL (1985) Visual and oculomotor signals in nucleus reticularis tegmenti pontis in alert monkey. Journal of Neurophysiology 54: 1326-1345

Cromer JA, Waitzman DM (2007) Comparison of saccade-associated neuronal activity in the primate central mesencephalic and paramedian pontine reticular formations. Journal of Neurophysiology 98: 835-850

Deubel H (1987) Adaptivity of gain and direction in oblique saccades. In: O'Regan JK, Levy-Schoen A (eds) Eye Movements from Physiology to Cognition. Elsevier, Amsterdam, pp 181-190

Frens MA, Van Opstal AJ (1994) Transfer of short-term adaptation in human saccadic eye-movements. Experimental Brain Research 100: 293-306

Golla H, Tziridis K, Haarmeier T, Catz N, Barash S, Thier P (2008) Reduced saccadic resilience and impaired saccadic adaptation due to cerebellar disease. Eur J Neurosci 27: 132-144

Hopp JJ, Fuchs AF (2006) Amplitude adaptation occurs where a saccade is represented as a vector and not as its components. Vision Research 46: 3121-3128

Inaba N, Iwamoto Y, Yoshida K (2003) Changes in cerebellar fastigial burst activity related to saccadic gain adaptation in the monkey. Neuroscience Research 46: 359-368

Kojima Y, Iwamoto Y, Yoshida K (2005) Effect of saccadic amplitude adaptation on subsequent adaptation of saccades in different directions. Neuroscience Research 53: 404-412

Lefevre P, Quaia C, Optican LM (1998) Distributed model of control of saccades by superior colliculus and cerebellum. Neural Networks 11: 1175-1190

May PJ, Hartwichyoung R, Nelson J, Sparks DL, Porter JD (1990) Cerebellotectal pathways in the macaque - implications for collicular generation of saccades. Neuroscience 36: 305-324

McLaughlin SC (1967) Parametric adjustment in saccadic eye movements. Perception & Psychophysics 2: 359-362

Noda H, Sugita S, Ikeda Y (1990) Afferent and efferent connections of the oculomotor region of the fastigial nucleus in the macaque monkey. Journal of Comparative Neurology 302: 330-348

Noto CT, Watanabe S, Fuchs AF (1999) Characteristics of simian adaptation fields produced by behavioral changes in saccade size and direction. Journal of Neurophysiology 81: 2798-2813

Ohtsuka K, Noda H (1995) Discharge properties of purkinje-cells in the oculomotor vermis during visually guided saccades in the macaque monkey. Journal of Neurophysiology 74: 1828-1840

Palkovits M, Mezey E, Hamori J, Szentagothai J (1977) Quantitative histological analysis of cerebellar nuclei in cat .1. numerical data on cells and on synapses. Experimental Brain Research 28: 189-209

Prsa M, Dash S, Catz N, Dicke PW, Thier P (2009) Characteristics of Responses of Golgi Cells and Mossy Fibers to Eye Saccades and Saccadic Adaptation Recorded from the Posterior Vermis of the Cerebellum. Journal of Neuroscience 29: 250-262

Quaia C, Lefevre P, Optican LM (1999) Model of the control of saccades by superior colliculus and cerebellum. Journal of Neurophysiology 82: 999-1018

Scudder CA, McGee DM (2003) Adaptive modification of saccade size produces correlated changes in the discharges of fastigial nucleus neurons. Journal of Neurophysiology 90: 1011-1026

Sparks DL, Holland R, Guthrie BL (1976) Size and distribution of movement fields in monkey superior colliculus. Brain Research 113: 21-34

Takagi M, Zee DS, Tamargo RJ (2000) Effects of lesions of the oculomotor cerebellar vermis on eye movements in primate: Smooth pursuit. Journal of Neurophysiology 83: 2047-2062

Thier P, Dicke PW, Haas R, Barash S (2000) Encoding of movement time by populations of cerebellar Purkinje cells. Nature 405: 72-76

Wallman J, Fuchs AF (1998) Saccadic gain modification: Visual error drives motor adaptation. Journal of Neurophysiology 80: 2405-2416

Behavioral/Systems/Cognitive

# Characteristics of Responses of Golgi Cells and Mossy Fibers to Eye Saccades and Saccadic Adaptation Recorded from the Posterior Vermis of the Cerebellum

**Mario Prsa, Suryadeep Dash, Nicolas Catz, Peter W. Dicke, and Peter Thier**
Department of Cognitive Neurology, University of Tübingen, Hertie Institute for Clinical Brain Research, 72076 Tübingen, Germany

**The anatomical organization of the granular layer of the cerebellum suggests an important function for Golgi cells (GC) in the pathway conveying mossy fiber (MF) afferents to Purkinje cells. Based on such anatomic observations, early proposals have attributed a role in "gain control" for GCs, a function disputed by recent investigations, which assert that GCs instead contribute to oscillatory mechanisms. However, conclusive physiological evidence based on studies of cerebellum-dependent behavior supporting/dismissing the gain control proposition has been lacking as of yet. We addressed the possible function of this interneuron by recording the activity of a large number of both MFs and GCs during saccadic eye movements from the same cortical area of the monkey cerebellum, namely the oculomotor vermis (OMV). Our cellular identification conformed to previously established criteria, mainly to juxtacellular labeling studies correlating physiological parameters with cell morphology. Response patterns of both MFs and GCs were highly heterogeneous. MF discharges correlated linearly with eye saccade metrics and timing, showing directional preference and precise direction tuning. In contrast, GC discharges did not correlate strongly with the metrics or direction of movement. Their discharge properties were also unaffected by motor learning during saccadic adaptation. The OMV therefore receives a barrage of information about eye movements from different oculomotor areas over the MF pathway, which is not reflected in GCs. The unspecificity of GCs has important implications for the intricacies of neuronal processing in the granular layer, clearly discrediting their involvement in gain control and instead suggesting a more secluded role for these interneurons.**

*Key words:* **Golgi cells; mossy fibers; cerebellum; saccades; saccadic adaptation; oculomotor**

## Introduction

The cerebellar cortex is anatomically organized in three distinct layers: the molecular layer, the Purkinje cell (PC) layer and the granular layer (see Fig. 1). The pathways carrying the two known inputs to the cerebellum [climbing fibers and mossy fibers (MFs)] converge at the level of Purkinje cells, which in turn provide the only output of the cerebellar cortex, with their axons terminating in the deep cerebellar and vestibular nuclei.

Whereas the climbing fibers excite the PCs and possibly some interneurons directly, the MF pathway to PC dendrites is indirect. The MF afferents first synapse with cellular elements in the granular layer before the information is transmitted to the PCs via parallel fibers (for a review, see Ito, 2006). Golgi cells (GCs) process the information carried by MFs to the cerebellum before this signal reaches the PC layer. They are the most numerous interneurons in the granular layer [apart from granule cells (GrC)] (Simat et al., 2007), have comparatively larger somata than other interneurons (Barmack and Yakhnitsa, 2008), receive direct excitation from both parallel and mossy fibers (Palay and Chan-Palay, 1974), and in turn exhibit an exclusive inhibition of thousands of GrCs (Hámori and Szentágothai, 1966). The GCs could also potentially modulate the MF signals directly, namely by spillover of GABA through $GABA_B$ receptors found on MF rosettes (Mitchell and Silver, 2000).

Early studies on the cerebellum (Eccles et al., 1967; Marr, 1969; Albus, 1971; Ito, 1984) postulated a number of concepts purely based on anatomical and theoretical considerations that greatly influenced subsequent investigations. One such concept was that cerebellar GCs perform gain control over the MF transmission to PCs [for a detailed discussion, see the study by De Schutter et al. (2000)]. In short, a greater excitation of GrCs by the MFs would lead to an increased inhibition of the same GrCs by the activated GCs, resulting, overall, in limiting the amount of excitation that is transmitted to the PCs. However, more recent physiological findings about cerebellar GCs (Dieudonne, 1998; Vos et al., 1999a, 1999b; Holtzman et al. 2006) have proven to be inconsistent with this classical view. Instead, they led to alternative concepts about their functional role, such as their implication in launching oscillatory mechanisms in the granular layer (Maex and De Schutter, 1998; De Schutter et al., 2000). Still, such propositions remain speculative. Very little is in fact known about the specific properties of or the role GCs might have,

Received Oct. 6, 2008; revised Nov. 27, 2008; accepted Dec. 1, 2008.
This work was supported by Deutsche Forschungsgemeinschaft Sonderforschungsbereich 550 A7.
Correspondence should be addressed to Peter Thier, Department of Cognitive Neurology, University of Tübingen, Hertie Institute for Clinical Brain Research, Ottfried Müller Strasse, 72076 Tübingen, Germany. E-mail: thier@uni-tuebingen.de.
DOI:10.1523/JNEUROSCI.4791-08.2009
 0270-6474/09/290250-13$15.00/0

mainly because *in vivo* recordings from animals involved in well controlled behaviors are lacking.

Consequently, with the intention to shed more light on their properties and eventual function they might have in the cerebellar processing of information, we recorded from a substantial number of both GCs and MF terminals in the oculomotor vermis (OMV) (the narrow strip along the midline of lobules VIc and VIIa of the cerebellum), while monkeys executed visually guided saccades. Eye saccades, a model of cerebellum-dependent motor behavior, provide a comparative advantage over other types of motor behavior resulting from the small number of degrees of freedom and simpler kinematics-to-dynamics transformations.

## Materials and Methods

### *Animals*

Two rhesus monkeys (*Macaca mulatta*) A and N were prepared for eye position recording using the magnetic scleral search coil technique (Judge et al. 1980). To painlessly immobilize the monkeys' heads, a titanium pole was attached to the skull with titanium bone screws. Titanium was used for its high biocompatibility and for compatibility in magnetic resonance imaging (MRI) settings. Recording chambers (also titanium) were implanted over the posterior part of the skull to gain access to the posterior cerebellum for extra-cellular recordings. The middle of the cylinder axis was aimed to the interaural position (0, 0, 0 in stereotaxic coordinates) and inclined by 40° in the posterior direction about the axis perpendicular to the interaural plane. All surgical procedures were conducted under general anesthesia (introduced with ketamine and maintained by inhalation of isoflurane and nitrous oxide, supplemented by intravenous remifentanil) with control of vital parameters (body temperature, $CO_2$, $O_2$, blood pressure, electrocardiogram), followed the guidelines set by the National Institutes of Health and national law and were approved by the local committee supervising the handling of experimental animals. After the surgery, monkeys were supplied with analgetics until full recovery.

### *Behavioral tasks*

During all behavioral tasks, the monkeys sat head-fixed in a primate chair in total darkness. They were trained to make saccadic eye movements to a white target dot (0.2° diameter) displayed on a monitor screen positioned 42 cm in front of the animals. The eye position signal measured by the scleral search coil method was calibrated and sampled at 1 kHz. The monkey received an automatic liquid reward each time he successfully executed the eye saccade; i.e., maintained gaze inside an eye position window (±1.5°) during initial fixation until the target jump, and displaced the eyes back inside the window and maintained fixation no later than 300 ms after the jump.

### *Directional selectivity paradigm*

To test for the directional preference of the recorded units, the monkeys executed visually guided saccades from an initial central fixation point toward targets located at 10° eccentricity in eight different directions in the frontoparallel plane. We designated each direction by their angular polar coordinate. Directions included two horizontal (rightward: 0° and leftward: 180°), two vertical (upward: 90° and downward: 270°), and four diagonal (right-up: 45°, left-up: 135°, left-down: 225°, and right-down: 315°) directions. The monkeys initially fixated a central fixation point for 1000 ms, after which the peripheral target appeared with the simultaneous disappearance of the fixation target. After the saccadic eye movement, the monkeys had to fixate the peripheral target for 300–500 ms. Target directions were randomly chosen from trial to trial.

### *Amplitude tuning paradigm*

To test for the tuning of cells to saccades of different amplitudes, the animals executed visually guided saccades from a central fixation point toward targets at eight different peripheral eccentricities (from 2.5° to 20° in 2.5° steps) in the single radial direction for which the neuron had preferentially responded. The central and peripheral fixation times were as in the directional selectivity paradigm. The target amplitude was randomly chosen for each trial.

### *Saccadic adaptation paradigm*

Saccades were adapted using the standard "McLaughlin" paradigm (McLaughlin, 1967). The monkeys were asked to make saccades from a central fixation point toward a peripheral target in the preferred direction of the neuron and at a fixed eccentricity. During the execution of the saccade, the target spot was shifted either back toward the fixation point (inward adaptation) or in the direction away from it (outward adaptation). The monkey shifted its gaze to the initial target location and then produced a corrective saccade toward the shifted target. This procedure was repeated up to 1000 trials during which the monkey progressively learned to either decrease or increase the amplitude of the initial saccades [see the study by Catz et al. (2005) for examples illustrating saccadic adaptation]. The initial target amplitudes, as well as the sizes of target shifts, were varied between different adaptation sessions. The percentage of gain change was calculated as $\pm|1\text{-saccade\_amplitude/initial\_target\_amplitude}| \times 100$. Gain change percentiles were defined as positive for outward and negative for inward adaptation.

### *Electrophysiology*

Postsurgical MRI was used to facilitate the anatomic localization of cerebellar lobules VI and VIIa. The identification of this area was confirmed by extra-cellular recordings characterized by frequent saccade-related multiunit background bursts and a large number of saccade-related single units. All extra-cellular action potentials were recorded with commercially available glass-coated tungsten microelectrodes (Alpha Omega Engineering) with 1–2 MΩ impedances that were driven to the cerebellum by means of a high precision motor (1 μm movement steps). Single units were isolated on-line with the Multi Spikes Detector software (Alpha Omega Engineering) by detecting and sorting waveforms according to shape. We did not attempt to discern what side of the OMV we were recording from.

### *Data analysis*

*Processing of eye position and neuronal activity data.* All analyses were performed off-line with custom programs compiled in Matlab (Mathworks). The recorded horizontal and vertical eye position traces were smoothed with a Savitzky-Golay filter (window = 10 points, polynomial degree = 4), which replaces the data points in the specified window by a polynomial regression fit of the chosen degree. With a window of 10 points and a fourth degree polynomial, the eye position data are low-pass filtered with a bandwidth of ~100 Hz, which is appropriate for frequencies of natural eye movements (20–30 Hz). Two-dimensional velocity vectors were computed and we used the 20 °/s velocity criterion for detecting saccade onset and end. Saccades with maximal velocity <100 °/s or with durations longer than 100 ms were discarded (this comprised <1% of saccades).

We estimated the instantaneous firing rate of the recorded neurons with a continuous spike density function, generated by convoluting the spike train with a Gaussian function of width $\sigma = 20$ ms. A Poisson spike train analysis (Hanes et al., 1995) was applied to detect the time stamps of onset and end of bursts for the relevant neurons. This analysis relies on a surprise index (SI) defined as $\mathrm{SI} = -\log(P)$, where $P$ is given in Equation 1 and is the probability that, given a mean discharge rate $r$ of the entire spike train being analyzed, a spike train of a time interval $T$ contains $n$ or more spikes. Burst peaks were then calculated as the maximum value of the estimated spike density function between these two time stamps.

$$P = e^{-rT}\sum_{i=n}^{\infty}(rT)^i/i! \qquad (1)$$

The sample average of the dependence of burst peaks on saccade amplitude (see Fig. 8*A*,*C*) was computed by first dividing the range of amplitudes for saccades in the preferred direction of the unit into 10 equally sized bins of 2°. Mean burst peaks were then calculated for each bin for each neuron. The average amplitude tuning data were then computed as the average of all the mean values in each bin across all neurons that had been tested at the amplitude represented by that particular bin. The population activity of all neurons (see Fig. 8*B*,*D*) was computed by dividing the range of saccade durations into 21 equally sized bins of 2 ms.

Recorded spike trains were then assigned to their corresponding bins, and the population mean was computed so as to have each neuron contribute equally to the population response. The spike density function was estimated for the averaged spike trains in each bin as described above. The end of the population response in each bin was determined as the time when the burst decreased below a subjectively chosen value of five SDs above the mean of activity during the first 750 ms of fixation. Calculating population averages this way is not intended to have any anatomic significance, it is instead used as a pertinent method in capturing the temporal information conveyed by a particular group of neurons.

*Statistical analysis and data fitting.* We performed a Student's (when the two samples had equal variances) or Welch's (when the two samples had unequal variances) *t* test whenever we wished to evaluate whether two data samples come from the same distribution with equal means. Normality of data were tested with the Kolmogorov–Smirnov test. We deemed the difference to be statistically significant when the probability ( *p* value) of having distributions with equal means did not surpass the 5% level. Where appropriate, the computed *p* value was multiplied by the number of performed tests to correct for multiple comparisons (Bonferroni correction).

Linear and quadratic fits to data points were computed using the method of least squares. The coefficient of determination $r^2$ was used to evaluate how well the model fitted the data and the *F*-statistic was calculated to evaluate the probability ( *p* value) that all parameters in the model fit were equal to zero. Furthermore, the *F* test with $\nu_1$ and $\nu_2$ degrees of freedom was performed to evaluate whether fitting the data with a quadratic rather than a linear model was justified. The *F* test gives the probability ( *p* value) that the model with added parameters yields the same noise variance as the initial linear one. We deemed the quadratic model as being justified when the probability of having the same noise variance was $<5\%$.

The directional tuning curves shown in Figure 5 were intended for a qualitative description only and were least squares fits to the data points using Equation 2 with $N = 4$ ($\beta$ are the free parameters, $\tau$ the angle in radians is the independent variable). This polar equation produces a periodic smooth curve that passes through the eight data points in a polar plot, as follows:

$$y(\tau) = \beta_0 + \beta_{i1}\sin(i\tau) + \beta_{i2}\cos(i\tau) + \ldots + \beta_{N1}\sin(N\tau) + \beta_{N2}\cos(N\tau)$$

for

$$i = 1 \ldots N \qquad 0 \le \tau < 2\pi\,. \qquad (2)$$

Nonlinear regression was used to fit Gaussian curves to the directional data (see Figs. 5, 6*B*). Perisaccadic activity was computed as the average spike density from 50 ms before saccade onset until 200 ms after saccade onset, and activity during central fixation was computed as average spike density from 500 to 200 ms before saccade onset. The perisaccadic data were first normalized by subtracting the mean activity during central fixation and then by dividing all the points by the maximum (or minimum for pausing units) value. Accordingly, in the normalized perisaccadic activity ratios (see Figs. 5, 6*B*), a value of one indicates maximum (or minimum for pausing units) activity, and the zero level corresponds to the baseline activity (during central fixation). The goodness of fit was evaluated uniquely by the coefficient of determination $r^2$, and a Gaussian fit was deemed to be inappropriate when 95% confidence intervals on the estimated parameters were unreasonable. The preferred direction of each tested neuron was defined to be the angular value corresponding to the peak of the fitted Gaussian curve; only where a Gaussian fit was judged appropriate.

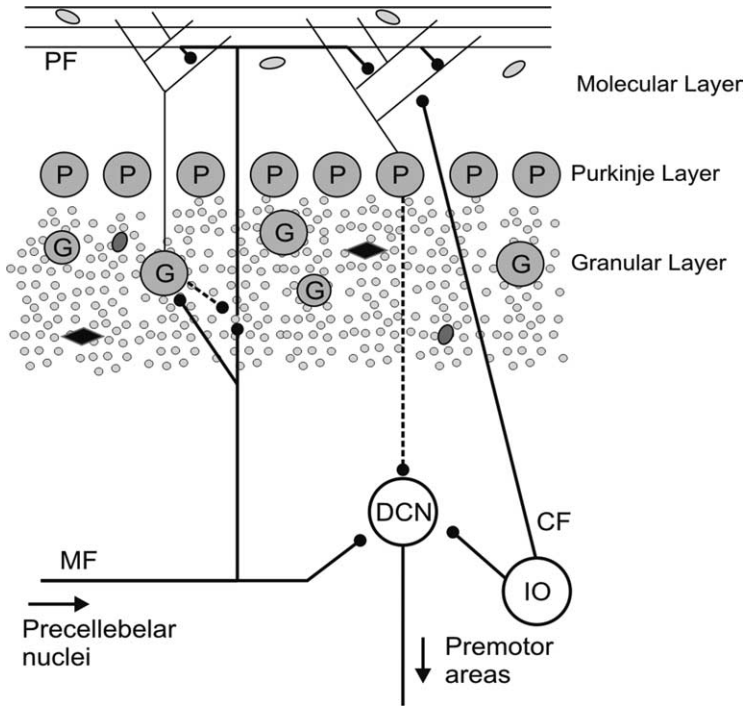


**Figure 1.** Schematic of the cerebellar cortex organization. Excitatory and inhibitory synapses are distinguished with solid and dotted lines respectively. PF, Parallel fibers; DCN, deep cerebellar nuclei; IO, inferior olive; CF, climbing fibers; G, Golgi cells; P, Purkinje cells. Small gray circles represent granule cells and the other undefined symbols represent other interneurons found in the granular and molecular layers.

## Results

### Identification of Golgi cells and mossy fibers

Before any attempt in trying to record action potentials from specific neuronal types, we made sure that the recording electrode was situated in the granular layer. The PC layer was used as a landmark for this purpose (Fig. 1). PCs were readily identified by the simultaneous presence of simple and complex spikes (Eccles et al. 1967; Thach 1968) (Fig. 2*A*). Further advancing the electrode past the PC layer, depending on the orientation of the cerebellar folia, either the molecular or the granular layer could be encountered. The molecular layer was characterized by prominent complex spikes with any other action potentials being highly infrequent (Fig. 2*B*). Otherwise, if the electrode was advanced into the granular layer, complex spikes disappeared completely and action potentials from other cellular elements could be encountered and clearly isolated, albeit less frequently than in the PC layer, where the large-sized neurons are more densely distributed (Fig. 2*C*). Another important criterion which permitted the distinction between granular and molecular layers was the beehive-like saccade-related background activity. Whereas the molecular layer remained relatively silent, saccade-related multiunit activity often dominated the background of the granular layer. These criteria are in line with previous electrophysiological identification of cerebellar layers confirmed by histological verification of electrolytic lesion sites in monkeys (Miles et al., 1980; van Kan et al. 1993).

With the recording electrode located in the granular layer of the OMV, GCs were recognized mainly on the basis of a unique

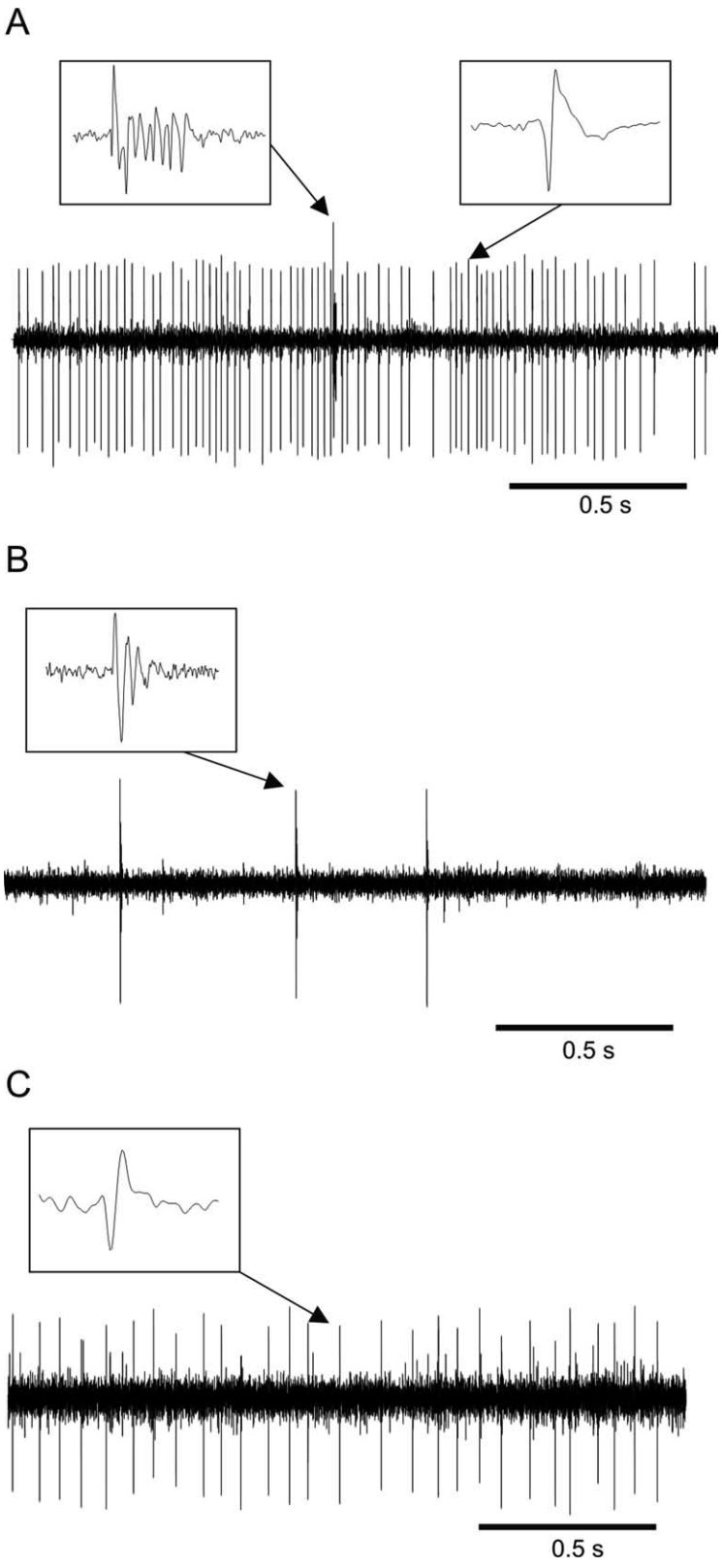


**Figure 2.** Electrophysiological identification of different layers of the cerebellar cortex. ***A–C***, Typical signals recorded from electrodes located in the Purkinje cell (***A***), molecular (***B***), and granular (***C***) layers. Insets, Enlarged waveforms of spikes pointed to by the arrows.

electrophysiological signature established by Barmack and Yakhnitsa (2008) (in the mouse cerebellum), and Holtzman et al. (2006) and Simpson et al. (2005) (in the rat cerebellum) who compared a number of electrophysiological parameters based on extracellular recordings with the morphology of cells as revealed by subsequent juxtacellular labeling. In accordance with these studies, units we identified as GCs were characterized by the absence of complex spikes and by action potentials that all showed tonic activity at rest with low mean firing frequencies (2–30 Hz), distinctive interspike interval (ISI) histogram shapes lacking high frequency components (Fig. 3*A*) and well pronounced, long (> 1 ms) and di/tri-phasic action potential wave shapes (Fig. 3*C*). In accordance with previous work (Holtzman et al., 2006), a comparison of the ISI distributions of individual cells we identified as either Golgi or Purkinje revealed that the two types of units possessed different discharge properties at rest (Fig. 3*B*). Whereas median ISI values of GCs covered a wide range of intervals, those of PCs fell into a much narrower range of 5 to 40 ms with very little overlap between the distributions of median ISIs of the two populations of neurons. This comparison provides an additional guideline for distinguishing GCs from the PC simple spike discharges when the latter is not necessarily accompanied by complex spikes.

Other cellular elements that could give rise to action potentials in the granular layer include GrCs, unipolar brush cells (UBC), Lugaro cells, and MF terminals. More often than the putative GCs, we encountered very short and faint action potentials rather randomly in the granular layer (Fig. 3*C*). They were often followed by a negative after-wave (NAW) and were difficult to keep isolated for longer times. Based on previous similar descriptions from awake monkey recordings (Kase et al., 1980; Miles et al. 1980; Ohtsuka and Noda, 1992; van Kan et al. 1993), we assigned these action potentials to be emanating from MF terminals. The ISI histograms computed for these units were, however, highly diverse and unlike for GCs, typical histograms exemplifying the putative MFs could not be provided. The main criteria for identifying MFs (with the electrode in the granular layer) were either the presence of the NAW, or action potential durations significantly shorter than those of units thought to reflect cellular elements (Fig. 3*D*). van Kan et al. (1993) furthermore confirmed this identification by asynaptic activation of such units from electrical stimuli of the peduncle. We excluded GrCs as the possible origin of such potentials because the size of their somata (4–6 $\mu$m) seems to be much smaller than that of MF rosettes, which makes their recording possible only if high impedance electrodes (>15 M$\Omega$) are used (Barmack and Yakhnitsa, 2008). Climbing fibers

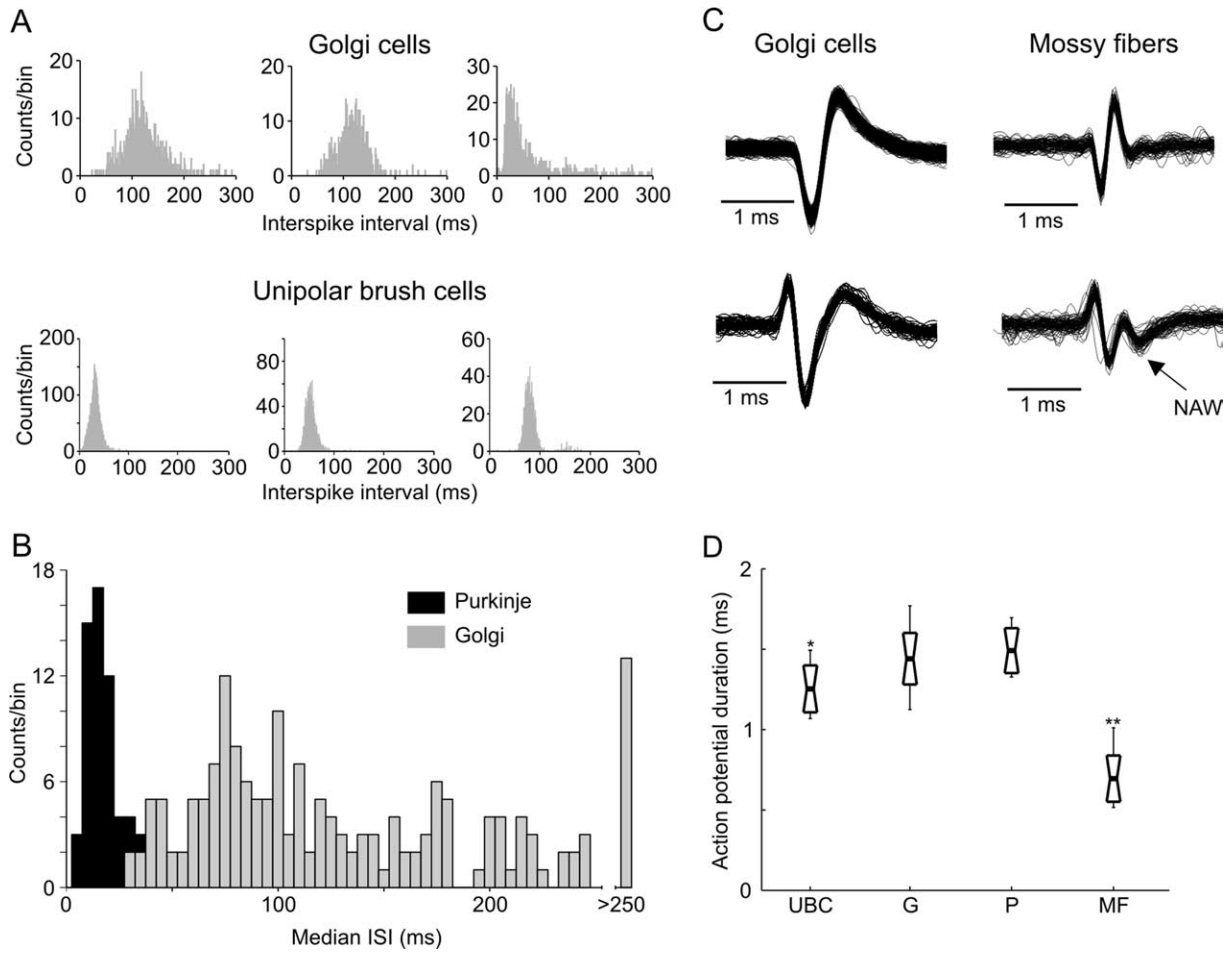


**Figure 3.** ***A***, Exemplary ISI histograms characterizing individual Golgi cells and unipolar brush cells. ***B***, Comparison between median ISI values of Golgi and Purkinje cells. ***C***, Comparison between typical action potential wave shapes recorded from Golgi cells and mossy fibers. ***D***, Distribution of action potential durations calculated from 10 randomly chosen UBCs, Golgi cells (G), Purkinje cells (P), and MF. Durations were measured from the beginning of the wave, up to the last moment the wave again crossed the initial level (the long negative rebound period was not included). The thick black line indicates mean values, short delimiters the SD, and long delimiters the full data range. The distribution of action potential durations of all units are compared with that of Golgi cells; $*p < 0.03$, $**p < 10^{-7}$.

that branch through the granular layer are also excluded as possible sources because, in addition to being ~50 times less frequent than MFs (Ito, 1984), they fire at very low rates (0.5–2 Hz) (Thach, 1968), unlike the high frequency bursts we recorded.

The units we identified as GCs could potentially also be mistaken for UBCs or Lugaro cells, the other two large-sized interneurons of the granular layer. Luckily, UBCs have been identified and characterized in juxtacellular labeling studies of Barmack and Yakhnitsa (2008) and Simpson et al. (2005). They discharge at highly regular firing rates and hence show narrow ISI histograms, with a wide range of possible median values. We have indeed encountered cells in the granular layer corresponding to this description (Fig. 3*A*) and have excluded them from our GC population, although recorded spike trains with similar properties have also been attributed to Golgi units after juxtacellular labeling (Holtzman et al., 2006). We also found that the presumed UBCs we recorded have action potential durations significantly shorter than GCs (Fig. 3*D*), which would be consistent with their comparatively smaller somata sizes (Barmack and Yakhnitsa, 2008). Unfortunately, we cannot exclude the possibility that some Lugaro cells were erroneously included in our GC group, simply because, to our knowledge, Lugaro cells have never been physiologically characterized *in vivo*; only in slice preparations of the rat cerebellum (Dieudonné and Dumoulin, 2000). It should however be noted that GCs largely outnumber the Lugaro cells in the granular layer [the ratio of Golgi to Lugaro cells is ~67/15 in the mouse cerebellum according to Simat et al. (2007)]. Finally, unlike previously reported (Edgley and Lidierth, 1987), we did not find that PC action potentials were shorter than those of GCs (Fig. 3*D*) were. The GC action potential durations were, however, more variable, which would be in agreement with their morphological heterogeneity (Geurts et al., 2003).

As a final point, it is important to state that we did not confirm the identity of Golgi cells or mossy fiber terminals morphologically, nor did we perform electrolytic lesions at recording sites. Our identification therefore remains putative.

### Heterogeneity of response patterns evoked by eye saccades

We recorded eye saccade responses of 177 putative GCs and 103 putative MFs. Both types of units exhibited a variety of response patterns including burst only [69% for MFs (Fig. 4*A1–3*); 65% for GCs (Fig. 4*B1*)] and pause only [14% for MFs (Fig. 4*A4*); 25% for GCs (Fig. 4*B4–5*)], while other cells/fibers exhibited a burst-followed-by-a-pause or pause-followed-by-a-burst pattern [17% for MFs (Fig. 4*A5–6*); 10% for GCs (Fig. 4*B3,6*)]. Both saccade-related (phasic) and position-related (tonic) increases (bursts) and decreases (pauses) in firing rate levels were observed.

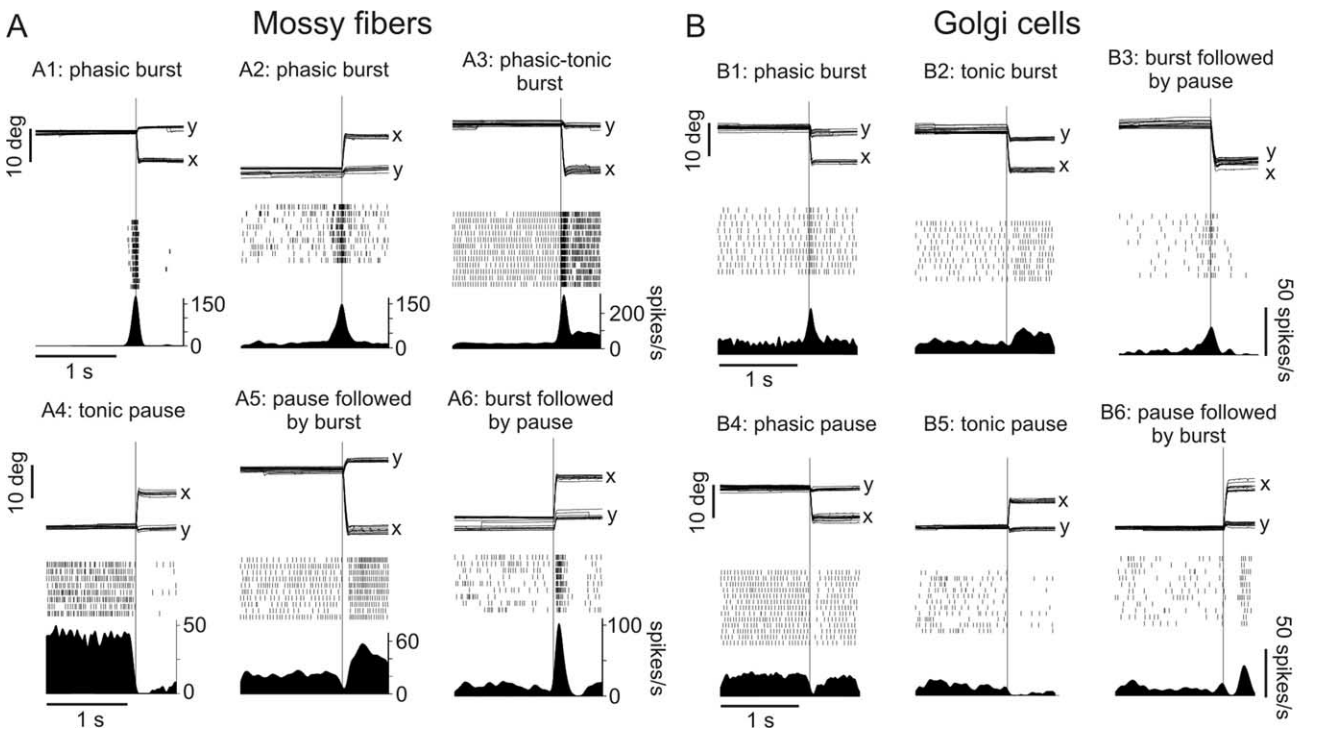


**Figure 4.** ***A***, ***B***, Diversity of response patterns recorded from six exemplary mossy fibers (***A***) and Golgi cells (***B***). In each panel, the upper trace represents horizontal (*x*) and vertical (*y*) eye movements, the middle trace shows the spike raster plot, and the lower trace is the estimated mean spike density function for all trials. All trials are aligned on saccade onset represented by the thin vertical line.

High unit-to-unit variability in start timings of the bursting responses (as detected by a Poisson spike train analysis; see Materials and Methods) relative to saccade onset [median (lower quartile, upper quartile): −14 (−64, 10) ms, $n = 87$ for MFs; −11 (−58, 7) ms, $n = 126$ for GCs] and end timings relative to saccade end [median (lower quartile, upper quartile): 10 (−27, 74) ms, $n = 87$ for MFs; 24 (−20, 81) ms, $n = 126$ for GCs], as well as highly variable durations of the related bursts [median (lower quartile, upper quartile): 94 (56, 145) ms, $n = 87$ for MFs; 104 (67, 155) ms, $n = 126$ for GCs] and pauses (subjectively evaluated), was observed without any obvious relationship to their classification as GCs or MFs. Where the GCs strikingly differed from MFs however, was in the peak frequency of the burst responses. GCs only rarely displayed saccade-evoked bursts >100 spk/s [median (lower quartile, upper quartile): 40.6 (32.8, 53.45) spk/s, $n = 126$], whereas MFs exhibited very strong bursts of activity often in the range of 100–200 spikes/s [median (lower quartile, upper quartile): 67.9 (49.2, 97.7) spikes/s, $n = 87$]. Further qualitative differences could be observed between the responses of MFs and GCs, namely in the pause and position-related burst patterns. The position-related bursts recorded from GCs had wavering firing rate levels and often decreased to baseline during prolonged eccentric fixation. Although most position-related responses of MFs approximately resembled those of GCs, many also showed distinct constant tonic levels maintained during prolonged peripheral fixation. These were often accompanied by phasic components and resemble the discharge of motor units in the abducens nucleus (Fig. 4*A3*). Whereas the pause responses of GCs could either be very precise and short (Fig. 4*B4*) or long and position-related (Fig. 4*B5*), those of MFs all persisted for longer durations, often throughout peripheral fixation (Fig. 4*A4*).

### Golgi cells and mossy fibers have differing directional selectivity properties

The identified GCs and MFs were tested for directional selectivity while the monkeys executed saccades in eight different directions in the frontoparallel plane (see the directional selectivity paradigm in Materials and Methods). For each tested unit, the perisaccadic activity (see Materials and Methods) was computed on a trial by trial basis and mean values were obtained for each of the eight directions of movement. The maximum (or minimum for pausing units) mean value was compared with the means of the other seven directions; when the difference was not statistically significant in more than four neighboring directions (meaning that directions >90° apart have similar activities), the unit was labeled as not directionally selective (see Fig. 6*A*). If, on the contrary, the unit showed directional selectivity, the preferred direction was evaluated as the angular value at which a Gaussian fit to the data points reached its peak.

From the 63 MFs (26 from monkey A and 37 from monkey N) tested using this paradigm, most (47, i.e., 74.6%) showed a clear directional tuning as illustrated by two typical examples in Figure 5*A*,*B*. Furthermore, the directionally selective MFs differed in the amount of suppression of their discharge relative to baseline for the direction opposite to the preferred one; some held their activity close to baseline (Fig. 5*B*), while others ceased firing (Fig. 5*A*). The 111 GCs (52 from monkey A and 59 from monkey N) tested for directional selectivity were found to exhibit a remarkably different behavior than the MFs. A minority of GCs (45, i.e., 40.5%) were directionally selective while the majority showed no clear directional preference as depicted in two typical examples in Figure 5*C*,*D*. Moreover, as many as 35 GCs (31.6%) showed no significant difference in their perisaccadic activity, when compared with the "optimal" direction, for all other seven neighbor-

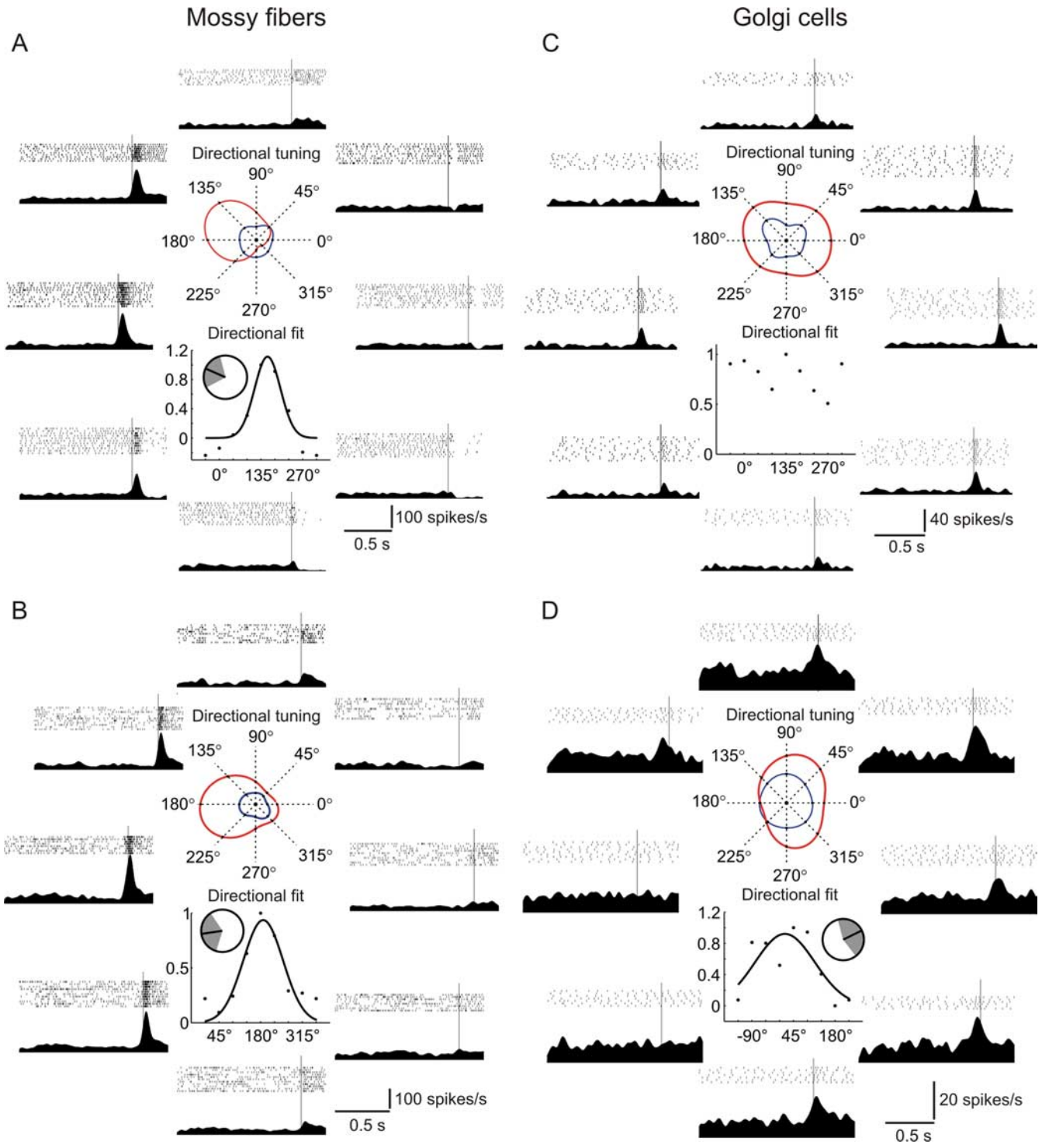


**Figure 5.** ***A–D***, Directional tuning properties of two exemplary mossy fibers (***A***, ***B***) and Golgi cells (***C***, ***D***). In each figure, the top central panel shows the directional tuning of the perisaccadic activity (in red) and activity during fixation (in blue) to the eight directions of movement. The bottom central panel shows a Gaussian fit to the normalized perisaccadic activity ratio points (see Materials and Methods) for the eight directions, and the inset depicts the preferred direction of movement of the cell (angle corresponding to the peak of the Gaussian fit), with the shaded area corresponding to the SD of the Gaussian curve. Each exterior panel is aligned with one of the eight movement directions and shows the raster plot and the mean spike density for that direction. All trials are aligned on saccade onset represented by the thin vertical line. The absence of a curve fit in ***C*** indicates that a Gaussian function was inappropriate to describe the data.

ing directions (Fig. 6*A*), while this was true in the case of only eight MFs (12.7%).

To ascertain a categorical description of the directional selectivity behavior of the MF and GC populations, it was first of interest to establish to what extent the eight different directions of movement tested were represented in the perisaccadic discharge of the GCs and MFs respectively. To address this question, circular data of preferred directions of individual units was compiled (Fig. 6*C*; see figure legend for details). Both Rao's spacing test and Rayleigh's uniformity test (both evaluate the probability of the null hypothesis that circular data are uniformly distributed along the 360° range) yielded lower $p$ values for MFs (Rao: $p = 0.05$,

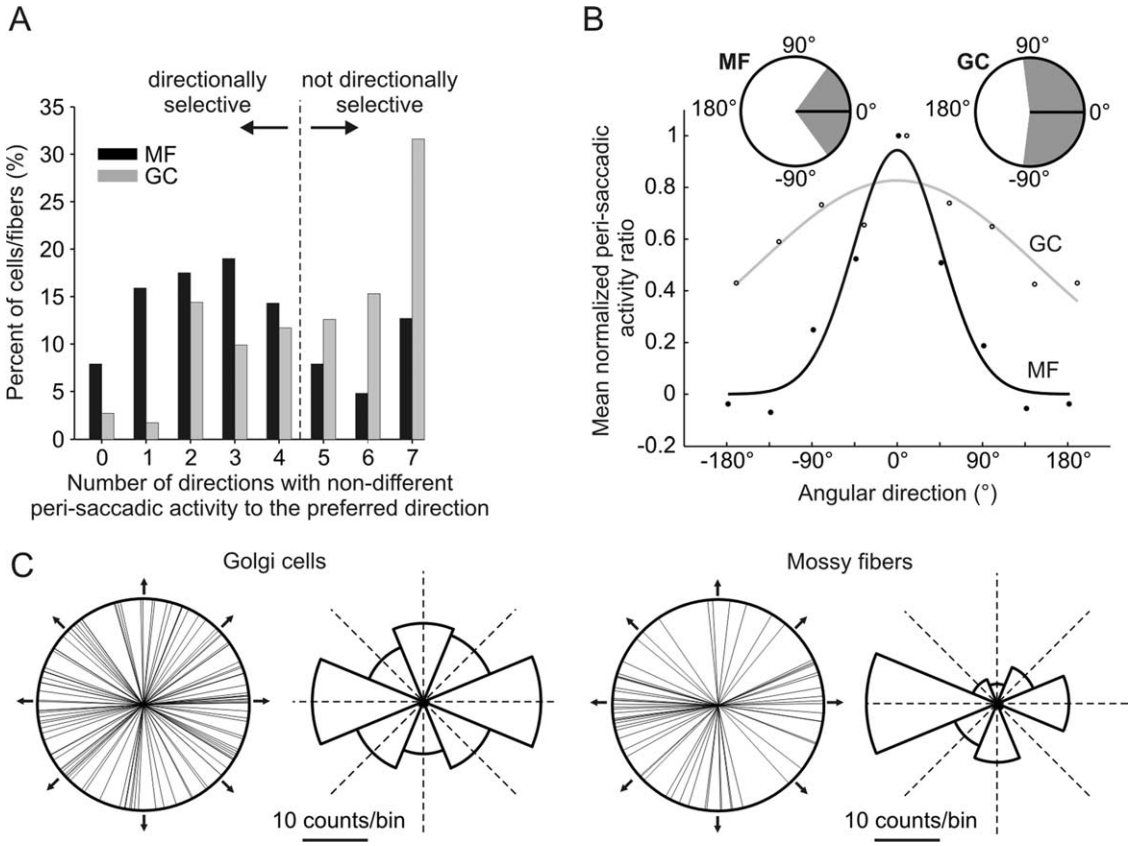


**Figure 6.** Directional selectivity properties of GC and MF. ***A***, Histogram showing the percentage of cells/fibers considered to be directionally selective. Only units in which mean perisaccadic activities in the preferred direction of movement were not significantly different from the mean in four or less neighboring directions were considered to be directionally selective. ***B***, Gaussian fits to the mean normalized perisaccadic activity ratio points (see Materials and Methods) of the eight tested directions of 111 and 63 Golgi cells (empty circles) and mossy fibers (filled circles) respectively, aligned to the direction where their mean perisaccadic activity is maximal. Insets, The SD (shaded area) around the preferred direction of the average cell/fiber. ***C***, Circular plots showing the preferred directions of 97 Golgi cells and 61 mossy fibers (only units with appropriate Gaussian fits to the directional data points were included, see Materials and Methods), together with histograms in which these directions were binned into octants. The arrows and dotted lines designate movement directions.

Rayleigh: $p = 0.07$) than for GCs (Rao: $p = 0.17$, Rayleigh: $p = 0.81$). The circular histograms provided in Figure 6*C* furthermore show that for both GCs and MFs, the two bins with maximum number of counts correspond to the two horizontal directions. These horizontal-preferring units constitute 51% of our MF sample but only 36% of our GC sample (25% would be expected for uniformly distributed data). It is therefore apparent that the octants corresponding to the other six nonhorizontal directions contain a proportionately larger number of counts for GCs than for MFs. Together, these findings suggest that MFs in the OMV are biased toward encoding horizontal movements, confirming previous findings of Ohtsuka and Noda (1992), but, in the same cortical area, all directions of movement seem to be more equally represented in the population response of GCs.

To directly compare the amount of direction selectivity of the two groups of units, we calculated the average normalized perisaccadic discharge of the two groups. For this purpose, the perisaccadic activity means of all individual cells/fibers were normalized in a way to always have the same direction (0°) as the preferred one (i.e., the tuning data were rotated so as the maximal perisaccadic activity value is pointing in the 0° direction). Least squares Gaussian fits to the population averages of such normalized data points (Fig. 6*B*) (see Materials and Methods for details) reveal that the MFs have a much narrower tuning than the GCs [variance parameter of the Gaussian curve with 95% confidence bounds: 64.35° (49.95°, 78.75°) for MFs and 208.35° (144.45°, 272.7°) for GCs]. Because the 95% confidence bounds on the variance estimates do not overlap for the two groups, the difference in direction tuning affinity is judged to be statistically significant.

### Mossy fibers carry information about saccade metrics, Golgi cells do not

After having established the directional preference of the recorded GCs and MFs, the monkeys executed saccades toward targets at eight different eccentricities in the preferred direction of the cell/fiber (see amplitude tuning paradigm in Materials and Methods). Because saccades toward increasing target eccentricities are associated with increasing saccade amplitude, velocity and duration, this paradigm allows us to establish if and how movement metrics are encoded by the activity of the recorded cells/fibers.

We first examined the GCs/MFs with burst responses using a Poisson spike train analysis (Hanes et al. 1995). Bursts were detected with this method in 105 (60 from monkey A and 45 from monkey N) and 86 (55 from monkey A and 31 from monkey N) of the recorded GCs and MFs, respectively, in the amplitude tuning paradigm. The peak discharge rate of the detected bursts was plotted as a function of increasing saccade amplitude for all the individual cells/fibers. Among the highly diverse tuning profiles that could be observed for all of the 105 GCs, two leading trends stand out and are illustrated by typical examples in Figure 7. As

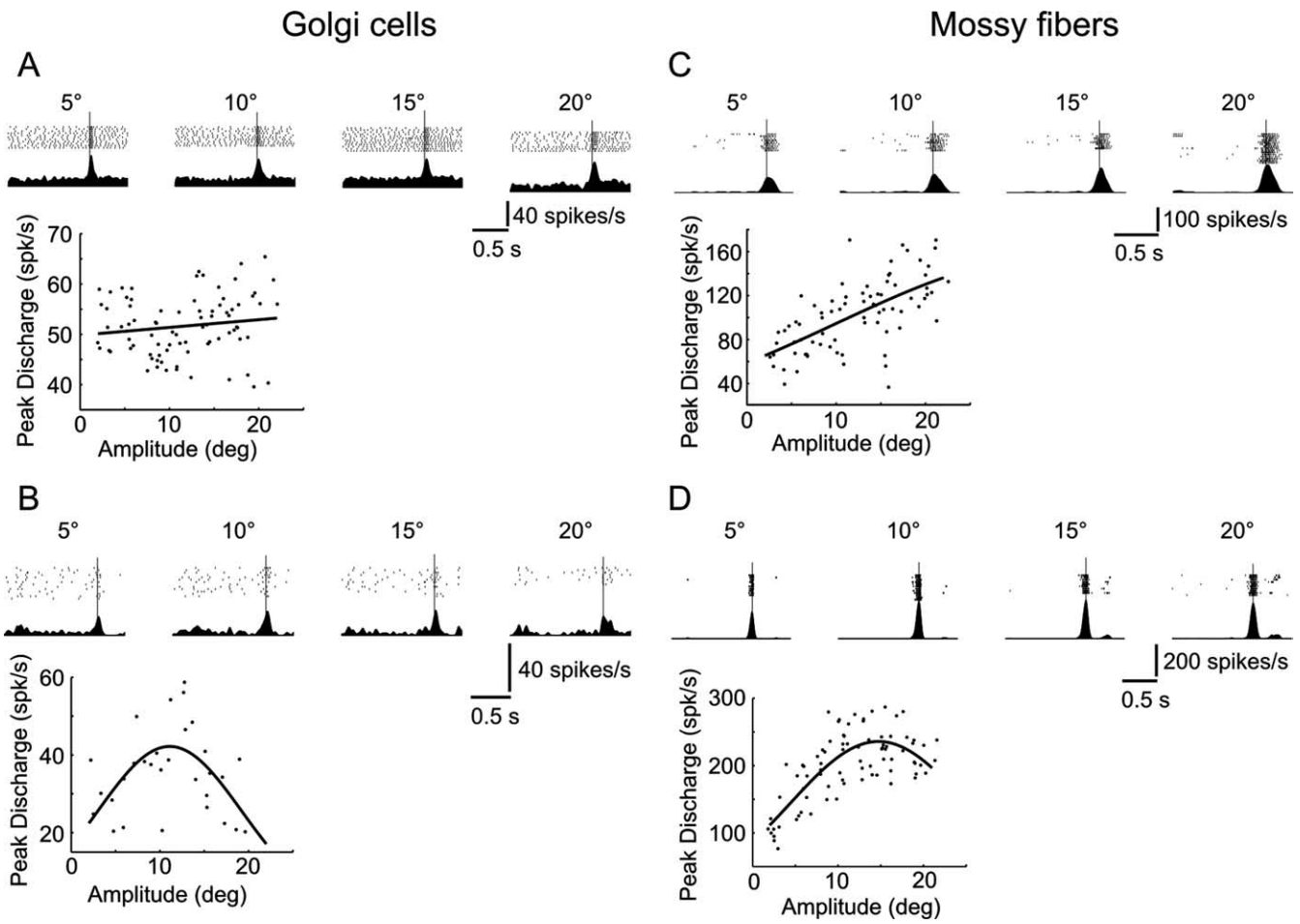


**Figure 7.** ***A–D***, Amplitude tuning characteristics of two exemplary Golgi cells (***A***, ***B***) and mossy fibers (***C***, ***D***). In each figure, the top panels each show the spike raster plot and the mean spike density for the indicated saccade amplitude (5°, 10°, 15° or 20°). All trials are aligned on saccade onset (vertical line). The bottom panels shows the peak discharge data points as a function of saccade amplitude and a corresponding least squares fit of a linear or Gaussian function.

shown in these figures, the peak burst discharge of most GCs either increased weakly or not at all with increasing saccade amplitude (Fig. 7*A*), or showed clear preference for intermediate saccade sizes (Fig. 7*B*). Also, the bursts of individual MFs could be characterized by two predominant tuning profiles that were most often observed. However, unlike the GCs, burst peaks of many MFs correlated positively and distinctly with saccade size (Fig. 7*C*), while others reached their maximum at intermediate amplitudes (Fig. 7*D*). To obtain a statistical description of the GC and MF mean population burst responses, increasing saccade amplitudes were divided into bins and all of the detected bursts were averaged for each bin (see Materials and Methods for details), regardless of what the preferred direction of the cell/fiber was. The resulting population data (Fig. 8*A*,*C*) reveal that the MF peak burst discharge increases linearly with increasing amplitude (linear fit: $r^2 = 0.92, p < 10^{-4}$), whereas the relationship between saccade sizes and burst maxima for the GCs is best described with a comparatively flat inverse parabola (quadratic fit: $r^2 = 0.9$, $p = 0.0003$; *F* test for quadratic vs linear fits: $F = 18.13$, $v_1 = 1$, $v_2 = 8$, $p = 0.0028$).

Second, we sought to analyze how the timing properties of GC and MF activities modulate with saccades of increasing duration. To this end we ordered all the recorded saccades and the associated cell/fiber spike trains by increasing saccade duration, divided the record into equally sized bins, and computed the average spike activity for each bin (see Materials and Methods for details). In this manner, the mean population activity of 177 GCs (112 from monkey A and 65 from monkey N) (Fig. 8*B*) and 103 MFs (66 from monkey A and 37 from monkey N) (Fig. 8*D*), tested with the amplitude tuning paradigm regardless of their response patterns and preferred directions, could be evaluated. The onset of the MF population response relative to saccade onset (mean ± SD: −83.71 ± 21.17 ms) was found to precede that of the GC population (mean ± SD: −74 ± 15.7 ms) in a statistically significant manner (*t* test: $p = 0.017$). Both population bursts thereafter persisted beyond the end of the saccadic eye movement, but differed greatly in the timing properties of their cessation. On the one hand, the ending of the MF response correlated linearly with increasing saccade duration (linear fit: $r^2 = 0.89$, $p < 10^{-9}$) and on the other, the end of the GC population burst was best fitted with an inverse parabola as a function of saccade duration (quadratic fit: $r^2 = 0.86$, $p < 10^{-7}$; *F* test for quadratic vs linear fits: $F = 31.18$, $v_1 = 1$, $v_2 = 19$, $p < 10^{-4}$). Moreover, the MF population response lasted far beyond that of the GCs [response end relative to saccade end, median (lower quartile, upper quartile): 138 (80, 231) ms, for MFs; 65 (54, 79.5) ms, for GCs], suspected to be caused by the strong position-related response patterns characterizing some of these units (Fig. 4*A3*).

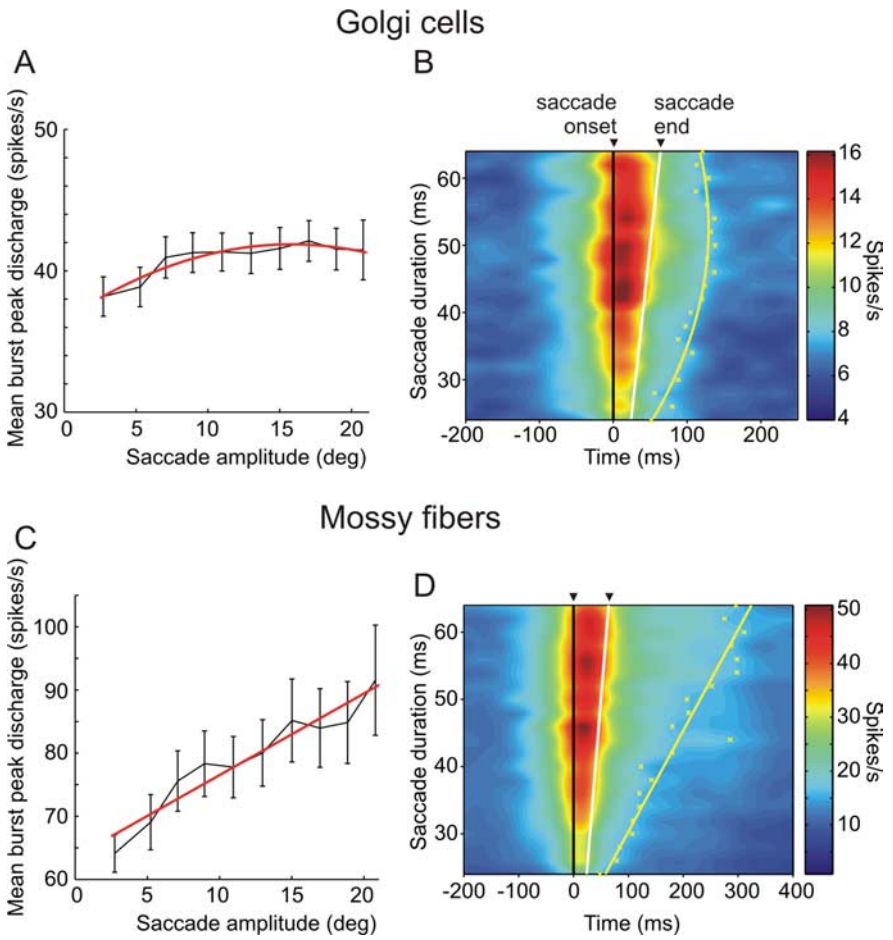


**Figure 8.** Amplitude tuning properties of the average peak discharge of Golgi cell and mossy fiber bursting units (***A***, ***C***) and timing properties of the mossy fiber and Golgi cell population responses. ***A***, Mean burst peak discharge as a function of saccade amplitude calculated for 105 Golgi cells. The delimiters indicate SEs, and the red line is a quadratic least squares fit to the data points. ***B***, Population response of 177 Golgi cells. Yellow crosses indicate the estimation of the burst end for each duration bin, and the yellow line is a least squares quadratic fit to those points. ***C***, Same data as in ***A*** but for 86 mossy fibers fitted with a linear function. ***D***, Same data as in ***B*** but for 103 mossy fibers with the yellow line being a linear least squares fit.

### Golgi cells do not seem to display plasticity during saccadic adaptation

Overall, 40 GCs could be kept isolated long enough to be tested during saccadic adaptation in the preferred direction of the cell/fiber [19 cells (13 from monkey A and 6 from monkey N) for inward and 21 cells (15 from monkey A and 6 from monkey N) for outward adaptation]. This form of short-term learning (see saccadic adaptation paradigm in Materials and Methods) allowed us to examine how GCs behave, compared with what is already known about the plasticity of PCs, during a recalibration of the saccadic system.

On an individual cell basis, we never observed obvious changes in the firing profiles of the recorded neurons. Despite progressively increasing or decreasing saccade amplitudes associated with a recalibrated saccadic command, individual GCs generally maintained their initial pattern of activity throughout the course of adaptation (Figs. 9*A*, 10*A*). Furthermore, the population mean activity was computed for the GCs tested for inward (Fig. 9*B*) and outward (Fig. 10*B*) adaptation. It was of interest to see whether and how peak activity, onset latency, and end latency estimates of the population average changed with increasing/decreasing saccade amplitude gains (see figure legends and Materials and Methods for details). Peak activity and onset latency showed no significant linear changes (linear fits: $r^2 = 0.19$, $p = 0.053$ and $r^2 = 0.06$, $p = 0.28$, respectively) during the course of inward adaptation, whereas the end latency of the burst showed a marginally significant decrease (linear fit: $r^2 = 0.26$, $p = 0.02$). In the case of outward adaptation, the onset latency of the population burst exhibited a barely significant increase (linear fit: $r^2 = 0.23$, $p = 0.032$), and peak discharge and end latency remain unchanged (linear fits: $r^2 = 0.03$, $p = 0.48$ and $r^2 = 0.04$, $p = 0.38$, respectively), while the amplitude of saccades increased.

Unfortunately, we could not test the MFs during the adaptation paradigms, mainly because the recording stability of MFs was often poor, making it difficult to keep their action potentials well isolated for longer times.

## Discussion

### What does the diversity of observed response patterns of MFs and GCs imply?

Previous recordings from the OMV and the flocculus during eye movements in monkeys are in accordance with our results about the different patterns of activity recorded from MFs (Kase et al., 1980; Miles et al., 1980; Ohtsuka and Noda, 1992). Similarly, recordings from monkeys in the intermediate cerebellar cortex during forelimb manipulations (van Kan et al., 1993) describe various combinations of tonic and phasic discharges of MFs. In the case of the OMV, the MF afferents have been shown to arise mainly in the pontine nuclei, the nucleus reticularis tegmentis pontis (NRTP), and the paramedian pontine reticular formation (PPRF), suggesting that the cerebellum is provided by both cortical and subcortical information about visually guided eye movements (Thielert and Thier, 1993). Based on their recordings, Ohtsuka and Noda (1992) have, however, concluded that the MFs destined for the OMV are restricted to the PPRF and superior colliculus (via NRTP), because the end of their MF bursting responses always precluded the completion of the saccade. Our own data show a much higher variability of MF burst timings, and such heterogeneity indeed conforms to the fact that the MF input to the cerebellum originates from various movement-related sources in the brainstem.

The cell-to-cell variability of movement-related discharges in GCs was also observed for various eye and head movements (Miles et al., 1980) and forelimb manipulations (van Kan et al., 1993) in the monkey, as well as during cat locomotion (Edgley and Lidierth, 1987). This was vexingly not the case for electrical and somatosensory stimuli of vibrissal pads and limbs in rats (Vos et al., 1999b; Holtzman et al., 2006), in which the evoked GC responses were more stereotypical. This variability observed in GCs could simply reflect excitations, direct or indirect, from the heterogeneous MFs. However, the Golgi group included substantially more pause units, often phasic, which we never observed in

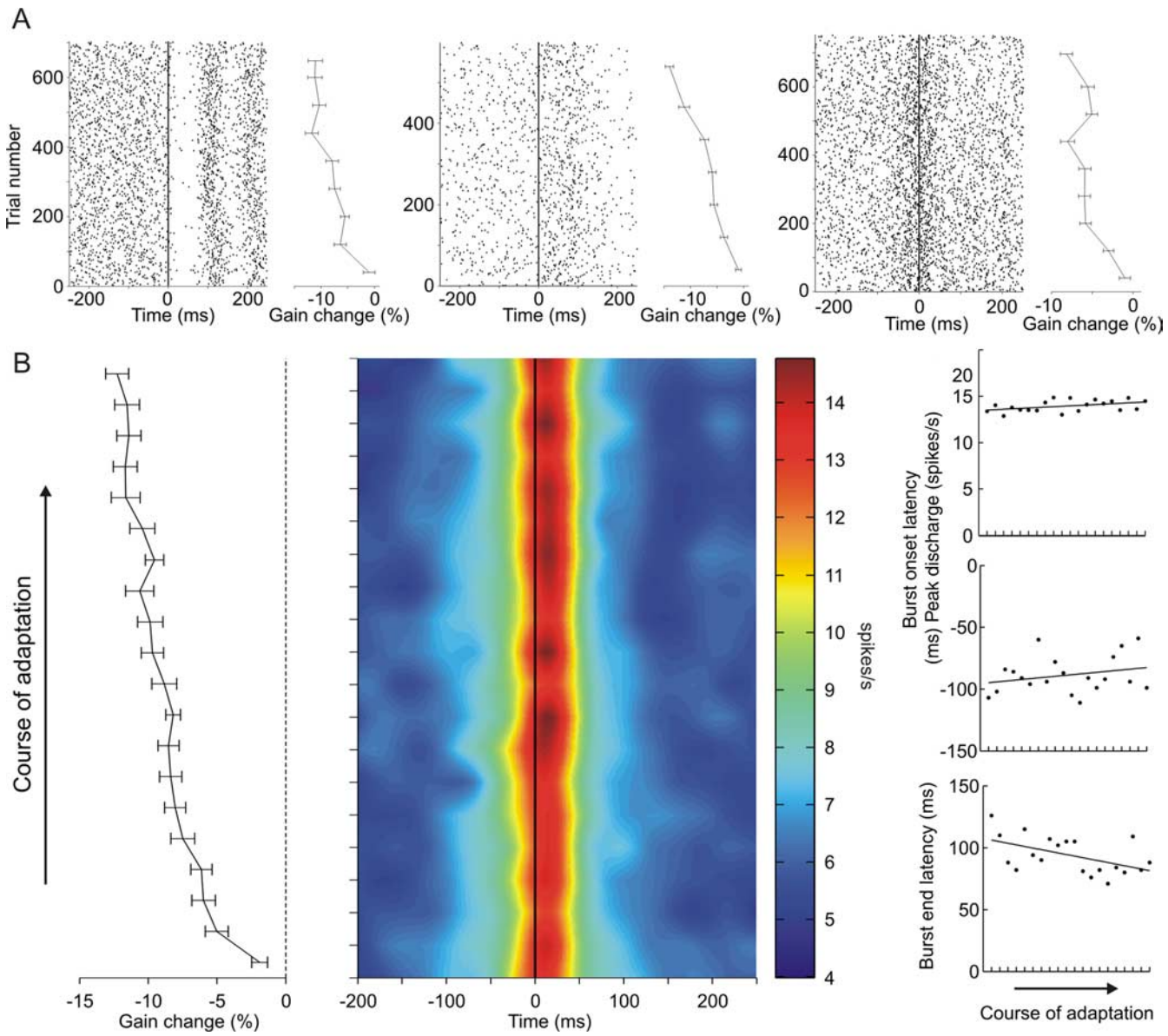


**Figure 9.** ***A***, Spiking activity of three exemplary Golgi cells during the course of inward adaptation. Left panels in each example show spike raster plots for all trials aligned on saccade onset (vertical line). Right panels indicate mean (± SE) percentage gain changes during the course of adaptation. The mean percentage gain change was evaluated for each 80 consecutive trials. ***B***, Population response of 19 Golgi cells during the course of inward adaptation. Middle panel, Mean population activity aligned at saccade onset (vertical line); left panel, mean (± SE) percentage gain change during the course of adaptation. Data from individual cells were all divided in increasing trial order into 20 equally sized bins, and population means were computed for each bin. Right panel, Peak discharge, burst onset latency, and burst end latency evaluated for the population activity for each of the 20 bins during the course of adaptation. Lines indicate linear least squares fits to the data points.

MFs. The additional modulation of GCs by inhibitory interneurons seems pertinent in this context. The axonal plexus of individual GCs are known to branch within generally nonoverlapping parasagittal planes (Barmack and Yakhnitsa, 2008). Combined with the heterogeneity of their discharge patterns, this suggests, as previously speculated by Edgley and Lidierth (1987), that subpopulations of thousands of GrCs organized in sagittal zones are under different patterns of inhibitory control.

### The disparity of directional selectivity between MFs and GCs has functional implications

van Kan et al. (1993) reported that most MFs responded reciprocally to extension and flexion movements and exhibited strong device specificity (showed preference for shoulder, elbow, wrist, or finger manipulation), whereas GCs fired identically for both flexion and extension, and lacked device specificity. Similarly, Edgley and Lidierth (1987) stated that the majority of GCs were responsive to stimuli of both forelimbs of the cat, and the eye saccade-related responses of MFs recorded in the flocculus (Miles et al., 1980) or the OMV (Kase et al., 1980; Ohtsuka and Noda, 1992) generally showed strong directional preference. Finally, electrical and tactile stimuli of the rat face or limbs (Vos et al., 1999b; Holtzman et al., 2006) revealed that responses in GCs could be elicited from widespread areas. All these findings are in accordance with our own results about the disparity of directional selectivity between MF and GC populations (Fig. 5, 6).

The strong directional selectivity of MFs entails that restricted groups of GrCs [400–600 per MF according to Ito (2006)] are excited preferentially for movements in a particular direction. The broad directional tuning of GCs then suggests that these

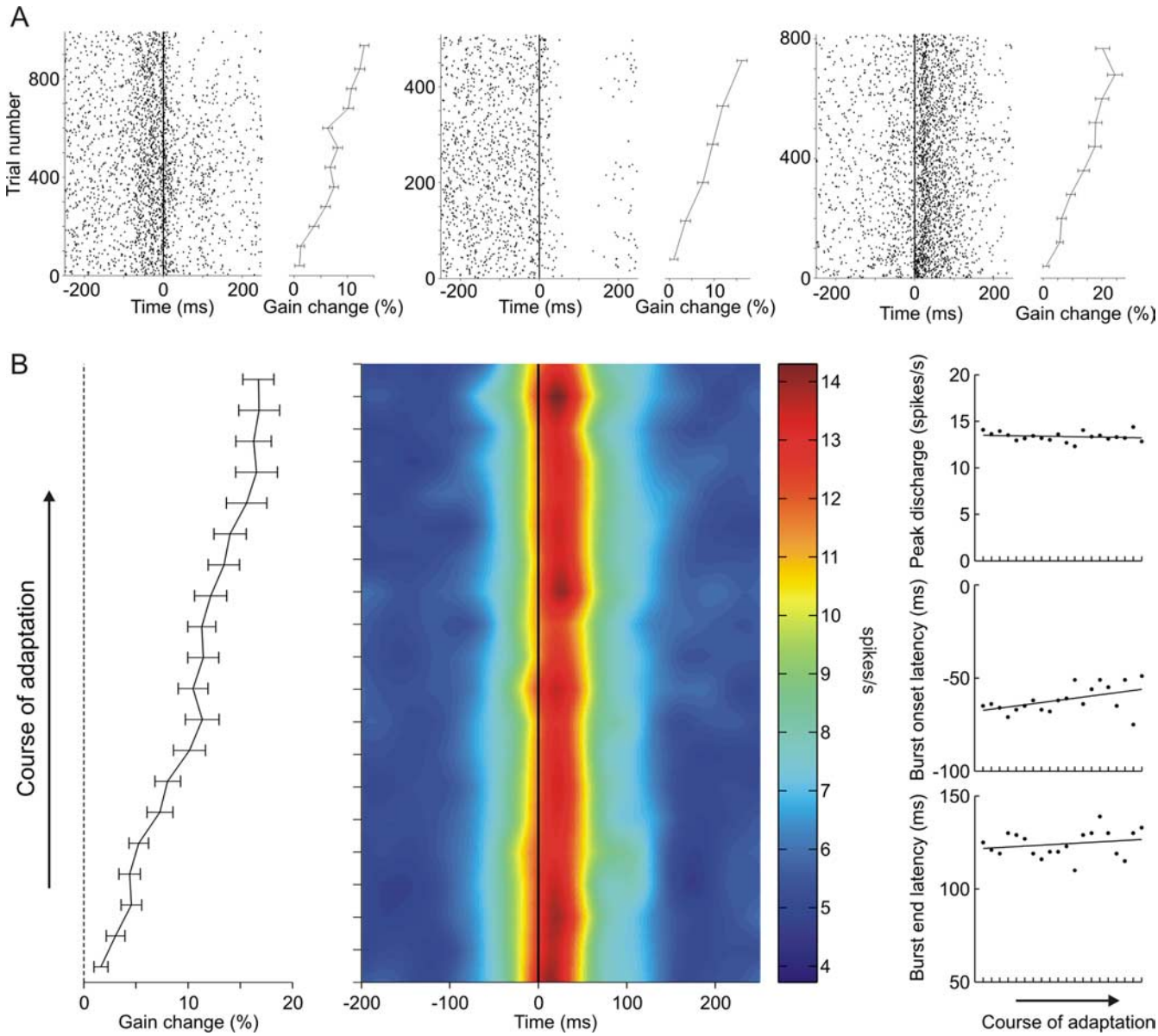


**Figure 10.** ***A***, Spiking activity of three exemplary Golgi cells during the course of outward adaptation. ***B***, Population response of 21 Golgi cells during the course of outward adaptation. The panels are as in Figure 9.

neurons are well suited to individually inhibit large groups [thousands according to Hámori and Szentágothai (1966)] of GrCs regardless of movement direction. In principle, the excitation of a GC by numerous parallel fibers originating from GrCs, each tuned to a particular direction, could account for the broad directional field of that neuron. However, the efficacy of the parallel fiber input to GCs has been demonstrated to be too weak to modulate their firing (Dieudonne, 1998), leading to assertions that the activity of GCs is determined mainly by direct MF excitation. Because MFs fire preferentially for eye saccades in a single direction, the absence of directional preference in GCs would require a substantial convergence of direct MF excitatory inputs onto single neurons. Still, compared with the vast majority of GC dendrites that ascend toward the molecular layer, only few are thought to branch within the granule layer (Pellionisz and Szentágothai, 1973). This observation would alternatively lend credit to the assumption that GCs are modulated by a climbing fiber-dependent signal and other cerebellar interneurons (Barmack and Yakhnitsa, 2008). If the GC modulation were, however, climbing fiber-dependent, it would be expected to show changes during saccadic adaptation, which we found not to be the case.

### The nonspecificity of GC activity to saccade metrics is inconsistent with the gain control theory

The population activity of MFs showed distinct linear relationships with saccade metrics (Fig. 8*C*,*D*). Therefore, the abundance of information carried by MFs to the cerebellum is movement specific. Ohtsuka and Noda (1992) reported tuning curves to saccade amplitude of MFs similar to ours, and van Kan et al. (1993) further confirmed that several properties of MF firing correlated with joint angle, movement velocity, and duration. Conversely, the GC population did not reflect any features specific to the metrics or timing of eye saccades (Fig. 8*A*,*B*). The study by Edgley and Lidierth (1987) is the only other one to our knowledge to examine the specificity of GCs to movement metrics. In line with our own results, they reported that different

speeds of locomotion and platform inclination angles resulted in unaltered timing patterns and discharge rates of most GCs. Therefore, the observation that MFs convey movement-specific data to the cerebellum and that GCs are oblivious to this information, suggests that these neurons are not well suited to perform gain control over PC discharge. In contradiction with the gain control theory, our results suggest that larger and/or longer eye saccades will result in a higher/longer excitation of GrCs by MFs, but the same GrCs will not receive a proportionately larger inhibition from GCs that would be needed to limit the amount of MF transmission to PCs.

**Comparison with saccade-related properties of Purkinje cells**

The population response of PCs has been shown to be characterized by an intriguingly precise reflection of saccade timing (Thier et al., 2000), while our present results show that GCs fail to provide any alike information. It is clear that any influence GCs might have on PCs via their inhibition of GrCs cannot be responsible for this feature of the PC population. Our other finding is that MFs, the input to the cerebellar cortex, encode an abundance of movement-specific information, which contrasts the much more restricted information found on the output side at the level of PCs. Unlike PCs, the MF population response does not end simultaneously with saccade end but lasts much beyond (Fig. 8*D*), and furthermore, bursting MFs fire on average more for larger saccades (Fig. 8*C*), which is not characteristic of PCs (Thier et al., 2000). A confinement of the input information seems thus to be necessary on its pathway toward the PC layer, in which the inhibitory GCs, although anatomically in an ideal position, are hardly involved. More generally, if one assumes that the firing properties of a major interneuron are indicative of the saccade-related properties of the granular layer at large, than the saccade-related timing of the PC population is not a mere reflection of a previous processing in the granular layer of the movement-specific MF input. Alternatively, climbing fibers and molecular layer interneurons may be more important in modulating this unique activity of PCs, which might also be an emerging property of the circuitry rather than reflective of input.

Another distinctive feature of GCs is that they fail to exhibit the kind of plasticity observed in PC simple spikes (Catz et al., 2008) during saccadic adaptation. Our results do not suggest any strong correlation between changes in GC firing and changes in the adapting amplitude of saccades (Fig. 9, 10). Therefore, the PC simple spike activity modulation of saccade dynamics during adaptation [see the study by Catz et al. (2008) for details] seems not to be caused by a previous processing of the MF input in the granular layer, but is instead a consequence of adjusting the complex spike activity (Catz et al., 2005). Our results thus show that behaviorally relevant cerebellar plasticity emerges only at the level of PCs, where the climbing fiber input seems to play the major role.

## References


Albus JS (1971) A theory of cerebellar function. Math Biosci 10:25–61.

Barmack NH, Yakhnitsa V (2008) Functions of interneurons in mouse cerebellum. J Neurosci 28:1140–1152.

Catz N, Dicke PW, Thier P (2005) Cerebellar complex spike firing is suitable to induce as well as to stabilize motor learning. Curr Biol 15:2179–2189.

Catz N, Dicke PW, Thier P (2008) Cerebellar-dependent motor learning is based on pruning a purkinje cell population response. Proc Natl Acad Sci U S A 105:7309–7314.

De Schutter E, Vos B, Maex R (2000) The function of cerebellar Golgi cells revisited. Prog Brain Res 124:81–93.

Dieudonne S (1998) Submillisecond kinetics and low efficacy of parallel fibre-Golgi cell synaptic currents in the rat cerebellum. J Physiol 510:845–866.

Dieudonné S, Dumoulin A (2000) Serotonin-driven long-range inhibitory connections in the cerebellar cortex. J Neurosci 20:1837–1848.

Eccles JC, Ito M, Szentagothai J (1967) The cerebellum as a neuronal machine. Berlin: Springer.

Edgley SA, Lidierth M (1987) The discharges of cerebellar Golgi cells during locomotion in the cat. J Physiol 392:315–332.

Geurts FJ, De Schutter E, Dieudonné S (2003) Unraveling the cerebellar cortex: cytology and cellular physiology of large-sized interneurons in the granular layer. Cerebellum, 2:290–299.

Hámori J, Szentágothai J (1966) Participation of Golgi neuron processes in the cerebellar glomeruli: an electron microscope study. Exp Brain Res 2:35–48.

Hanes DP, Thompson KG, Schall JD (1995) Relationship of presaccadic activity in frontal eye field and supplementary eye field to saccade initiation in macaque: poisson spike train analysis. Exp Brain Res 103:85–96.

Holtzman T, Rajapaksa T, Mostofi A, Edgley SA (2006) Different responses of rat cerebellar purkinje cells and Golgi cells evoked by widespread convergent sensory inputs. J Physiol 574:491–507.

Ito M (1984) The cerebellum and neural control. New York: Raven.

Ito M (2006) Cerebellar circuitry as a neuronal machine. Prog Neurobiol 78:272–303.

Judge SJ, Richmond BJ, Chu FC (1980) Implantation of magnetic search coils for measurement of eye position: an improved method. Vision Res 20:535–538.

Kase M, Miller DC, Noda H (1980) Discharges of purkinje cells and mossy fibres in the cerebellar vermis of the monkey during saccadic eye movements and fixation. J Physiol 300:539–555.

Maex R, De Schutter E (1998) Synchronization of Golgi and granule cell firing in a detailed network model of the cerebellar granule cell layer. J Neurophysiol 80:2521–2537.

Marr D (1969) A theory of cerebellar cortex. J Physiol 202:437–470.

McLaughlin SC (1967) Parametric adjustment in saccadic eye movements. Percept Psychophys 2:359–362.

Miles FA, Fuller JH, Braitman DJ, Dow BM (1980) Long-term adaptive changes in primate vestibuloocular reflex. III. Electrophysiological observations in flocculus of normal monkeys. J Neurophysiol 43:1437–1476.

Mitchell SJ, Silver RA (2000) Gaba spillover from single inhibitory axons suppresses low-frequency excitatory transmission at the cerebellar glomerulus. J Neurosci 20:8651–8658.

Ohtsuka K, Noda H (1992) Burst discharges of mossy fibers in the oculomotor vermis of macaque monkeys during saccadic eye movements. Neurosci Res 15:102–114.

Palay SL, Chan-Palay V (1974) Cerebellar cortex: cytology and organization. New York: Springer.

Pellionisz A, Szentágothai J (1973) Dynamic single unit simulation of a realistic cerebellar network model. Brain Res 49:83–99.

Simat M, Parpan F, Fritschy JM (2007) Heterogeneity of glycinergic and gabaergic interneurons in the granule cell layer of mouse cerebellum. J Comp Neurol 500:71–83.

Simpson JI, Hulscher HC, Sabel-Goedknegt E, Ruigrok TJH (2005) Between in and out: linking morphology and physiology of cerebellar cortical interneurons. Prog Brain Res 148:329–340.

Thach WT (1968) Discharge of purkinje and cerebellar nuclear neurons during rapidly alternating arm movements in the monkey. J Neurophysiol 31:785–797.

Thielert CD, Thier P (1993) Patterns of projections from the pontine nuclei and the nucleus reticularis tegmenti pontis to the posterior vermis in the rhesus monkey: a study using retrograde tracers. J Comp Neurol 337:113–126.

Thier P, Dicke PW, Haas R, Barash S (2000) Encoding of movement time by populations of cerebellar purkinje cells. Nature 405:72–76.

van Kan PL, Gibson AR, Houk JC (1993) Movement-related inputs to intermediate cerebellum of the monkey. J Neurophysiol 69:74–94.

Vos BP, Maex R, Volny-Luraghi A, De Schutter E (1999a) Parallel fibers synchronize spontaneous activity in cerebellar Golgi cells. J Neurosci 19:RC6.

Vos BP, Volny-Luraghi A, De Schutter E (1999b) Cerebellar Golgi cells in the rat: receptive fields and timing of responses to facial stimulation. Eur J Neurosci 11:2621–2634.

Behavioral/Systems/Cognitive

# The Absence of Eye Muscle Fatigue Indicates That the Nervous System Compensates for Non-Motor Disturbances of Oculomotor Function

**Mario Prsa, Peter W. Dicke, and Peter Thier**
Department of Cognitive Neurology, Hertie Institute for Clinical Brain Research, University of Tübingen, 72076 Tübingen, Germany

**The physical properties of our bodies are subject to change (due to fatigue, heavy equipment, injury or aging) as we move around in the surrounding environment. The traditional definition of motor adaptation dictates that a mechanism in our brain needs to compensate for such alterations by appropriately modifying neural motor commands, if the vitally important accuracy of executed movements is to be preserved. In this article we describe how a repetitive eye movement task brings about changes in eye saccade kinematics that compromise accurate motor performance in the absence of a proper compensatory response. Surgical lesions in animals and human patient studies have previously demonstrated that an intact cerebellum is necessary for the compensation to arise and prevent the occurrence of hypometric movements. Here we identified the dynamic properties of the eye plant by recording from abducens motoneurons responsible for the required movement and measured the muscle response to microstimulation of the abducens nucleus in rhesus monkeys. The ensuing results demonstrate that the muscular periphery remains intact during the fatiguing eye movement task, while internal sources of noise (drowsiness, attentional modulation, neuronal fatigue etc.) must be responsible for a diminished oculomotor performance. This finding leads to the important realization that while supervising the accuracy of our movements, the nervous system takes additionally into account and adapts to any disruptive processes within the brain itself, clearly unrelated to the dynamical behavior of muscles or the environment. The existence of this supplementary mechanism forces a reassessment of traditional views of cerebellum-dependent motor adaptation.**

## Introduction

While quickly ascending a flight of stairs, one heavily relies on the ability of her CNS to produce motor commands that will accurately guide the limb to the desired target at each step. After extensive physical exercise and with fatigued limb muscles, the individual is still able to perform the climbing task with identical accuracy, albeit with slower displacements. This is because our motor commands are continuously adjusted to produce accurate movements while the properties of our body change; a neural mechanism called motor adaptation. Previous experimental investigations of motor adaptation have almost exclusively been concerned with the ability to adapt motor behavior to novel dynamics of the body or external environment, by for instance imposing force fields to ongoing arm movements (Shadmehr and Mussa-Ivaldi, 1994; Li et al., 2001).

Suppose now that the person climbs up the flight of stairs after having performed mentally exhausting nonphysical work. This would intuitively lead to slower movement kinematics even though the physical dynamics of the limb being displaced are unaltered. This example highlights our contention that, as opposed to peripheral physical changes, movement accuracy can additionally be compromised by central cognitive processes that deteriorate the reliability of converting the desired displacement plan into the actual movement. We then further argue that the concept of motor adaptation needs to be extended to include the ability of the CNS to cope not only with external physical changes but with disruptive sources of noise present within the brain itself. The existence of this supplemental compensatory mechanism seems to be of even higher importance; because the manifestation of such central disturbances during a person's daily activities are ostensibly more recurrent than modifications of the motor periphery.

Here we provide the first conclusive evidence that during a motor task, a neural mechanism actively compensates for changes unspecific to the muscular periphery that would otherwise cause movements to become inaccurate. We trained rhesus monkeys to perform a strenuous task during which the oculomotor system, due to extensive repetitive use, undergoes significant physiological changes as reflected by progressively slower saccadic eye movements. Accuracy is however maintained because of a compensatory upregulation of movement duration. Previous investigations of the effects of repetitive eye movements on oculomotor performance (Brozek, 1949; Bahill and Stark, 1975; Schmidt et al., 1979; Fuchs and Binder, 1983; Straube et al., 1997; Chen-Harris et al., 2008; Xu-Wilson et al., 2009) were all based on psychophysical measures and the reached conclusions about the

Received July 27, 2010; revised Aug. 26, 2010; accepted Sept. 20, 2010.

This work was supported by Deutsche Forschungsgemeinschaft Grants SFB 550 A7 and EU PITN-GA-2009-238214.

Correspondence should be addressed to Prof. Dr. Peter Thier, Center for Neurology, Hertie Institute for Clinical Brain Research, Department of Cognitive Neurology, Hoppe-Seyler-Strasse 3, 72076 Tübingen, Germany. E-mail: thier@uni-tuebingen.de.

DOI:10.1523/JNEUROSCI.3901-10.2010

 0270-6474/10/3015834-09$15.00/0

origin of fatigue remained suggestive at most. We demonstrate from single motor unit recordings in the monkey abducens nucleus that the system dynamics of the peripheral eye plant remain unaltered during the "fatigue" experiment. This result indicates that the slower eye kinematics are not the consequence of a muscular fatigue, but supports our hypothesis that cognitive factors (i.e., mental fatigue) are degrading the oculomotor functioning and are being successfully compensated to preserve accurate movements.

## Materials and Methods

### *Animals*

Three rhesus monkeys (*Macaca mulatta*) were prepared for eye position recording using the magnetic scleral search coil technique (Judge et al., 1980). To painlessly immobilize the monkeys' heads, a titanium pole was attached to the skull with titanium bone screws. Titanium was used for its high biocompatibility and for compatibility in functional magnetic resonance imaging settings. Recording chambers (also titanium) were implanted over the posterior part of the skull to gain access to the abducens nuclei for extracellular recordings by advancing electrodes through the cerebellum (Prsa et al., 2009). All surgical procedures were conducted under general anesthesia (introduced with ketamine and maintained by inhalation of isoflurane and nitrous oxide, supplemented by remifentanil) with control of vital parameters (body temperature, $CO_2$, $O_2$, blood pressure, ECG), followed the guidelines set by the National Institutes of Health and national law and were approved by the local committee supervising the handling of experimental animals. After the surgery, monkeys were supplied with analgesics until full recovery.

### *Behavioral tasks*

During all behavioral tasks, the monkeys sat head-fixed in a primate chair in total darkness. They were trained to make saccadic eye movements to a white target dot (0.2° diameter) displayed on a monitor screen positioned 43 cm in front of the animals. The eye position signal measured by the scleral search coil method was calibrated and sampled at 1 kHz. The monkey received an automatic liquid reward at the end of a successful trial. A trial counted as successful, if the animal maintained gaze inside an eye position window ($\pm$1.5°) during initial fixation until the target jump, and displaced the eyes back inside the window in its new position and maintained fixation no later than 300 ms after the jump.

*Saccadic fatigue paradigm.* The monkeys were trained to execute large numbers of visually guided eye saccades from a central fixation point toward a peripheral target in the horizontal direction. During each experiment the target always appeared at the same eccentricity but was varied from session to session anywhere between 8° and 24°, with 10–12° being the most frequent amplitude range (Fig. 1*C*). The central point was fixated for 400–500 ms, after which the peripheral target appeared with the simultaneous disappearance of the fixation target. After the saccadic eye movement, the monkeys had to fixate the peripheral target for 250–400 ms. To maximize the rate of consecutive saccades, the intertrial interval was set to zero (the next trial was initiated as soon as the previous one finished).

*Amplitude tuning paradigm.* To test for the tuning of cells to saccades of different amplitudes, before the fatigue experiment, the animals executed visually guided saccades from a central fixation point toward targets at eight different peripheral eccentricities (from 2.5° to 20° in 2.5° steps) in the horizontal direction. Ten saccades on average (but never less than six) were performed for each eccentricity. The central and peripheral fixation times in this paradigm were 900–1000 ms and 500–700 ms. The intertrial interval was varied between 100 and 500 ms and the target amplitude was randomly chosen for each trial. The post-fatigue amplitude tuning had the same fixation and intertrial interval durations as in the saccadic fatigue paradigm, and was performed as an immediate continuation of the latter.

### *Electrophysiology and microstimulation*

Postsurgical MRI was used to facilitate the anatomic localization of the abducens nucleus. The identification of this area was confirmed by extracellular recordings characterized only by the typical burst-tonic discharge patterns during ipsilateral saccades of single isolated units and more often of a noisy multiunit background response, which could be continuously kept on the electrode signal for long tuning distances (up to 2 mm). We therefore exclude the possibility of having recorded from neurons with similar responses in the immediately adjacent nucleus prepositus and medial vestibular nuclei, which additionally harbor neurons with distinctly different discharge patterns that were never encountered. Furthermore, we attempted to map the limits of the abducens nucleus by slightly modifying each time the coordinates of the penetrating electrode inside the recording chamber. An effort was then made to record from the central portion of the abducens nuclei to avoid the units innervating nontwitch muscle fibers lying around its periphery (Büttner-Ennever et al., 2001).

All extracellular action potentials were recorded with commercially available enamel-coated tungsten microelectrodes (Frederick Haer) with 1–10 M$\Omega$ nominal impedances that were driven to the brainstem by means of a high precision motor (1 $\mu$m movement steps). Single units were isolated on-line with the Multi Spikes Detector software (Alpha Omega Engineering) by detecting and sorting waveforms according to shape. Only well isolated waveforms, clearly distinguishable from the ever present background activity, were considered for further recording.

In the abducens microstimulation manipulations, the stimulus consisted of a sequence of constant current biphasic pulses (each phase lasting 0.2 ms) and was applied for 100 ms at four different frequencies (300 Hz, 400 Hz, 500 Hz and 600 Hz). The current intensity was varied between 25 and 35 $\mu$A between different sessions but was held constant throughout each individual session. For the purpose of the stimulation experiments, one monkey was trained to fixate a central fixation point for a random time interval (700–1000 ms) after which the point was extinguished and a gap interval of 500 ms followed before a peripheral target appeared randomly in any of eight peripheral directions. The stimulation was applied 50–200 ms into the gap period in 20–30% of the trials randomly interleaved, at least four times for each of the four stimulus frequencies. A liquid reward was delivered to the monkey each time it successfully made a saccade toward the final peripheral target.

### *System identification and data analysis*

All analyses were performed off-line with custom programs compiled in Matlab (MathWorks). The recorded horizontal eye position signals were sampled at 1 kHz, smoothed with a Savitzky–Golay filter (window = 10 points, polynomial degree = 4) and velocity traces were computed by taking digital derivatives. We used the 20 °/s velocity criterion for detecting saccade onset and end. Saccades with maximal velocity below 100 °/s or with durations longer than 100 ms were discarded. We estimated the instantaneous firing rate of the recorded neurons with a continuous spike density function, generated by convoluting the spike train with a Gaussian function of width $\sigma = 5$ ms.

The parameters of the two models in Equations 1 and 2 were evaluated for each recorded neuron using a system identification technique similar to the one previously developed for the analysis of pontine burst neurons (Cullen et al., 1996) and also applied to the discharges of abducens neurons (Sylvestre and Cullen, 1999). Briefly, each of the model formulations in the continuous time domain was first mapped into discrete time using the finite differences transform and assuming an output-error model structure. The parameters of the discrete time formulation were then evaluated using a prediction error method with preprogrammed functions available in the Matlab System Identification Toolbox. The method consists of an iterative numerical search for a parameter set that minimizes the distance between the predicted outputs (according to the parameter set at each iteration) and the actual measured outputs. The iterative update of each parameter is done according to the damped Gauss–Newton method (Ljung, 2002). This was preferred to a linear regression algorithm because of the partially correlated inputs (position, velocity, acceleration) and the dependence of the current on the previous output values in the second-order model. Only the saccadic portions of eye movements and spike density functions (traces between saccade onset and end) were used and data from multiple trials (always $N/2$ of the total set of $N$ trials (see below); $N = 80$ on average) were merged for the

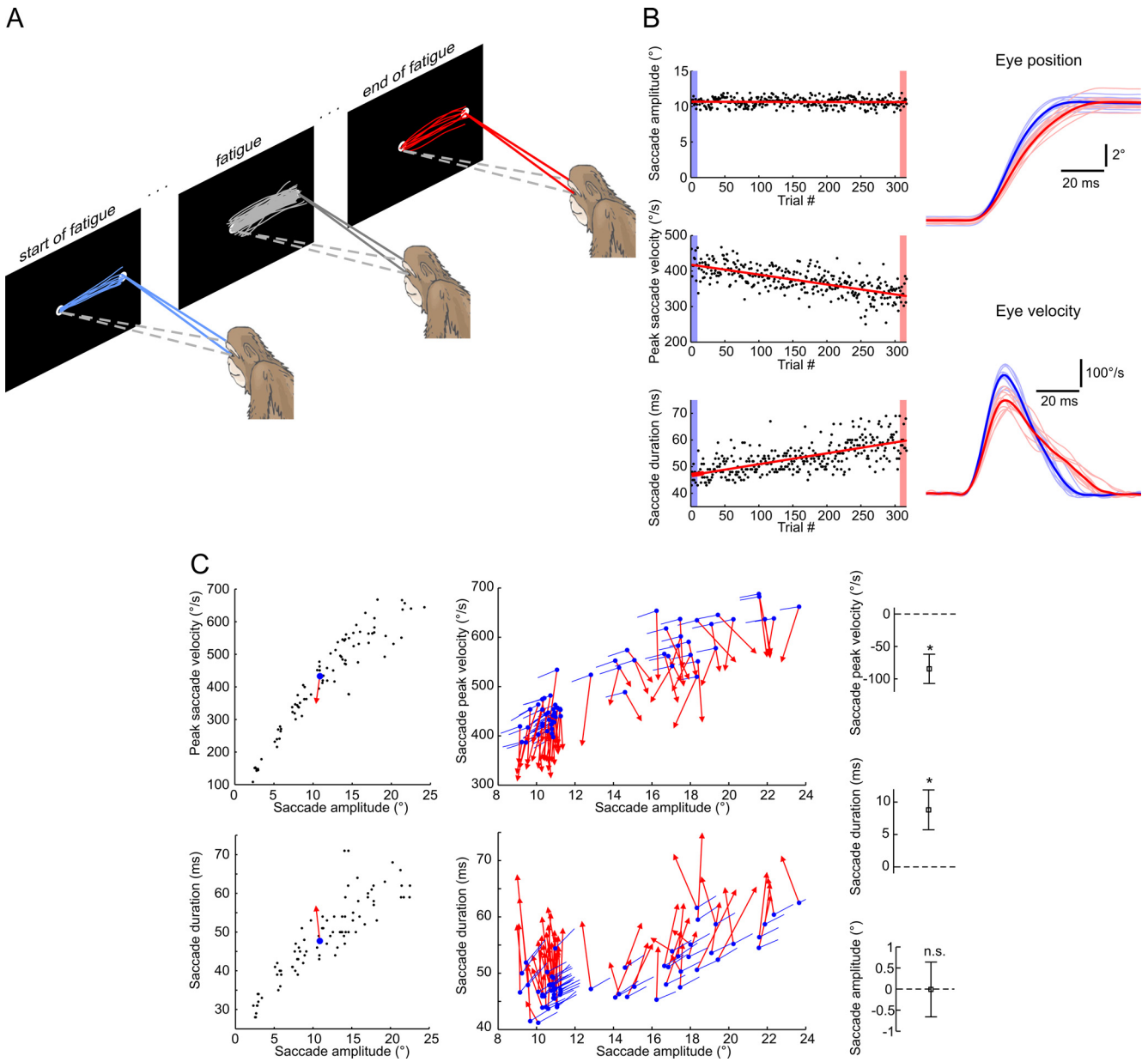


**Figure 1.** Typical changes in eye saccade kinematics during saccadic fatigue. ***A***, Illustrative depiction of the fatigue experiment. The selected convention was to define the first and last 10 trials as the start and end of fatigue. ***B***, Saccade peak velocity and duration, but not amplitude, progressively change during the fatigue experiment. Left, Lines are least-squares linear fits to the three saccade metrics plotted for each consecutive trial. Right, Eye position and eye velocity individual (thin) and mean (bold) traces at the start (blue) and end (red) of the fatigue experiment. ***C***, Eye saccade kinematics move away from their pre-fatigue main sequences. Left, Average data points at the start (blue dots) and end (red arrowheads) of one fatigue session with the pre-fatigue peak saccade velocities and durations plotted against amplitude (black dots). Middle, Same average data points for all 62 fatigue sessions. Blue lines indicate the direction of change predicted by the corresponding pre-fatigue main sequences. Right, Mean $\pm$ SD changes in peak saccade velocity and duration across all fatigue sessions were statistically different from zero (*t* tests, $*p < 10^{-30}$) while the mean amplitudes did not significantly (n.s.) change (*t* test, $p = 0.91$).

identification analysis. Because the burst of spikes in abducens units leads saccade onset by a few milliseconds (Fig. 2*A*), the spike density functions had to be shifted forward in time to be aligned with the movement of the eyes. This lead time was evaluated both subjectively and by the dynamic estimation method (Cullen et al., 1996). The latter consists of repeating the identification for a range of lead times and choosing the one the gives the highest goodness of fit measure. The initial conditions were always taken from the measured data.

A bootstrap analysis provided confidence intervals for each evaluated model parameter (Fig. 2*B*) and allowed a statistical comparison between the pre-fatigue and post-fatigue estimates for individual neurons (Fig. 3). It consisted of repeating the system identification for each neuron 1300 times on different subsets of the data each time. The different subsets were formed by taking at random, *without* replacement, $N/2$ trials from the total set of $N$ trials (for $N = 80$ trials, $10^{23}$ such combinations are possible). The models were then validated at each repetition on the other, independent, $N/2$ half of the trials by computing the variance accounted for (VAF). The VAF is calculated as $\{1 - [\mathrm{var}(F_{est} - F_m)/\mathrm{var}(F_m)]\}$ where $F_m$ is the measured and $F_{est}$ the estimated firing rate, and provides a normalized measure of how much of the variability in a unit's discharge is explained by the model.

The population activity of all neurons (Fig. 3*B*) was computed by dividing the range of saccade amplitudes into equally sized bins of 0.5°. Eye position traces and the associated spike density functions were then assigned to their corresponding bins and average saccades and firing rates were then computed across all trials and all neurons for each bin.

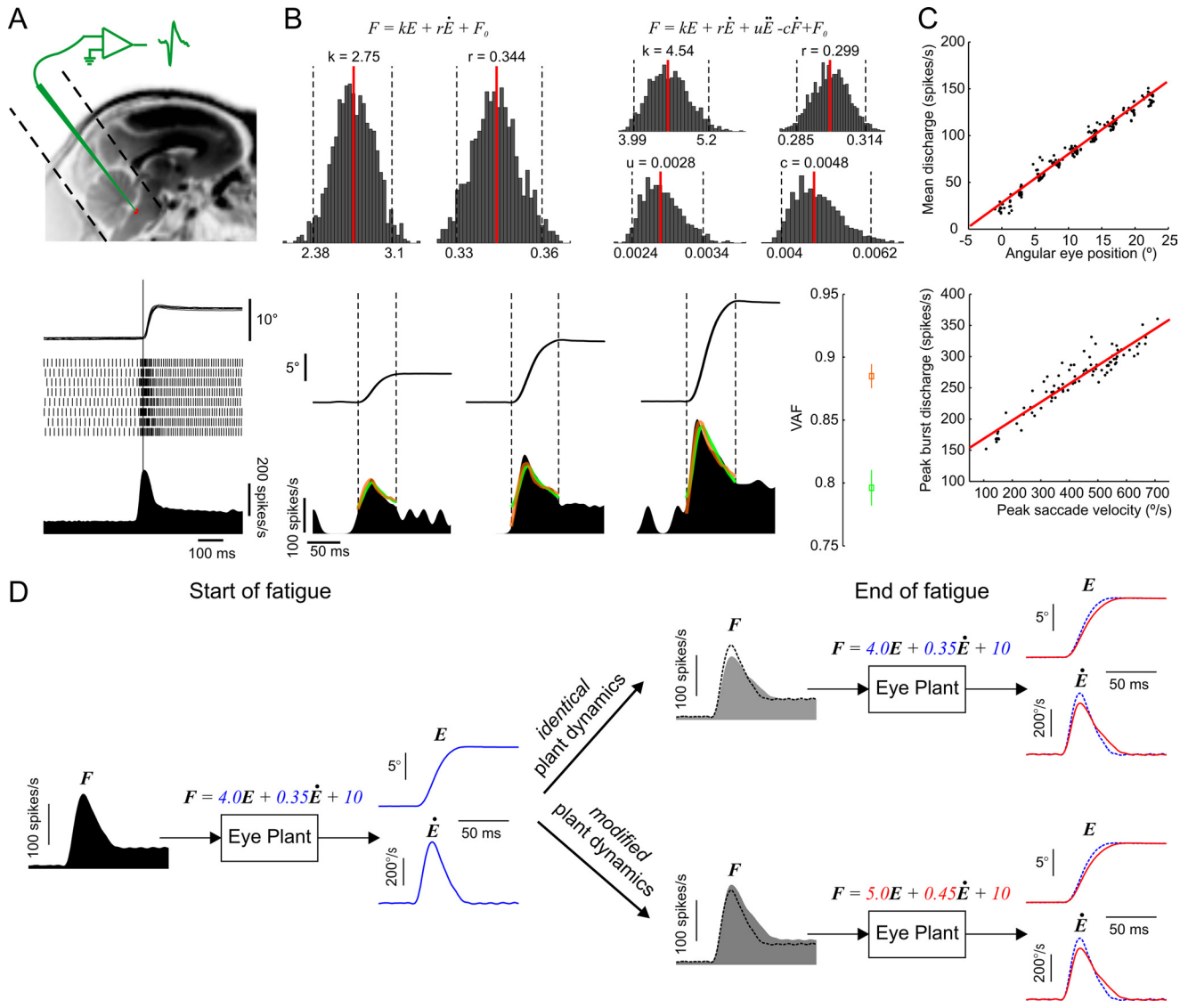


**Figure 2.** Characterization of abducens neurons' activity. ***A***, Recording neurons from the abducens nucleus. Top, Approximate anatomical location of the abducens nucleus in an MRI image of a rhesus monkey. Dotted lines reveal the placement and orientation of the recording chamber. Bottom, A typical saccade-related discharge pattern of an abducens neuron. The superimposed eye traces, detected action potentials and the average spike density function are aligned on saccade onset (vertical line). ***B***, Quantitative assessment of abducens discharges. Top, Spiking rates were fitted with the two model formulations and bootstrap histograms were computed for each model parameter. Median values (red lines) and limits of the 95% confidence intervals (dotted lines) are provided. Bottom, Examples of eye traces and spike density functions recorded during three saccades of increasing amplitude. The VAF measure (mean ± SD) was used to evaluate how well the models fit the data. The predicted activity is superimposed on the actual one for the first-order (green) and second-order (orange) model fits. Dotted vertical lines indicate the onset and end of each saccade. ***C***, Position and velocity sensitivity measures. Data from the same example neuron with least-squares linear regression fits (red lines). ***D***, Simulation of eye plant dynamics with the first-order model showing changes in firing rates of abducens motoneurons that would be expected under the muscular and nonmuscular fatigue hypotheses. Left, Simulated motoneuron spike density profile (***F***) given the pre-fatigue eye position (***E***) and velocity ($\dot{\boldsymbol{E}}$) traces (in blue) with the indicated model parameters. Right, Same simulation with a slower and longer post-fatigue eye saccade (in red) in the two cases where the eye plant parameters are either modified or remain unchanged. The simulated pre-fatigue data (dotted traces) are superimposed for comparison purposes. With identical plant dynamics, the expected changes in firing rates parallel those in eye saccade kinematics, whereas in the case of modified dynamics they do not. In the latter case, the neuron's sensitivity to eye position and velocity (as measured in ***C***) would be altered, and attempting to predict the firing rate with the pre-fatigue eye plant dynamics (as in ***B***) would underestimate the actual rate.

The duration versus amplitude main sequence was fit with a straight line and that of the peak velocity versus amplitude with an exponential function. The direction of change predicted by the main sequences during fatigue (Fig. 1*C*, blue lines) was then evaluated as the tangent to these two fitting curves evaluated at the relevant data points. The peak burst discharge and the mean discharge during fixation were evaluated respectively as the spike density function (after being shifted by its lead time) maximum value between saccade start and end, and its mean value in an interval of 400 ms, 50 ms after/before saccade end/start.

We performed paired or unpaired Student's $t$ tests whenever we wished to evaluate whether two data samples came from distributions with equal means. Normality of data was tested with the Kolmogorov–Smirnov test. We deemed the difference to be statistically significant when the probability ( $p$ value) of having distributions with equal means did not surpass the 5% level.

## Results

### Fatiguing the oculomotor system

We trained three rhesus monkeys to execute large numbers of visually guided eye saccades from a central fixation point toward a peripheral target at a very fast rate (Fig. 1*A*). Each experiment consisted of 500 saccades on average, performed at a mean rate of 1 saccade every 2 s. Changes in saccade kinematics are readily observed throughout the course of such an experiment; peak

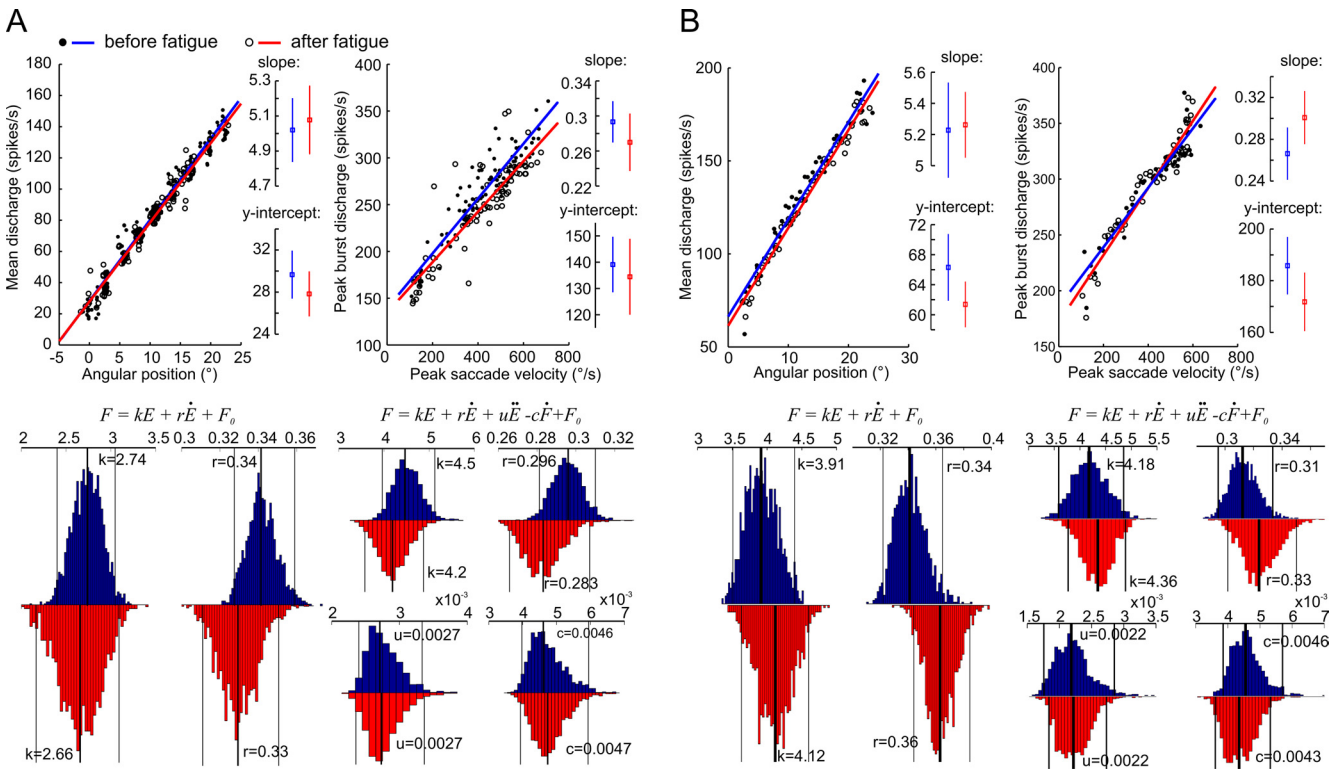


**Figure 3.** Eye plant dynamics are not altered by saccadic fatigue. ***A***, Comparison of pre-fatigue and post-fatigue discharge properties of a single abducens neuron. Top, Position and velocity sensitivity data with their least-squares linear regression fits before and after the fatigue experiment. Insets provide the slopes and *y*-intercepts (with their 95% confidence intervals) of the regression lines. Bottom, Bootstrap distributions of the first- and second-order model parameters evaluated before (blue) and after (red) fatigue. On each histogram, the median values (thick lines) with their 95% confidence intervals (thin lines) are provided. ***B***, Comparison of pre-fatigue and post-fatigue saccade-related properties of a population response of 62 neurons. Same measures as in ***A***. The population activity was computed by dividing the range of saccade amplitudes into equally sized bins of 0.5°. Eye position traces and the associated spike density functions were then assigned to their corresponding bins and average saccades and firing rates were then computed across all trials and all neurons for each bin.

velocity decreases while accuracy is maintained because duration increases in a fully compensatory manner (Fig. 1*B*).

Eye saccades are otherwise considered to be very stereotypical movements. Their velocity traces typically have bell-shaped profiles and a precise nonlinear association exists between peak saccade velocity and amplitude on the one hand, and a linear relation between saccade duration and amplitude on the other; referred to as the "saccadic main sequence." The main sequence dictates that higher amplitude saccades become increasingly both longer and faster. Our results show that fast repetitive eye movements largely skew the velocity profiles (Fig. 1*B*) and cause the saccade kinematics to move away from their main sequence (Fig. 1*C*). Explicitly put, the slower saccades caused by the fatigue should normally be indicative of a neural command leading to smaller amplitude movements, yet a late extension in movement duration brings the saccade to the intended target and keeps amplitude constant. Both saccade duration and velocity change, while the amplitude remains constant; the fatigue experiment therefore disrupts the normal mode of operation of saccadic eye movements. The increase in saccade duration seems furthermore to be reflective of a compensatory cerebellum-dependent mechanism, since it is only present in healthy subjects, whereas it does not accompany the drop in peak velocity in cerebellar patients (Golla et al., 2008; Xu-Wilson et al., 2009) and monkeys with cerebellar lesions (Barash et al., 1999) and hence does not prevent the expected hypometric saccades in those cases. Therefore, the preservation of accuracy despite a breakdown of ordinary motor behavior during saccadic fatigue is clearly indicative of an adaptive neural process.

We look next at whether the compensation observed during saccadic fatigue falls into the traditional definition of motor learning alluded to in the introduction. In other words, does the cerebellum-dependent mechanism adapt to changes in the dynamic properties of the peripheral eye plant (i.e., muscular fatigue) or to some other physiological changes in the oculomotor system?

### Identification of eye plant dynamics

The abducens nucleus located in the pontomedullary brainstem just beneath the floor of the fourth ventricle (Fig. 2*A*) harbors mainly two functional cell groups; motor neurons and internuclear neurons. The axons of motor neurons give rise to the sixth cranial nerve and innervate the lateral rectus muscle of the eye. The internuclear neurons project axons to the subgroup of motor units in the contralateral oculomotor nucleus which directly innervate the medial rectus muscle of the other eye. Therefore, a burst of spikes in neurons of the abducens nucleus is translated into muscle force and then into eye movement in a fairly direct way. It has the effect of rotating the ipsilateral eye temporally and the contralateral eye nasally, effectively producing a horizontal ipsiversive binocular eye movement.

A typical abducens neuron discharge during ipsiversive saccades displays a strong phasic burst of spikes during the saccade, followed by a constant tonic firing rate that lasts throughout peripheral fixation (Fig. 2*A*). The phasic burst accelerates the eyes during the saccadic component of movement against the viscous forces acting on the eye globe, and the tonic discharge holds the eyes fixed at the peripheral position by counteracting

**Table 1. The parameters of the evaluated models as well as the position and velocity sensitivity curves did not change as a result of fatigue for the population of abducens neurons**

| | Parameter | Before fatigue | After fatigue | Paired *t* test ( *p* value) |
|---|---|---|---|---|
| First-order model | *k* | 5.3 (7.6, 3.9) | 5.6 (7.6, 3.5) | 0.47 |
| | *r* | 0.35 (0.43, 0.3) | 0.37 (0.45, 0.3) | 0.035 |
| VAF (mean ± SD) | | 0.63 ± 0.1 | 0.62 ± 0.1 | |
| Second-order model | *k* | 5.8 (8.2, 2.6) | 5.6 (9.4, 2.9) | 0.49 |
| | *r* | 0.52 (0.82, 0.27) | 0.5 (0.79, 0.28) | 0.63 |
| | *u* | 0.014 (0.02, 0.009) | 0.015 (0.021, 0.011) | 0.62 |
| | *c* | 0.037 (0.043, 0.03) | 0.036 (0.046, 0.027) | 0.92 |
| VAF (mean ± SD) | | 0.67 ± 0.1 | 0.67 ± 0.1 | |
| Position sensitivity | slope | 5.61 ± 2 | 5.61 ± 2.2 | 0.99 |
| | *y*-intercept | 53.3 ± 43.6 | 52.7 ± 39.4 | 0.78 |
| Velocity sensitivity | slope | 0.32 ± 0.16 | 0.33 ± 0.16 | 0.41 |
| | *y*-intercept | 194.6 ± 84.3 | 191 ± 90.6 | 0.49 |

Values followed by parenthetical values are medians (upper/lower quartile). Values followed by ± values are means ± SD.

the elastic forces that pull the eye back toward midline. This typical phasic-tonic pattern of discharge reflects the dynamic properties of the "eye plant" (production of muscle force and the action of that force on the eye globe and supporting orbital tissues) that need to be overcome to produce the desired saccadic eye movement (Robinson, 1964, 1970). The eye plant dynamics thus seem to be dominated by its viscoelastic properties and can be modeled as a first-order system (Eq. 1) between the firing rate of abducens neurons ($F$) at input and instantaneous eye position ($E$) at output ($k$, elasticity constant, $r$, viscosity constant, $F_0$, bias term).

$$F = kE + r\dot{E} + F_0. \quad (1)$$

In a notable study evaluating a number of different eye plant model formulations (Sylvestre and Cullen, 1999), the first-order model in Equation 1 was indeed shown to be an adequate descriptor of motor neuron discharges during saccades. A second-order formulation (Eq. 2) including an acceleration term ($u\ddot{E}$) and a slide term ($-c\dot{F}$), was however shown to significantly improve the quality of fit and best account for the dynamics between firing rate and the saccadic eye movement.

$$F = kE + r\dot{E} + u\ddot{E} - c\dot{F} + F_0. \quad (2)$$

Before the fatigue experiment, we recorded single neurons in the abducens nucleus while the monkeys made saccades to targets of varying amplitudes (80 saccades on average between 2.5° and 20°). We used these data to run a system identification analysis of the two model formulations in Equations 1 and 2, obtained bootstrap confidence intervals of each evaluated parameter and validated the identified models on an independent set of data (see Materials and Methods for details). The identification and validation results are provided for one example neuron in Figure 2*B*. The mean (±SD) percentage of variance in the firing rates of the recorded neurons that could be accounted for (VAF) by the first- and second-order model fits were 0.63 (±0.1) and 0.67 (±0.1) respectively. From the same data, we also computed the traditional velocity and position sensitivity tuning curves (relationship between peak saccade velocity and peak burst discharge, and between eye position and firing rate during fixation) for each recorded neuron (Fig. 2*C*). The latter provides an additional, more qualitative, description of the relationship between abducens neuron discharges and eye saccade metrics.

We then continuously kept recording the same neurons throughout the fatigue experiment and repeated the above task and identification analysis immediately after. The muscular fatigue hypothesis predicts that after the fatigue experiment, the system identification should yield significantly larger parameters of eye plant dynamics as well as increased slopes of the position and velocity sensitivity curves compared with before fatigue. The model simulations in Figure 2*D* describe the expected changes in the firing rates of abducens motoneurons under the muscular and nonmuscular fatigue hypotheses. We recorded a total of 62 neurons from three monkeys (31 from monkey R, 9 from monkey N and 22 from monkey H) and present the obtained results in the following section.

### Eye plant dynamics are not altered by fatigue

The single example in Figure 3*A* illustrates the consistent finding that the dynamics of the eye plant, evaluated from single neuron data by the traditional first-order and a more complex second-order model, did not show any significant changes as a result of fatigue. The corresponding pairs of model parameters, evaluated with the pre-fatigue and post-fatigue data separately, systematically showed an overlap between their 95% confidence intervals. A distribution of each parameter evaluated from all 62 different neurons, showed a marginally significant increase after fatigue in the mean value of the $r$ parameter in the first-order model, while the difference remained highly insignificant for the distributions of all other parameters (Table 1). Moreover, the neurons' sensitivities to peak saccade velocity and static eye position did not change after the fatigue experiment, as revealed by the single cell example (Fig. 3*A*) and a paired comparison between the distributions of the sensitivity curves' slopes and $y$-intercepts of all neurons evaluated before and after fatigue (Table 1).

Extraocular muscles however do not contract in response to a discharge from a single abducens neuron but from a population of many neurons. It is then conceivable that changes in the properties of eye plant dynamics due to muscular fatigue appear in the responses of single neurons in absolute terms only but never reach significant levels. We therefore computed a population response where each average saccadic eye movement was now associated with an average discharge of as many as 62 abducens neurons (see Materials and Methods for details). The identification of eye plant dynamics was then repeated with the population response computed with both the pre-fatigue and post-fatigue sets of data. A comparison of the 95% confidence intervals of the system parameter estimates still revealed large overlaps for all parameters between the two independently evaluated sets (Fig. 3*B*). The velocity and position sensitivity curves based on these average discharges were also not significantly modified by the fatigue sessions.

We next looked at whether any changes of the oculomotor periphery became apparent during the course of the saccadic

fatigue experiment itself. As previously noted, the fast repetitive series of eye saccades brought about significant changes in movement kinematics. For all 62 fatigue sessions during which individual abducens units were being recorded, the monkeys produced the typical pattern of reduced peak saccade velocity and increased duration, all while the amplitude of saccades remained constant. Accordingly, each fatigue experiment moved the relationship between saccade amplitude and each of the two movement metrics (peak velocity and duration) away from their characteristic pre-fatigue main sequences (Fig. 1*C*). The relationship between the firing rates of abducens neurons and these altered saccade kinematics however did not change. First, the drop in peak velocity was accompanied by a decreased peak discharge as predicted by the neuron's velocity sensitivity curve (Fig. 4*A*). When normalized by their corresponding velocity sensitivity regression fits evaluated with the pre-fatigue data, the average peak discharge values plotted against the average peak velocity, at the start and end of the fatigue sessions, fell along the normalized line of unity slope passing through the origin (Fig. 4*A*). The lines connecting the average data points of the first and last 10 trials of the fatigue experiment had a mean (±SD) slope of 0.91 (±0.59) which was not significantly different from one (*t* test, $p = 0.25$). Second, the previously computed dynamic model fits for each neuron could fit equally well both the abducens discharges at the start of fatigue, and those that eventually give rise to the saccades with slower kinematics (Fig. 4*B*). Had the physical dynamics of the eye plant progressively changed during the fatigue experiments, one would expect the identified models to ever more underestimate the actual motor neuron discharges, thus increase the residual variance (variance of the difference between actual and predicted signals) and lead to significantly lower VAF values. No significant differences were however found between the distributions of mean VAF values at the start and end of fatigue for both the first- and second-order models (*t* test, $p = 0.13$ and $p = 0.44$ respectively) for the entire population of 62 neurons.

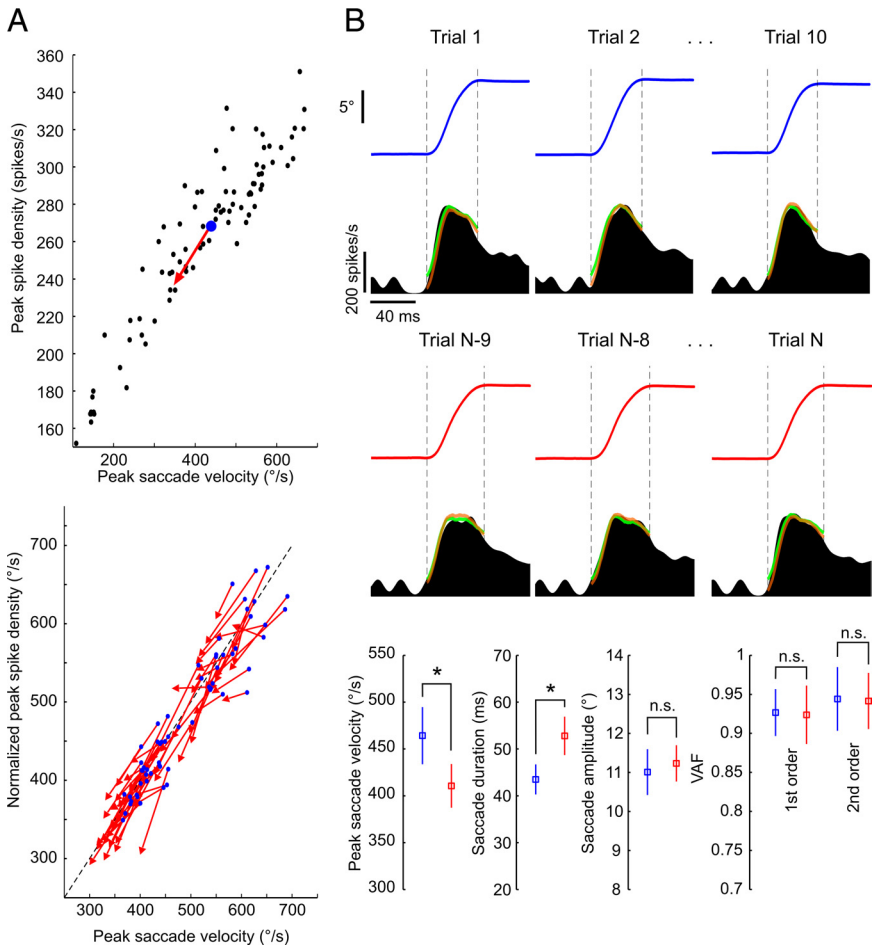


**Figure 4.** No changes in eye plant dynamics occur during the course of fatigue. ***A***, Progressively slower eye saccades are accompanied by parallel decreases in peak discharges of abducens neurons. Top, Average data points at fatigue start (blue dots) and end (red arrowheads) with pre-fatigue peak discharges plotted against saccade peak velocity (black dots) for one example neuron. Bottom, Same average data points for all 62 neurons normalized to the unity-slope line (dotted line) with their respective pre-fatigue velocity sensitivity regression fits [$Y_n = (Y - b)/a$, where $Y_n$ is the normalized version of the peak spike density measure $Y$, and $a$ and $b$ are, respectively, the slope and $y$-intercept of the velocity sensitivity regression line]. ***B***, The evaluated models predicted the activity of abducens neurons equally well throughout fatigue. Top, Eye traces and corresponding abducens neuron spike density functions of an example neuron, with superimposed first (green)- and second (orange)-order model fits, for three trials taken from the start (blue) and end (red) of a fatigue experiment. Bottom, Between the start (blue) and end (red) of the fatigue, mean (±SD) values of peak saccade velocity and duration showed significant changes (*) (*t* tests, $p = 0.0004$ and $p = 0.00003$, respectively), whereas those of saccade amplitude ( $p = 0.36$) and the VAF by the first ( $p = 0.85$)- and second ( $p = 0.88$)-order model fits did not (n.s.).

Our results indicate that the observed changes in eye saccade kinematics were accompanied by parallel changes in the discharge rates of abducens neurons; the dynamic relationship between the two was sustained. The physiological changes that disrupt habitual saccadic performance therefore originate upstream of the abducens nucleus, away from the oculomotor periphery.

### Confirming the absence of muscular fatigue by microstimulation

As an additional control experiment we electrically stimulated the abducens nucleus before and after the long repetitive sequence of saccades. We applied a stimulating current of constant intensity and duration at four different frequencies through the electrode's tip located in the abducens nucleus while the monkey held its gaze fixed in the straight-ahead position (see Materials and Methods for details). The amplitudes and peak velocities of the ipsilaterally evoked saccades were then compared between three different stimulation periods; before the fatigue experiment, immediately after, and following a rest period which allowed voluntary saccades to regain their pre-fatigue velocity and duration levels. If the fatigue sessions caused a weakening of eye muscles, then the current applied at the same site with identical parameters should evoke significantly slower and/or lower amplitude saccades compared with the before fatigue and after rest periods.

We repeated the above described sequence of stimulation experiments during 15 sessions in one monkey, each time at a different site within the abducens nucleus. While increasing the stimulation frequency consistently evoked faster and larger eye

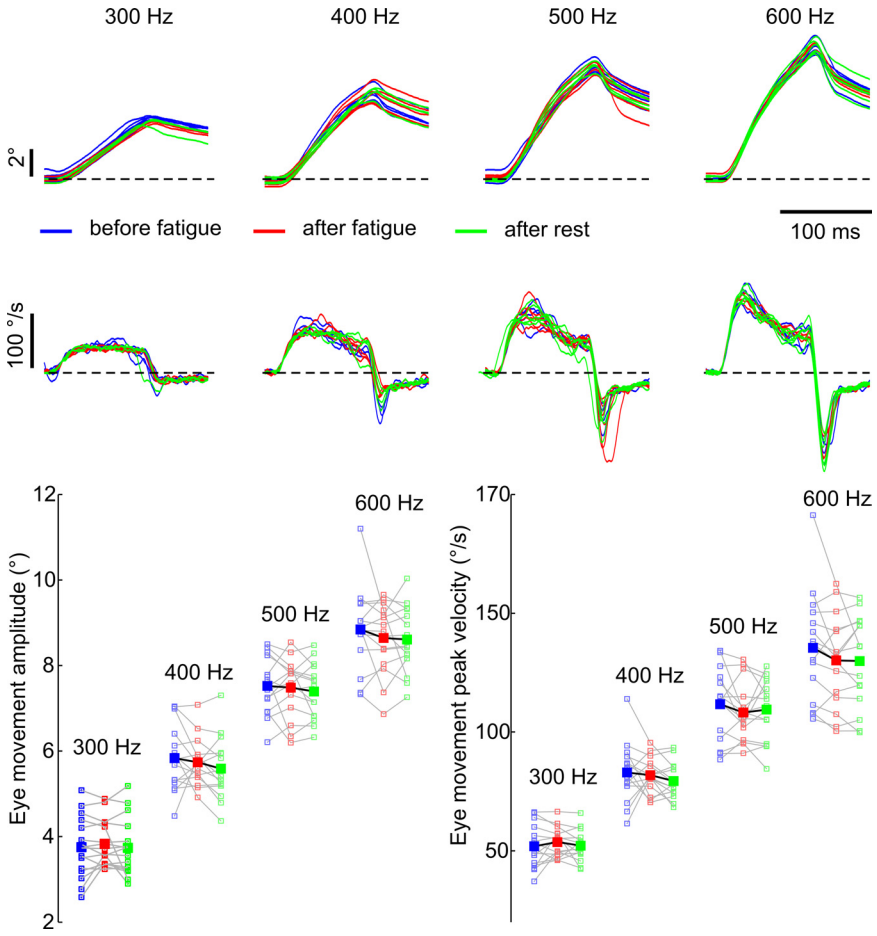


**Figure 5.** Microstimulation of the abducens nucleus confirms the absence of muscular fatigue. Top, Eye position (first row) and velocity (second row) traces of the stimulation-evoked eye movements at four different stimulus frequencies were highly similar before (blue) and after (red) a fatigue session, and after a subsequent rest period (green). The traces are aligned on saccade onset. Bottom, Mean amplitudes and peak velocities of the stimulated saccades for all 15 experimental sessions (small open squares) together with their average values (large filled squares).

movements, no discernable differences could be observed between the three different stimulation periods (Fig. 5). A two-way ANOVA analysis (the two factors being stimulus frequency and stimulation period) confirmed that across the 15 individual sessions, there was a significant main effect of stimulus frequency on peak velocities ( $p = 0$) and amplitudes ( $p = 0$) of the evoked movements. The null hypothesis that either saccade amplitudes or peak velocities were equal for the three stimulation periods could however not be rejected at a significant level ( $p = 0.5$ and $p = 0.52$ respectively). There were also no significant interactions between the two factors for either the amplitude ( $p = 0.99$) or the peak velocity ( $p = 0.96$) measures. It therefore seems that the rectus muscles of the eye respond without change to microstimulation of their motor neurons following a fatiguing eye movement task.

## Discussion

In traditional views of motor adaptation, the neural control of movement is continuously adapted to compensate for any changes in the physical properties of the body or the external environment (due to age, injury, muscular fatigue, carrying weighty objects etc.). The first descriptions of adaptive changes in eye movement control adhered to this view; the observed adaptive processes were implied to compensate for alterations in the oculomotor plant (Kommerell et al., 1976; Abel et al., 1978; Optican and Robinson, 1980; Optican and Miles, 1985; Grossberg, 1986; Scudder and McGee, 2003) and were moreover shown to depend on the cerebellum (Optican and Robinson, 1980; Scudder and McGee, 2003). In studies of arm displacements under external force fields, the ability to learn to move accurately with novel limb dynamics also depends on an intact cerebellum (Smith and Shadmehr, 2005). The prevalent theory suggests that the nervous system adapts to the external perturbation by computing/updating an internal model of either inverse (Shadmehr and Mussa-Ivaldi, 1994; Wolpert and Miall, 1996) or forward dynamics (Wolpert and Miall, 1996) of the actual physical plant. The progressive regulation of eye saccade kinematics during the fatigue experiment that we described is a characteristic example of a cerebellum-dependent motor adaptation that preserves accurate movements (Barash et al., 1999; Golla et al., 2008; Xu-Wilson et al., 2009). A number of early (Brozek, 1949; Bahill and Stark, 1975; Schmidt et al., 1979; Fuchs and Binder, 1983) and more recent (Straube et al., 1997; Chen-Harris et al., 2008; Xu-Wilson et al., 2009) investigations have already speculated that when subjects were engaged in repetitive eye movements, cognitive processes such as mental tiredness might be responsible for a diminished oculomotor performance. By a direct electrophysiological identification of eye plant dynamics, we here provide the first conclusive evidence that the oculomotor periphery remains intact during an exhausting eye movement task. Consistent with *in vitro* studies suggesting that preparations of extraocular muscles of rabbit (Frueh et al., 1994) and mouse (Kaminski and Richmonds, 2002) are particularly fatigue resistant, our results show that even in natural behaviors, primate extraocular muscles do not display any fatigue characteristics analogous to those of skeletal muscles. More remarkable is the implication that saccadic fatigue must be of premotor origin, reflecting altered saccade commands due to modified cognitive modulation or to neuronal adaptation; factors which collectively tend to deteriorate the precision and reliability of the conversion of the initial saccade plan into the actual movement. This deterioration due to "non-motor" noise is prevented by a compensatory mechanism in the cerebellum, which does not subscribe to the above description of classical motor adaptation.

The origin of fatigued saccades is necessarily a corruption of the neural encoding of the planned movement. For instance, the reliability by which the desired displacement is eventually encoded in the superficial and intermediate layers of the superior colliculus (SC) (Schiller et al., 1980; Hanes and Wurtz, 2001) might be gradually diminished during fatigue. This could be caused by either a neuronal habituation to the consequences of the same repeating visual stimulus or by modulation from cortical areas reflecting a state of "mental tiredness" (reduced alertness, motivation, attention etc.) of for instance neurons in the SC which have been found to reflect arousal or attentive states

(Sparks and Mays, 1980). As a result, the SC deep layers would provide a command to the saccade generator in the pons (Raybourn and Keller, 1977; Keller et al., 2000) to move the eyes with inappropriately reduced amplitude, naturally associated with a lower velocity than the initial nonfatigued saccades. The oculomotor cerebellum, which integrates eye movement information from all key cortical and subcortical areas (Thielert and Thier, 1993), then actively increases saccade duration and prevents this inaccuracy by prolonging the saccade-related discharges via its notable projections to the pontine brainstem area (Noda et al., 1990). This plausible hypothesis makes testable predictions which could and should be verified by further electrophysiology and modeling studies of the oculomotor system. What remains certain however is that the typical pattern of cerebellum-dependent changes in saccade kinematics during fatigue is not attributable to a modification in the dynamic properties of the eye plant. In agreement with more recent models of the saccadic system (Quaia et al., 1999; Glasauer, 2003), this observation suggests that instead of solely adapting for long-term alterations in the oculomotor periphery (e.g., weakening of eye muscles), the cerebellum continuously monitors the progress of each movement and passively compensates for sources of inaccuracy regardless of their origin. Alternatively, the cerebellum could actively discriminate between the different potential errors in movement accuracy, estimate the sources of these errors, and adapt to each independently.

## References


Abel LA, Schmidt D, Dell'Osso LF, Daroff RB (1978) Saccadic system plasticity in humans. Ann Neurol 4:313–318.

Bahill AT, Stark L (1975) Overlapping saccades and glissades are produced by fatigue in saccadic eye-movement system. Exp Neurol 48:95–106.

Barash S, Melikyan A, Sivakov A, Zhang M, Glickstein M, Thier P (1999) Saccadic dysmetria and adaptation after lesions of the cerebellar cortex. J Neurosci 19:10931–10939.

Brozek J (1949) Quantitative criteria of oculomotor performance and fatigue. J Appl Physiol 2:247–260.

Büttner-Ennever JA, Horn AK, Scherberger H, D'Ascanio P (2001) Motoneurons of twitch and nontwitch extraocular muscle fibers in the abducens, trochlear, and oculomotor nuclei of monkeys. J Comp Neurol 438:318–335.

Chen-Harris H, Joiner WM, Ethier V, Zee DS, Shadmehr R (2008) Adaptive control of saccades via internal feedback. J Neurosci 28:2804–2813.

Cullen KE, Rey CG, Guitton D, Galiana HL (1996) The use of system identification techniques in the analysis of oculomotor burst neuron spike train dynamics. J Comput Neurosci 3:347–368.

Frueh BR, Hayes A, Lynch GS, Williams DA (1994) Contractile properties and temperature sensitivity of the extraocular-muscles, the levator and superior rectus, of the rabbit. J Physiol 475:327–336.

Fuchs AF, Binder MD (1983) Fatigue resistance of human extra-ocular muscles. J Neurophysiol 49:28–34.

Glasauer S (2003) Cerebellar contribution to saccades and gaze holding: a modeling approach. Ann N Y Acad Sci 1004:206–219.

Golla H, Tziridis K, Haarmeier T, Catz N, Barash S, Thier P (2008) Reduced saccadic resilience and impaired saccadic adaptation due to cerebellar disease. Eur J Neurosci 27:132–144.

Grossberg S (1986) Adaptive compensation to changes in the oculomotor plant. In: Adaptive processes in the visual and oculomotor systems (Keller E, Zee DS, eds), pp 341–345. Oxford: Pergamon.

Hanes DP, Wurtz RH (2001) Interaction of the frontal eye field and superior colliculus for saccade generation. J Neurophysiol 85:804–815.

Judge SJ, Richmond BJ, Chu FC (1980) Implantation of magnetic search coils for measurement of eye position: an improved method. Vision Res 20:535–538.

Kaminski HJ, Richmonds C (2002) Extraocular muscle fatigue. In: Neurobiology of eye movements: from molecules to behavior (Kaminski HJ, Leigh RJ, eds), pp 397–398. New York: New York Academy of Sciences.

Keller EL, McPeek RM, Salz T (2000) Evidence against direct connections to PPRF EBNs from SC in the monkey. J Neurophysiol 84:1303–1313.

Kommerell G, Olivier D, Theopold H (1976) Adaptive programming of phasic and tonic components in saccadic eye-movements - investigations in patients with abducens palsy. Invest Ophthalmol 15:657–660.

Li CS, Padoa-Schioppa C, Bizzi E (2001) Neuronal correlates of motor performance and motor learning in the primary motor cortex of monkeys adapting to an external force field. Neuron 30:593–607.

Ljung L (2002) Prediction error estimation methods. Circuits Syst Signal Processing 21:11–21.

Noda H, Sugita S, Ikeda Y (1990) Afferent and efferent connections of the oculomotor region of the fastigial nucleus in the macaque monkey. J Comp Neurol 302:330–348.

Optican LM, Miles FA (1985) Visually induced adaptive-changes in primate saccadic oculomotor control signals. J Neurophysiol 54:940–958.

Optican LM, Robinson DA (1980) Cerebellar-dependent adaptive-control of primate saccadic system. J Neurophysiol 44:1058–1076.

Prsa M, Dash S, Catz N, Dicke PW, Thier P (2009) Characteristics of responses of Golgi cells and mossy fibers to eye saccades and saccadic adaptation recorded from the posterior vermis of the cerebellum. J Neurosci 29:250–262.

Quaia C, Lefèvre P, Optican LM (1999) Model of the control of saccades by superior colliculus and cerebellum. J Neurophysiol 82:999–1018.

Raybourn MS, Keller EL (1977) Colliculoreticular organization in primate oculomotor system. J Neurophysiol 40:861–878.

Robinson DA (1964) Mechanics of human saccadic eye movement. J Physiol 174:245–264.

Robinson DA (1970) Oculomotor unit behavior in monkey. J Neurophysiol 33:393–403.

Schiller PH, True SD, Conway JL (1980) Deficits in eye-movements following frontal eye-field and superior colliculus ablations. J Neurophysiol 44:1175–1189.

Schmidt D, Abel LA, Dell'Osso LF, Daroff RB (1979) Saccadic velocity characteristics: intrinsic variability and fatigue. Aviat Space Environ Med 50:393–395.

Scudder CA, McGee DM (2003) Adaptive modification of saccade size produces correlated changes in the discharges of fastigial nucleus neurons. J Neurophysiol 90:1011–1026.

Shadmehr R, Mussa-Ivaldi FA (1994) Adaptive representation of dynamics during learning of a motor task. J Neurosci 14:3208–3224.

Smith MA, Shadmehr R (2005) Intact ability to learn internal models of arm dynamics in Huntington's disease but not cerebellar degeneration. J Neurophysiol 93:2809–2821.

Sparks DL, Mays LE (1980) Movement fields of saccade-related burst neurons in the monkey superior colliculus. Brain Res 190:39–50.

Straube A, Robinson FR, Fuchs AF (1997) Decrease in saccadic performance after many visually guided saccadic eye movements in monkeys. Invest Ophthalmol Vis Sci 38:2810–2816.

Sylvestre PA, Cullen KE (1999) Quantitative analysis of abducens neuron discharge dynamics during saccadic and slow eye movements. J Neurophysiol 82:2612–2632.

Thielert CD, Thier P (1993) Patterns of projections from the pontine-nuclei and the nucleus-reticularis tegmenti pontis to the posterior vermis in the rhesus-monkey: a study using retrograde tracers. J Comp Neurol 337:113–126.

Wolpert DM, Miall RC (1996) Forward models for physiological motor control. Neural Netw 9:1265–1279.

Xu-Wilson M, Chen-Harris H, Zee DS, Shadmehr R (2009) Cerebellar contributions to adaptive control of saccades in humans. J Neurosci 29:12930–12939.